



FATİH UNIVERSITY

The Graduate School of Sciences and Engineering

**Doctor of Philosophy in
Electrical and Electronics Engineering**

**MODELING OF ELECTROMAGNETIC
INTERACTION IN HUMAN TISSUES AND LOCAL
TEMPERATURE INCREASE FOR CANCER
TREATMENT AND DEVELOPMENT OF A
HYPERTHERMIA APPLICATOR**

by

Ömer IŞIK

July 2015



**MODELING OF ELECTROMAGNETIC INTERACTION IN
HUMAN TISSUES AND LOCAL TEMPERATURE INCREASE FOR
CANCER TREATMENT AND DEVELOPMENT OF A
HYPERThERmIA APPLICATOR**

by

Ömer IŞIK

A thesis submitted to

the Graduate School of Sciences and Engineering

of

Fatih University

in partial fulfillment of the requirements for the degree of

Doctor of Philosophy

in

Electrical and Electronics Engineering

July 2015
Istanbul, Turkey

APPROVAL PAGE

This is to certify that I have read this thesis written by Ömer IŞIK and that in my opinion it is fully adequate, in scope and quality, as a thesis for the degree of Doctor of Philosophy in Electrical and Electronics Engineering.

Assoc. Prof. Erdal KORKMAZ
Thesis Supervisor

I certify that this thesis satisfies all the requirements as a thesis for the degree of Doctor of Philosophy in Electrical and Electronics Engineering.

Prof. Onur TOKER
Head of Department

Examining Committee Members

Assoc. Prof. Erdal KORKMAZ

Prof. Nurullah ARSLAN

Asst. Prof. Hüseyin SAĞKOL

Assoc. Prof. Salih DEMİREL

Prof. Ahmet Serdar TÜRK

It is approved that this thesis has been written in compliance with the formatting rules laid down by the Graduate School of Sciences and Engineering.

Prof. Nurullah ARSLAN
Director

July 2015

MODELING OF ELECTROMAGNETIC INTERACTION IN HUMAN TISSUES AN LOCAL TEMPERATURE INCREASE FOR CANCER TREATMENT AND DEVELOPMENT OF A HYPERTHERMIA APPLICATOR

Ömer IŞIK

Ph.D. Thesis – Electrical and Electronics Engineering
July 2015

Thesis Supervisor: Assoc. Prof. Erdal KORKMAZ

ABSTRACT

Hyperthermia is a type of cancer treatment in which body tissue is exposed to high temperatures to damage and kill cancer cells. The objective of this treatment is to raise the temperature in tumor up to such a therapeutic level that cell death occurs. To meet with the above stated challenge, narrow band spiral antenna array is presented.

The aim of this thesis is to develop a system to be used for cancer treatment as an alternative method for the conventional treatment methods. In an RF setup the cancerous region will be exposed to external electromagnetic fields. In that way the aim is to increase the temperature in cancerous tissues between 42-44 ° C by exposing up to 60 minutes or more. When applying the regional hyperthermia the temperature has to be limited in surrounding healthy tissues. To that end a hyperthermia applicator has been designed for breast cancer treatment. The applicator consists of 24 directive Archimedean spiral antennas at 434 MHz in a hemispherical arrangement. All individual antennas are focused towards a target region and its phases are adapted to focus all the fields at the targeted region. The measurements are performed by submerging the in-house developed tissue mimicking materials inside the applicator which completely stand inside distilled water. By exposing the tissue mimicking materials to focused waves the temperature distribution with respect to time is observed. Both measurements and simulation results verify the capability of the applicator to focus a very small region in three dimensions.

Keywords: Hyperthermia breast applicator, directive compact antennas, breast cancer, SAR, Tissue mimicking gels.

KANSER TEDAVİSİNDE İNSAN DOKULARINDAKİ ELEKTROMANYETİK ETKİLEŞİM VE LOKAL ISI ARTIŞI MODELLEMESİ VE HİPERTERMİ APLİKATÖRÜNÜN GELİŞTİRİLMESİ

Ömer IŞIK

Doktora Tezi – Elektrik ve Elektronik Mühendisliği
Temmuz 2015

Tez Danışmanı: Doç. Dr. Erdal KORKMAZ

ÖZ

Bir kanser tedavi yöntemi olarak hipertermi, insan vücudunun yüksek ısıya maruz bırakılarak kanser hücrelerinin yok edilmesidir. Bu tedavinin amacı, tümördeki sıcaklığı tedavi edici seviyelere kadar yükselterek hücre ölümünü meydana getirmektir. Bu kriterleri sağlamak için dar hüzmeli döngüsel spiral anten sunulmuştur.

Bu tezin amacı, kanser tedavisinde geleneksel tedavi yöntemlerin dışında alternatif bir yöntem olan hipertermi yöntemini uygulayabilecek bir sistemin geliştirilmesidir. RF bir düzenek içerisinde kanserli bölgenin harici elektromanyetik alana maruz bırakılarak ısıtılması istenmektedir. Bu yöntemde amaç kanserli dokuyu 60 dakika veya daha uzun süreli elektromanyetik alana maruz bırakarak burdaki sıcaklığın 42-44 ° C sıcaklık değerlerine yükseltmektir. Bölgesel hipertermi uygulanırken sağlıklı dokuların zarar görmemesi için ısı artışı çevredeki sağlıklı dokularda minimize edilmelidir. Bu hedef doğrultusunda göğüs kanseri tedavisinde kullanılacak bir hipertermi aplikatörü geliştirildi. Aplikatör 434 MHz’de çalışan 24 adet yönlü Arşimet spiral antenlerin yarım küre şeklinde dizininden oluşmaktadır. Tüm antenler tek tek merkezi bir noktaya yönlendirilmiş ve fazları kontrol edilerek yönlendirilen bölgede odaklanma hedeflenmiştir. Ölçümler tamamen saf suya gömülü olan aplikatöre doku taklit malzemeleri daldırılarak yapılmıştır. Odaklanmış elektromanyetik alana maruz bırakılan doku taklit malzemelerindeki sıcaklık değişimi zamana göre gözlemlenmiştir. Ölçüm ve simülasyon sonuçları aplikatörün çok küçük bölgelere üç boyutlu olarak odaklanabilme kapasitesine sahip olduğunu doğrulamaktadır.

Anahtar Kelimeler: Göğüs Hipertermi Aplikatörü, Küçük Yönlü Antenler, Göğüs Kanseri, SAR, Taklit Dolu Jelleri.

To my parents

*To my lovely wife and my sisters and brothers who have supported me in many ways
along this journey.*

ACKNOWLEDGEMENT

In this thesis a hyperthermia applicator is designed, optimized and developed using spiral patch antennas in a hemispherical configuration. The task has been completed at the department of electrical and electronics engineering, RF Microwave laboratory at Fatih University.

I would like to express my sincere gratitude and respect to my advisor Assoc. Prof. Dr. Erdal KORKMAZ for his technical guidance and support throughout the research. His constructive criticism and advice are gratefully acknowledged.

I am thankful to the committee members, Prof. Dr. Nurullah ARSLAN, Assist. Prof. Dr. Hüseyin SAĞKOL, Prof. Dr. Ahmet Serdar TÜRK, and Assoc. Prof. Dr. Salih DEMİREL for giving their valuable time to serve in the defense committee.

I am also grateful to The Scientific and Technological Research Council of Turkey (TUBITAK) for the support of the project number 111E087 at which I could perform my PhD thesis.

I am also thankful to my colleagues Mohammed Ahmed NASSOR, Mamady KEBE, M. Emin ÖZTÜRK, Uğur ÇELİK, Assoc. Prof. Dr. Hüseyin KAVAS, Emre ÇEVİK, and Ömer KAKŞI and my other colleagues and friends who made my stay at the university a memorable and valuable experience.

Finally, and most importantly, I would like to thank my wife Zeynep. Her support, encouragement, quiet patience and unwavering love were undeniably the bedrock upon which the past five years of my life have been built. I thank my parents for their faith in me and allowing me to be as ambitious as I wanted.

TABLE OF CONTENTS

ABSTRACT.....	iii
ÖZ.....	iv
DEDICATION.....	v
ACKNOWLEDGMENT.....	vi
TABLE OF CONTENTS.....	vii
LIST OF TABLES.....	ix
LIST OF FIGURES.....	x
LIST OF SYMBOLS AND ABBREVIATIONS.....	xiv
CHAPTER 1 INTRODUCTION.....	1
1.1 Introduction.....	1
CHAPTER 2 LITERATURE SURVEY: HYPERTHERMIA IN CANCER	
TREATMENT.....	7
2.1 History of Hyperthermia.....	7
2.2 Basic Principles of Hyperthermia.....	12
2.2.1 Definition of Hyperthermia.....	15
2.2.2 Methods to Increase Temperature.....	18
2.3 Treatment Planning of Hyperthermia.....	20
2.3.1 Specific Absorption Rate (SAR) and Its Distribution.....	20
2.3.2 Temperature and Its Distribution.....	21
2.3.3 Treatment Planning.....	21
2.4 Hyperthermia Application Methods.....	21
2.4.1 Local Hyperthermia.....	22
2.4.2 Regional Hyperthermia.....	24
2.4.3 Whole-Body Hyperthermia.....	26
CHAPTER 3 SINGULAR ANTENNA FOR HYPERTHERMIA APPLICATOR ...	28
3.1 Design of Singular Antenna.....	28

CHAPTER 4	TISSUE MIMICKING GEL CHARACTERIZATION	40
4.1	Introduction.....	40
4.2	Characterization of Muscle Mimicking Material	41
4.3	Characterization of Skin Mimicking Material	42
4.4	Characterization of Fat Mimicking Material	46
4.5	Characterization of Cancer Tissue Mimicking Material	47
CHAPTER 5	HYPERTHERMIA APPLICATOR DESIGN	52
5.1	Forming a Model of Human Tissue.....	52
5.2	Applicator Design	54
5.3	Design of a Breast Applicator.....	60
5.4	Simulation with Real Breast Phantom	65
CHAPTER 6	IMPLEMENTATION AND MEASUREMENT WITH HEMISPHERICAL BREAST APPLICATOR	69
6.1	Design of Microwave Components.....	69
6.2	Measurement with Hemispherical Breast Applicator	72
CHAPTER 7	CONCLUSION.....	76
REFERENCES	79
APPENDIX A	DECLARATION STATEMENT FOR THE ORIGINALITY OF THE THESIS AND PUBLICATIONS FROM THE THESIS WORK.....	87
A.1	Declaration Statement for the Originality of the Thesis.....	87
A.2	Publications from the Thesis Work.....	87
APPENDIX B	ACKNOWLEDGEMENT	89
CURRICULUM VITAE	90

LIST OF TABLES

TABLE

2.1	The rate of complete response with irradiation or hyperthermia alone	17
4.1	Recipes for Muscle Mimicking Gels for ISM Band.....	42
4.2	Recipes for Skin Mimicking Gels for ISM Band.	42
4.3	Recipes for Fat Mimicking Gels for ISM Band.	47
4.4	Recipes for Cancerous Tissue Mimicking Gels for ISM Band	48
5.1	Dielectric properties of tissues at 434 MHz	60
5.2	Dielectric properties of tissues at 434 MHz	67

LIST OF FIGURES

FIGURE

1.1	Growth of cancer cells	2
1.2	According to the development of standardized rates per 100,000 person-years of age, cancer incidence rates in Turkey	2
1.3	The age-standardized rate per 100,000 population distribution according to type of cancer rates in the male age groups in Turkey.	3
1.4	Age standardized rate ratios of distribution by type of cancer in women age group per 100,000 in Turkey.....	4
2.1	Non-invasive measurement of temperature distribution in the hybrid hyperthermia applicator (Wust et al., 2002)	17
2.2	Cell survival curves (Dewey et al., 1977)	19
2.3	Scheme of a system for local hyperthermia (Wust et al., 2002).....	23
2.4	Applicator types for local hyperthermia, such as (a) waveguide applicator; (b) spiral applicator; and (c) current sheet applicator (Wust et al., 2002).	23
2.5	Sigma-60 applicators (four dipole pairs) with treatment couch of the BSD-2000 system for regional hyperthermia. (b) A novel multiantenna applicator Sigma-Eye (12 dipole pairs) mounted on the same treatment unit as shown in (a) (Wust et al., 2002)	25
2.6	Schematic drawing of the Aquatherm system for whole-body hyperthermia (Wust et al., 2002)	27
2.7	Schematic drawing of the Iratherm system for whole-body hyperthermia (Wust et al., 2002)	27
3.1	Top and Side views of the rectangular patch antenna.	30
3.2	Top and Side views of the spiral antenna	30
3.3	S_{11} values for patch (dashed line) and spiral (solid line) antennas	31
3.4	S_{11} characteristics obtained from parameter sweep for strip width of spiral antenna	32

3.5	S_{11} characteristics obtained from parameter sweep for height of spiral antenna	33
3.6	S_{11} characteristics obtained from parameter sweep for width of spiral antenna	33
3.7	Simulation (solid line) and measurement (dashed line) S_{11} values for patch antenna.....	34
3.8	Simulation (solid line) and measurement (dashed line) S_{11} values for spiral antenna.....	34
3.9	The polarization of the spiral antenna	35
3.10	Measurement setup for manual radiation pattern measurements	36
3.11	Simulated (solid line) and measured (dashed line) radiation patterns of spiral antenna at 434 MHz: for $\phi = 0$ plane (left) and $\phi = 90^\circ$ plane (right)	37
3.12	Three dimensional radiation pattern of spiral antenna at 434 MHz.....	37
3.13	Simulated radiation patterns of spiral antenna at 566 MHz (left) and at 716 MHz (right)	38
3.14	Simulated radiation patterns of patch antenna at 434 MHz	38
3.15	Three-dimensional radiation pattern of patch antenna obtained by simulation	38
3.16	S_{11} values for spiral antenna at different water bolus height.....	39
4.1	Relative dielectric permittivity comparison of Triton X-100, DGBE and deionized water.....	43
4.2	Conductivity comparison of Triton X-100, DGBE and deionized water	43
4.3	Process of preparing muscle and skin mimicking materials	44
4.4	Measurement set-up for electrical property measurement	44
4.5	Comparison of relative dielectric permittivity of characterized skin, muscle and fat mimicking gel at room temperature	45
4.6	Comparison of Conductivity of characterized skin, muscle and fat mimicking gel at room temperature	45
4.7	Process of preparing fat mimicking material.....	46
4.8	Relative dielectric permittivity of characterized breast cancer mimicking gel at room temperature	47
4.9	Conductivity of characterized breast cancer mimicking gel at room temperature.....	48

4.10	Relative dielectric permittivity changes of skin and muscle mimicking materials at room temperature	49
4.11	Conductivity changes of skin and muscle mimicking materials at room temperature	50
4.12	Relative dielectric permittivity changes of skin and muscle mimicking materials at +4 °C	50
4.13	Conductivity changes of skin and muscle mimicking material at +4 °C.....	51
5.1	Female breast anatomy	53
5.2	Side and top view of the breast model intended to be used in the simulation program.....	54
5.3	Spiral antenna model inside a water bolus (3cm) with tissues of skin, fat and muscle (left).....	55
5.4	Electric field lines of spiral antenna into tissues at $\phi = 0^\circ$ and $\phi = 90^\circ$ planes at 434 MHz.....	55
5.5	Electric field lines of spiral antenna into tissues at $\phi = 0^\circ$ and $\phi = 90^\circ$ planes at 434 MHz.....	56
5.6	A four antenna element head model where the antennas are embedded in water bolus covering the head	56
5.7	Laterally normalized electric field distribution (left) and longitudinal SAR distribution (right) for the spiral antenna.....	57
5.8	Laterally normalized electric field distribution (left) and longitudinal SAR distribution (right) when the patch antenna is positioned at the broad radiation angle	57
5.9	Coupling between each of four spiral antennas.....	58
5.10	Coupling between each of four patch antennas	58
5.11	Eight spiral antennas coupling between each other.....	59
5.12	Eight patch antennas coupling between each other	59
5.13	Side view of modeled female breast (left) and top view of twelve spiral antennas (right).	60
5.14	The SAR values at the center of cancer region in three orthogonal directions	61
5.15	The temperature increase during the 60 minutes at various locations of the model	62
5.16	Temperature distribution at the tumor center in three orthogonal directions	62

5.17	Side view of the modeled and top view of realized hemispherical breast applicator.....	63
5.18	Two dimensional temperature distribution at the cancerous point with three cross sections	64
5.19	One-dimensional temperature distribution in each of three orthogonal sections through the breast model at 434 MHz exposure for 30 minutes	65
5.20	Temperature increase during exposure in 30 minutes at various locations of the model at 434 MHz.	65
5.21	Side and top view of modeled detailed female breast model (Li X., et al, 2005)	66
5.22	Two dimensional temperature distribution at the cancerous point with three cross	67
5.23	Two dimensional temperature distribution at the cancerous point with three cross	67
5.24	Two dimensional temperature distribution at the cancerous point with three cross section.....	68
6.1	1x16 RF splitter used in applicator.....	69
6.2	Measurement results of 1x16 RF splitter.....	70
6.3	Voltage-controlled 1x16 RF phase shifter.....	71
6.4	Realized hemispherical breast applicator	72
6.5	General view of experimental setup	73
6.6	Different beakers used during the measurements and placement into the applicator	73
6.7	Temperature difference in time when all beakers are salty water	74
6.8	Temperature difference in time when beaker 1 is cancer mimicking gel.....	74

LIST OF SYMBOLS AND ABBREVIATIONS

SYMBOL/ABBREVIATION

σ	Conductivity
ε	Permittivity
μ	Permeability
η	Intrinsic Impedance
Γ	Reflection Coefficient
ω	Radian frequency
∇	Laplacian Operator
k	Thermal Conductivity (W/m/°C)
C_b	Heat Capacity of Blood (4000 J/kg/°C);
C_t	Heat Capacity of Tissue (4000 J/kg/°C);
ρ_b	Density of Blood (1000 kg/m ³);
ρ_t	Density of Tissue (1000 kg/m ³);
T	Temperature of the Tissue (°C)
w	Blood Perfusion Rate (kg/s-m ³)
ABC	Absorbing Boundary Conditions
ASTRO	The American Society For Therapeutic Radiology And Oncology
BHTE	Bio Heat Transfer Equation
CST	Computer Simulation Technology
FDA	Food and Drug Administration
FDTD	Finite Difference Time Domain
HDR	High Dose Rate
ISM	Industrial Scientific and Medical
MR	Magnetic Resonance
NCI	National Cancer Institute

RF	Radio Frequency
TE	Transverse Electric
TM	Transverse Magnetic
SAR	Specific Absorption Rate

CHAPTER 1

INTRODUCTION

1.1 INTRODUCTION

Cancer, almost everyone knows someone who has been seriously ill or died from is a disease caused by abnormal, uncontrolled cell division. Normal cells grow, divide and die. Unlike normal cells however, cancer cells continue to multiply in an abnormal, inordinate manner; continuing to grow and divide without dying. The uncontrolled growth causes a lump called as tumour. Cancer cells can also spread to healthy, surrounding tissue; compromising it and potentially causing damage. Growth of cancer cells is shown in Figure 1.1. There are over 200 types of cancer. For every different type of cancer, there are as many different methods of treatment. The complexity of the cancer tissue makes it hard to find out the real causes of the disease and to find a suitable cure method. Currently there are mass hypothesizes on the causes and treatments of some cancers but these are mere estimates as there is not enough exact knowledge about what perpetuates these diseases. The general aim of cancer therapy is to kill or damage the cancer cells without damaging the surrounding healthy tissue. All over the world, a significant increase is being observed in the proportion of deaths caused by cancer. According to a report released by Ministry of Health (2008), it is observed that there is an increase in cancer incidence value (see Figure 1.2). It is shown that the distribution of cancer among men and women in Figure 1.3 and Figure 1.4.

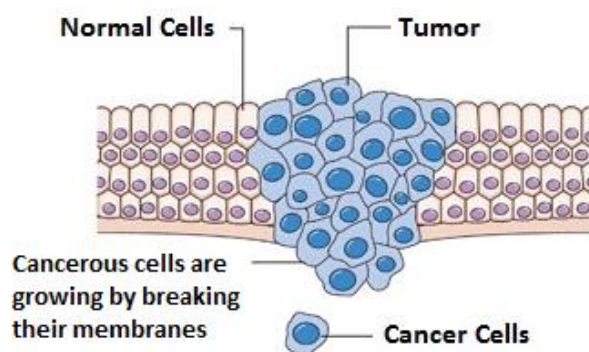


Figure 1.1 Growth of cancer cells.

Different types of cancer can behave very differently. The reason of some cancer types is known or is estimated however, it is still uncertain what causes most of cancer types. For example, smoking is known to cause a type of lung cancer. And skin cancer results from strong sunlight. Some other things that are thought to cause cancer are genetics, irregular nutrition, drinking alcohol and a polluted environment. Many risk factors that increase the chance of having cancer has identified as mentioned above. It can be said that some cancers are often caused by not a single factor but a variety factors.

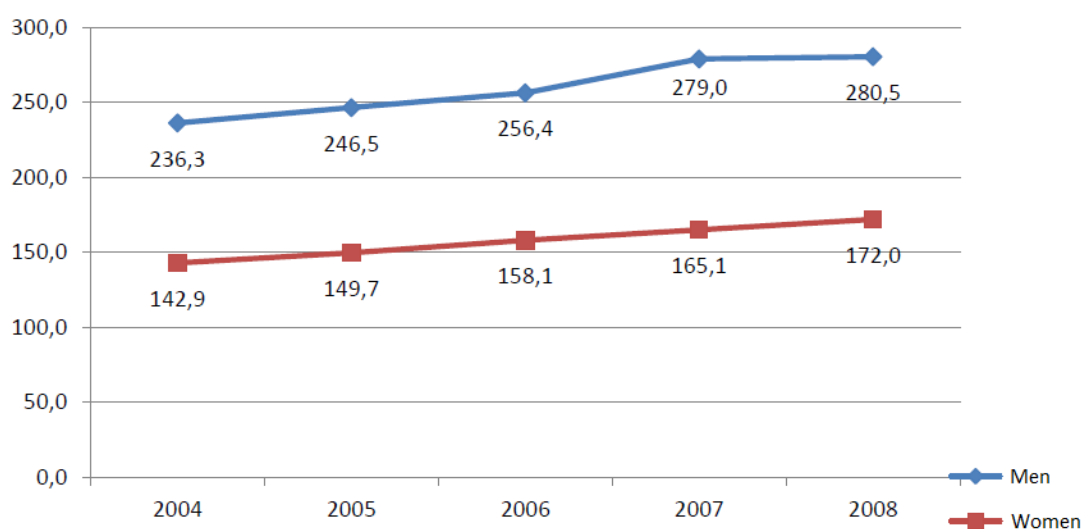


Figure 1.2 According to the development of standardized rates per 100,000 person-years of age, cancer incidence rates in Turkey.

Nowadays, common cancer types, if they are diagnosed in a timely fashion, can be treated with “traditional” treatments such as surgery, radiotherapy (radiation) and or chemotherapy. These methods can be applied individually or combined. Although traditional methods can be implemented efficiently according to the stage of the disease, there are also many disadvantages of these treatment methods. Unfortunately today, there is no certain cure for many types of cancer. Once a patient has been diagnosed with cancer, he or she may be given a life expectancy of up to five years even with the implementation of traditional treatment. Unfortunately, this is widely accepted as a positive, best-case scenario.

Surgery is the oldest form of cancer treatment. Cancerous tumor or tissue is physically removed from the body by surgery with an operation. There are many factors that cause the side effects after surgery. These side effects take shape by depending on the size and location of the tumor, the type of operation, and the patient’s general health (NCI Fact Sheet 6.7, 2005). Some pain may become after surgery, but this pain is controllable with some medical approaches. Surgery can be the greatest way for cure for some types of cancer. But it has a lot of risk factor. Because the removing cancer cells from the body without damaging is very difficult. Surgery needs an expert who must be very competent of this operation to achieve the best outcome.

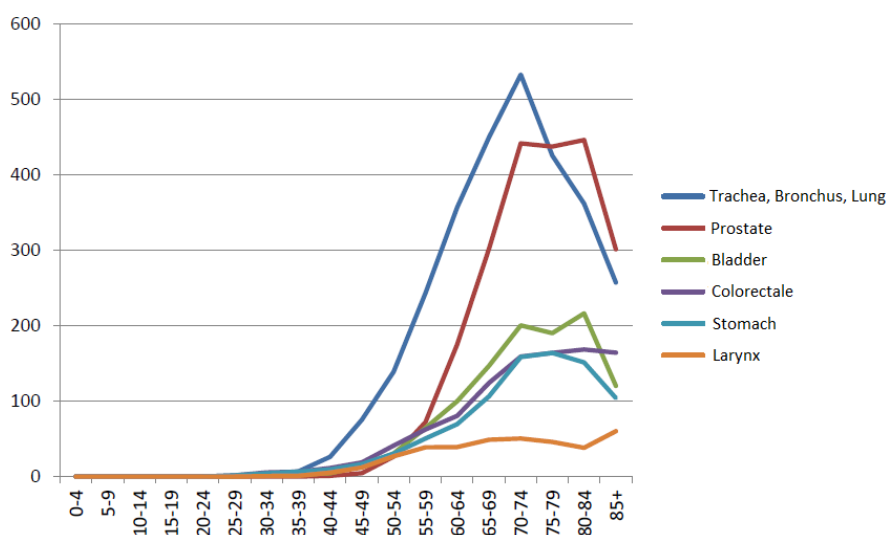


Figure 1.3 The age-standardized rate per 100,000 population distribution according to type of cancer rates in the male age groups in Turkey.

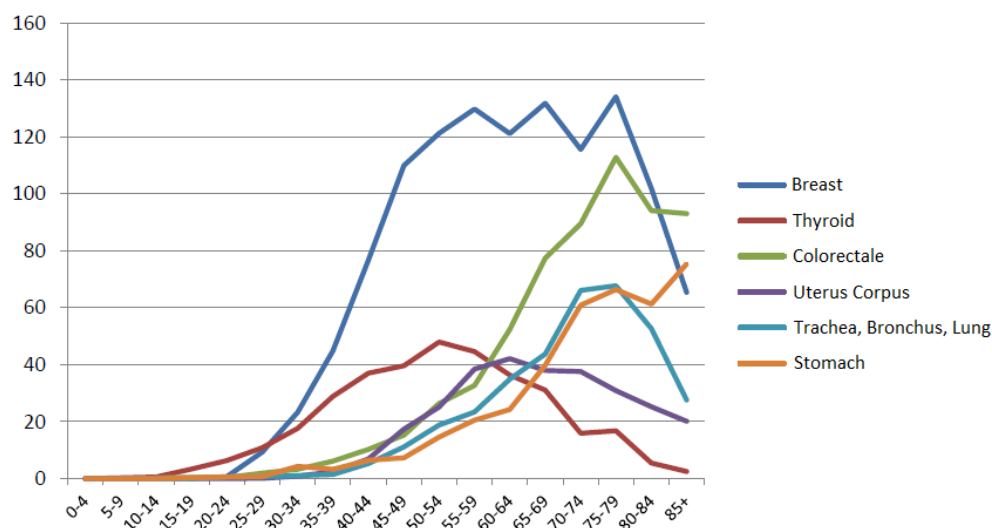


Figure 1.4 The age standardized rate ratios of distribution by type of cancer in women age group per 100,000 in Turkey.

The most common treatment type of cancer is chemotherapy. In chemotherapy, cancer cells throughout the body are killed with helping of drugs. One drug or a combination of drugs may be used within chemotherapy. These drugs can affect cancer cells anywhere in the body. Thus, chemotherapy can be referred as a systemic treatment (Cukier, 2005). Chemotherapy is applied alone or with other treatments. Although chemotherapy is effective method in cancer treatment, it has the side effects by depending mainly on the drugs and the doses. The disadvantage of chemotherapy is that healthy cells can also be harmed by anticancer drugs. Chemotherapy can also have several neurological side effects, such as fuzzy thinking and difficulty concentrating.

It is because of the poor prognosis that all too often comes with cancer that many scientists, doctors and researchers across broad fields of study are seeking alternative methods of treatment for the disease. These techniques are purposed to be more exact and much less invasive then current techniques. The new radiation techniques are recently started to get more significance in the treatment of cancer. One of the emerging and promising non-invasive treatment method is electromagnetic hyperthermia. Brought about in recent years, it shows promise in the revolutionizing of cancer treatment.

Hyperthermia also called thermal therapy or thermotherapy is a type of cancer treatment. The goal of electromagnetic hyperthermia is to increase the temprature of

cancer tissues by exposing them to non-invasive electromagnetic radiation. High temperature up to 45 °C is desirable in cancer tissues (NCI Fact Sheet 7.3, 2004), (Deufhard et al., 1997). Researches have shown that high temperatures can damage the protein build within the cell and hence kill the cancer cells, usually with minimal injury to normal tissues. When the tissues are heated the body naturally reacts on it an increase the blood circulation to cool down the heated tissues. As a result cytotoxic effect increases and that render cancerous cells more vulnerable to conventional chemotherapy and radiotherapy (Vernon et. Al., 1996; Vujaskovic et. al., 2010).

The main goal of this dissertation is to develop a hyperthermia applicator that implements the method of hyperthermia as a modern, advanced and alternative option for cancer patients that would be set apart from the traditional treatments available in clinics.. Superficial tumors can be heated relatively easier with microwave hyperthermia applicators. Tumors in deep locations are a challenge to bring therapeutic temperaturus with microwave applicators. Many factors such as penetration dept, inhomogeneous tissue properties, perfusion variations and irregular overlying tissue topology restrict the microwave heating. For deep located microwave hyperthermia applicators there are two essential problems to cope. First is the generation of therapeutic temperatures at the tumor location while avoiding hot spots in surrounding healthy tissues. Second problem is the monitoring and controlling of temperature within the tissues. A phased array antenna system where the fields constructively add at the targeted region and destructively add in other regions is a remedy for the first problem. Thermal monitoring can be conducted by MRI based systems (Salomir et al., 2000, 2001) or emerging microwave thermal monitoring techniques (Wust et al., 2006) which is out of scope of this dissertation. In order to avoid superficial heating and unwanted hot spots the use of directive antennas is preferable. Using directive antennas will allow us to mount antennas close to each other in a constrained region which will improve the efficiency of focusing. In addition the size of the antenna should be also small to use more antenna elements. Hence the design of an effective appropriate single antenna element is a crucial step in the development of a specific applicator. The design of a hyperthermia antenna differs much from the free space applications since the antenna is radiating directly into lossy mediums, for instance the water bolus and different tissue layers, which have to be considered as antenna loads.

The breast cancer is by far the most commonly diagnosed cancer type and the second leading cause of death among women (National Cancer Institute, 2014). The average size and quasi symmetrical shape with typical tumor location inside the breast was a reason to design a focused breast applicator. A cylindrically shaped phased array preclinical prototype breast cancer applicator is reported where a two dimensional focusing is obtained at 915 MHz (Korkmaz et al., 2012, 2013a, 2013b). This thesis presents the development of a preclinical breast applicator prototype that consists of 24 directive microstrip spiral antennas forming a hemispherical array at 434 MHz with 3D focusing capability. For the validation of measurements the tissue mimicking jels are characterized which are commonly used for preliminary hyperthermia measurements due to the no need for regulations, simplicity and cost reasons. As a central topic of this thesis, an introduction is presented in Chapter 1. The main purpose of this chapter is to make clear the aim of the thesis by giving background information about the dissertation. Cancer is firstly introduced in an abbreviated manner. General effects, causes, risks of cancer in human life are discussed. Briefly, the main treatment options or methods are mentioned.

Next, a literature survey about hyperthermia in cancer treatment is presented in Chapter 2. This chapter considers the basis of hyperthermia in cancer therapy. It represents the patient specific treatment approaches. Chapter 3 covers the characterization of some tissue materials. Recipes of characterized tissue mimicking materials are given in this chapter. Skin, muscle, breast fat and cancerous tissue are proposed for ISM Band. The detailed recipe for all these tissues and procedure to compose the materials are explained. A comparison between the electrical properties of these mimicking tissue materials and reference data (C. Gabriel et al., 1996, S. Gabriel et al., 1996) is given.

Chapter 4 discusses the design, simulation and measurement of single antenna element used for hyperthermia applicator. It also discusses potential applications of the proposed tissue mimicking materials. CST software is used to design the antennas. SEMCAD X software is used for thermal simulations. The simulation and measurement results regarding return loss, gain, coupling of antenna is given. Thermal simulation is represented. Chapter 5 concludes the thesis, briefly summarizes the results and discusses the potential applications.

CHAPTER 2

LITERATURE SURVEY: HYPERTHERMIA IN CANCER TREATMENT

For most of the cancer patients, chemotherapy and radiotherapy are two of the most popular and effective methods in the treatment of cancer. Cancer could be a very violent and sometimes an incurable disease. However, both chemotherapy and radiotherapy would damage the normal and abnormal tissues. Patients also have to suffer from great pain during these treatments. Alternatively, there are many promising cancer therapy techniques developed in last years. Hyperthermia cancer therapy is one of the promising approaches. This chapter describes all detailed applications about hyperthermia. And the following sections deal with the physical and biological basis of hyperthermia.

2.1 HISTORY OF HYPERTHERMIA

Written reports about the use of increasing temperatures in cancer treatment have existed for any centuries. As far as known that the oldest report was found in Egyptian Edwin Smith surgical papyrus, dated around 3000 B.C History of the treatment of cancer with hyperthermia can be traced back to 3000 B.C. (Chou, 1988). The current interest in hyperthermia came the center of attention in the early 1970s, where research activities were begun addressing both the biological and clinical usefulness of this modality (Nielsen et al., 2001). In 1975, It was initiated by the first international congress on hyperthermic oncology in Washington. This interest has followed a course as a new type of treatment. However hyperthermia was first employed as a treatment for malignant disease in the last century, it is only relatively recently that its mode of action

and clinical application have been subjected to scientific research (Dunscombe et al., 1989). The method of heating the tissue to treat its ailments is a traditional one. Even 5000 years ago the ancient Egyptians were known to have applied this form of healing via harmonic frequencies (Smith, 2002). The hyperthermia treatment method was applied firstly for the treatment of Hypocrites lung cancer circa 500-400 B.C. (Seegenschmiedt and Vernon, 1995). In 1912, from clinical studies taken on over 100 patients the many benefits of thermal therapy are touched upon (Muller, 1912). Pennes, in 1948, calculated the interaction of arterial blood and tissue temperature and showed that there is not only superficial heating but that the bio-heat equation founded by Pennes formed the basis for calculation of heat distribution. Using electromagnetic waves as a means of energy transfer for hyperthermia applications for oncologic hyperthermia is discussed in the symposium first in 1975 in Washington. The cellular phase transition was around 42°C in the tissues. Healthy cells were said to have sustained no damage under these temperatures but the cancer cells were found to be affected. High temperatures in the tissues impair the protein construction of cancerous cells and it inhibits their growth, potentially even killing them (Hildebrandt et al., 2002). It was also shown that the temperature of cancerous tissues is much higher than other tissues (van den Berg et al., 1983). In the first studies, it emphasized that the results are revealed more effective for superficial hyperthermia treatment of cancerous tissues (Abitbol et al., 1988). Specific Absorption Rate, temperature, and the appropriate configuration associated with these treatment techniques for design work began in 1989 (Dunscombe et al., 1989).

Studies summarized above are listed several reasons for the application of hyperthermia procedures and development but another advantage of this method can be used in addition to chemotherapy and radiotherapy (Wust et al., 2002). The positive results obtained with the use of methods in combination with other methods of hyperthermia are indicated (National Cancer Institute, 2014). Ultrasound to heat tissue, hot water tubes, ferromagnetic core and electromagnetic spread techniques have been tested (Yang and Liu, 2005). Externally applied electromagnetic regional hyperthermia methods, are referred to as the whole body (Wust et al., 2002). Whole-body hyperthermia application takes the principle to be heated entirely the body apart from the head (Yang et al., 2005; Babincov et al., 1999). Superficial hyperthermia method is

generally applied to a partial area of up to 4 cm deep. It is usually applied as an area of 50 cm² with a single antenna. A liquid bag is placed between the antenna and skin to reduce surface heat (Yang et al., 2005).

In my thesis what interests us is the actual application method regional hyperthermia. With this method is aim to not affected the healthy part by heating cancer in the region deeper (Deufhard et al., 1997). The biggest advantage of this method is to hold the person-specific treatment plans; one disadvantage is the difficulty the formation the plan. In other words, Proper use of parameters in the applicator is the creation of a special comprehensive geometric model for patient and electromagnetic on this model is possible by calculating the specific absorption rate and heat distribution. Some studies in the research and on regional hyperthermia applications and positive results have been reported (Kowalski et al., 2004). In this study, electromagnetic and thermal fields in the human tissue and results regarding the efficiency of numerical methods were published. Using array antennas in the deeper and large cancerous region was shown to be heated (Yang et al., 2005; Işık and Korkmaz, 2010; Korkmaz et al., 2013). Erasmus MC-Deniel den Hoed developed a hyperthermia applicator for neck-head model in the cancer center and he reported positive results (Paulides et al., 2007). In recent years, Similar studies have been launched or are continuing in many countries (Işık and Korkmaz, 2009; Işık, 2009; Seebass et al., 2001; Wust et al., 2005).

Despite all these efforts and expectations, there are many reasons not to applied microwave hyperthermia method so far at the clinical level. First, the solution of electromagnetic problems in the first year is generally only done with analytical solutions on rotational symmetric bodies, while numerical methods it was presented with the first simple applications. The fact that the electromagnetic behavior of in the complex environments can be solved by numerical methods has increased the importance of numerical methods with the development of computer technology. Initially, the software which is mostly based on asymptotic methods later on released with full electromagnetic solutions. It was brought to an acceptable level by improvements in the reliability of the simulation method. The objects used in numerical modeling methods are based on the solution of equation formed grilling according to the detailed of object and wavelength, there are an unknown number of millions in complex solution was not possible until a few years ago. The object used in numerical modeling

methods are based on the solution of equation by grilling according to object's detail and wavelength, the solution unknown number of millions in complex constructions was not possible until a few years ago. In recent years, The development of multi-core parallel computing based on specific hardware and the commercial simulation program updates software according to the these hardware, it was provided 20 times and more acceleration in the simulations. A second obstacle of the implementation of hyperthermia method so far is difficult to form detailed models of human-body tissue. Because method requires the person has applied to the body-tissue models, It constituted a major problem these models lack of detailed and reliable software from computer tomography images. The introduction of software to create these models in recent years, and electromagnetic simulation programs to make them compatible with gives promise for studies on hyperthermia method (ISEG, 2014; 3D-Doctor, 2014). Anymore, the current software can be created complex human body-tissue models by using details particulars in tissues.

These formed models can be calculated as using a more realistic way of electromagnetic interactions in tissues. These calculations for time domain finite difference method applicability to inhomogeneous model, resolution can be scaled in the same proportion with the increase, the model (the patient), and that included the interaction between the antenna and to accelerate the simulation of timing the hardware accelerator is preferable to because it is convenient (Taflov and Hagnes, 2005). The calculated value of electromagnetic fields is calculated specific absorption rate in tissues. Then, these values should be calculated temperature distribution in the tissue using the Pennes bio-heat equation (Pennes, 1948). Today, to do the segmentation of three-dimensional tissue, the electromagnetic interactions in tissues, which can calculate the specific absorption rate and effective heat dissipation and quick re-preparation software is not realistic. The literature and our own research work SEMCAD X commercial simulation program both time domain by using the finite difference method, the specific absorption rate, and conformity to calculate heat dissipation occurs with hyperthermia has the capacity to be able to observation method was used throughout the project. In addition, CST Studio Suite commercial simulation program was used in the antenna design and modeling.

In recent years, the portion applications is presented different applicators designed the result of in many studies (Paulides et al., 2014; Stang et al., 2012; Li v et al., 2011, Stauffer et al., 2010; Chen et al., 2010). Partial success was also obtained as a result of these practices. In fact, there is also a company that designs hyperthermia applicator (BSD Medical, 2014). These applicators are often used as a simple dipole antenna antenna. Radiation beam antenna to be used for an effective application of hyperthermia should be narrow, it should be able to operate at relatively low frequency in order to penetrate deep and also lateral size should be small in order to form opportunities to use multiple antennas. Thus, multiple antenna arrays can be used and provided a deeper increase in tissue temperature without damaging healthy tissue. For this purpose, our preliminary work and our ultimate antenna design has been reported in the part of our thesis (Korkmaz et al., 2012, 2013a, 2013b).

One of the deficiencies observed in the literature is the lack of application of hyperthermia in a general way for frequency selection based on the size and depth of cancer. Because focusing increases on high- frequency, penetrating the tissue of electromagnetic energy is reduced and it is formed opposite result in the low frequencies. In this context, 434MHz (ISM band) frequency which is reserved for Industry, Science and Health is used as applicator in our project. Furthermore, this improved antenna applicators must be calculated correctly in phase and amplitude parameters. Because this method is necessary for the implementation of future clinical expertise and with a reasonable time.

One of the major problems parallel to these developments how to confirmed to the calculated heat dissipation application on humans. In this context it is observed that the studies conducted in recent years that MR-based real-time measurement method and the method is performed using heat is developed(Salomir et al., 2000, 2001; Hynynen and McDonald, 2004; Wust et al., 2006; Gellermann et al., 2006; Paulides et al., 2014; Stang et al., 2012; Li et al., 2011, Stauffer et al., 2010; Chen et al., 2010). With this method will be monitored real-time, simultaneous heat distribution in the future application of hyperthermia, However, This method is very expensive method and is now out of the project scope. The experience gained through this project MR imaging-based heat is planned to work on alternative methods of microwave thermal imaging.

In the cancer treatment, chemotherapy and radiotherapy are two of the most effective and popular methods for most of the cancer patients. Cancer could be a very incurable and sometimes terrible disease. However, both of these therapies (chemotherapy and radiotherapy) may damage the normal and abnormal tissues. Alternatively, there are many promising cancer therapy techniques or approaches developed in last years. Hyperthermia cancer therapy is one of the promising approaches. There are several methods which hyperthermia can be applied: local hyperthermia by external or internal energy sources, regional hyperthermia by perfusion of organs or by irrigation of body cavities, and whole body hyperthermia. This chapter describes all detailed applications about hyperthermia. And the following sections deal with the physical and biological basis of hyperthermia.

2.2 BASIC PRINCIPLES OF HYPERTHERMIA

Nowadays the hyperthermia method is not yet at a level that it can be used commonly by oncologists in the clinic. It is necessary to overcome the many side effects the treatment can create. The human body stands as a lossy electromagnetic medium. When an electric field penetrates the human body, it is debilitated and part of that energy is absorbed into the body. This problem can be solved by increasing the number of sources that radiate the electromagnetic field into the deep tissue. By doing this, depending on the location and depth of the cancerous cells, the hyperthermia will be applied by using an array antenna that provides optimal absorption to the cancerous area. The same phase must be used repeatedly in the appropriated region in order to gather the desired harmonic electromagnetic field and focus it collectively on the concentrated area. In order to gather the waves at the desired location, the phase settings of the antennas should be calculated and set according to the tissues circulation in the isolated cancerous region that differs from the surrounding healthy tissue. Thus, the electromagnetic waves in the focused area are collected as constructive by the patient's body causing the temperature increment and phase settings to be disregarded by the healthy area. The total electromagnetic field and temperature rise absorbed is therefore minimized and destructive only to the cancerous tissue that was intended. The focus is to be both successful and have a relatively lower amount of energy that would be less

warming in the surrounding area. This would require the use of many antenna arrays even though the application area of human tissue is of a small size. The narrow beam of radiation and the antenna that operates it can function at low frequencies in order to penetrate deep into the tissue. In fact, although better focus can be achieved at high frequencies, the penetration degree is reduced. On the other hand, while operating at lower frequencies the penetration degree increases but the focusing is reduced. It is a matter of the correct frequency setting.

In addition, parameters, which will be used, cannot be generalized because electromagnetic interaction differs from model to model and it is only applied to a specific person or patient. Instead of a general model, each patient's own body-tissues should be uniquely tuned and created. Forming a detailed model is extremely difficult. Three-dimensional human tissue models can be created by using commercial software from computer tomography images. Here, segmentation of the tissues with certain sensitivity is required for focusing and phase calculation. Finite difference time domain method is preferred for applications to non-uniform patterns and working electromagnetic interference calculations. The resolution can be scaled into proportion with the increases and decreases that unify the interaction between the patient and antennas. This is preferred because it is in accordance with the features accelerator to accelerate simulation time (Taflove et al., 2005). A basic parameter about health risks of electromagnetic field power absorption in the human body is the specific absorption rate (SAR). SAR has been widely used with biological systems in expressing quantity interactions of electromagnetic fields in the radio and microwave frequency range. SAR at a point is defined for sinusoidal fields and for an infinitesimal volume element as in Eqn. (2.1).

$$\text{SAR} = \frac{\sigma}{2\rho} |E|^2 \quad (2.1)$$

Where $|E|$ is the magnitude of electric field (V/m), σ is conductivity (S/m) and ρ is mass density of the tissue (kg/m^3). Specific absorption rate in tissues is calculated by using calculated electromagnetic field value. The biothermal phenomena underlying hyperthermia are governed by Pennes (Pennes, 1998, Pennes, 1948). Then, heat distribution within the tissues is calculated by using these values in Pennes bio-heat

equation. This formulation expresses the balance of thermal energy in time and space and is also known as Pennes bio-heat transfer equation. It is shown in Eqn (2.2).

$$C_p(\mathbf{r})\rho(\mathbf{r})\frac{\partial T(\mathbf{r})}{\partial t} = \nabla \cdot (K(\mathbf{r})\nabla T(\mathbf{r})) + A_0(\mathbf{r}) + Q_0(\mathbf{r}) - B(\mathbf{r})(T(\mathbf{r}) - T_b) \quad (2.2)$$

Wherein C_p , ρ , T , K , T_b , Q_0 , A_0 , and B represent, the specific heat (J/kg/ °C), the physical density of the tissue (kg/m³), the temperature elevation (°C), the thermal conductivity (W/m/°C), the blood temperature (°C), the heating potential, the metabolic heat generation, and the capillary blood perfusion coefficient, respectively. The heating potential Q_0 is proportional to the square amplitude of the field, whereas all other terms depend on the tissue at hand.

When mentioning the hyperthermia method, it should also be understood that there are two different forms of carrying out the hyperthermia treatment. The first form utilizes an invasive probe that is heated to extreme temperatures and localized to the area affected by the cancer; this is known as Local Thermal Microwave Ablation (American Cancer Society, 2014). Microwave Ablation can only be effective and occurs when the temperature of the probing instrument meets or exceeds 45°C. The second form of hyperthermia treatment involves increasing the body temperature internally by exposing the patient to electromagnetic fields externally in a Microwave Apparatus (American Cancer Society, 2014; National Cancer Institute, 2014). The target goal of this method is to raise the temperature of the cancer tissue to 42-44°C within sixty minutes or more thus compromising the integrity of the cancer cells or killing the cancer cells outright. Several methods of implementing these two forms of hyperthermia treatment are currently under way; including Local Hyperthermia and Regional Hyperthermia; also known as Whole-body Hyperthermia. This doctoral thesis requires that Regional Hyperthermia by way of the Microwave Apparatus be the main focus of discussion in regards to these varying methods. Thermal Ablation is completely beyond the scope of this thesis.

As a means to prevent damage to healthy tissue while applying Regional Hyperthermia, special care should be given to avoid temperature increase in the surrounding healthy tissue. Although the desired temperature (42-44°C) is not enough

to destroy the cancer cells directly, it is known to impair the formation of the proteins inside the cancerous cells. Fortunately, cancerous cells are relatively less resistant to heat than healthy cells because, as indicated in previous studies, heat blocks the protein that is essential for the repair pathway (DNA) of the cancer cell to regrow. This method also holds the possibility of killing the cancer cell outright (Chou, 1988, Hildebrandt et al., 2002, Lagendijk, 2000).

This doctoral thesis is required to be developed with regional hyperthermia method and thermal ablation is completely beyond the scope of thesis. To prevent damage to healthy tissue while applying regional hyperthermia, temperature increase in the surrounding healthy tissue should be minimized. Although a desired temperature is not enough to destroy the cancer directly, it is known to impair protein form of cancerous cells. Cancerous cells are relatively less resistant to heat than healthy cell because it is indicated in previous studies that it inhibits the growth of cancerous part in this heat and it is even died (Chou, 1988; Hildebrandt et al., 2002; Lagendijk, 2000).

2.2.1 Definition of Hyperthermia

A dictionary explanation of the word “hyperthermia” is “heating of the body”. However, hyperthermia is an alternative cancer treatment as a therapy in which body tissue is exposed to high temperatures (Yang et al., 2005). The purpose of hyperthermia treatment of cancer is to increase the temperature in the related tumor volume above 42°C - 43°C for a sufficient period of time (Jordan et al., 1999). In the surrounding tissues, this process must protect normal physiological temperatures (well below 42 °C) (Converse et al., 2006). Scientist had shown that high temperatures can damage and kill cancer cells. This approach usually causes minimum injury to normal tissues. Hyperthermia is able to shrink tumor or cancer cells by killing them or damaging their proteins and structures (Hildebrandt et al., 2002). Hyperthermia is most often used to treat tumors that are close to the surface of the body. A special device called a surface applicator is used to the region of the tumor. That region is heated to a temperature of 43 °C (109°F) for approximately one hour. Hyperthermia treatments are given within one hour of radiation therapy or chemotherapy. Hyperthermia can also be used to treat deeper tumors when combined with high dose rate brachytherapy (HDR) (Dunscombe

et al., 1989). The HDR catheters are used for internal radiation treatments and for temperature measurements.

There is a clear reason for using hyperthermia in cancer treatment. At temperatures between 40 and 44°C, treatment is cytotoxic for cells in an environment with a low pO₂ and low pH, conditions that are found specifically within tumour tissue, because of insufficient blood perfusion. According to these conditions, radiotherapy is less effective, and systemically applied cytotoxic agents can arrive such areas in lower concentrations than in well perfused areas. And so, the addition of hyperthermia to chemotherapy or radiotherapy will result in at least an additive effect. Furthermore, the effects of both radiotherapy and many drugs are improved at an increased temperature (Wust et al., 2002).

Hyperthermia can be applied as an supplement therapy with different established cancer treatments such as radiotherapy and chemotherapy (Wust et al., 2002). Hyperthermia may make some cancer cells more sensitive to radiation or harm other cancer cells that radiation cannot damage.

When they are combined, hyperthermia and radiation therapy are frequently given within an hour of each other. The effects of certain anticancer drugs may be improved by hyperthermia. With numerous clinical trials have been tried by using hyperthermia method combination with radiation therapy and/or chemotherapy. These studies have focused on the treatment of many types of cancer, including sarcoma, melanoma, and cancers of the head and neck, breast, brain, lung, esophagus, bladder, rectum, liver, cervix, appendix and peritoneal lining (NCI Fact Sheet 7.3, 2004). Many of these studies, but not all, have shown an important progress in the treatment of cancer cells when hyperthermia is applied with other treatments methods. The combination of hyperthermia and radiation therapy may make the radio resistant tumor cells more sensitive to radiation (Abitbol et al., 1988). This is presented by comprehensive laboratory datas. Also, tumor cells in the synthetic phase of the reproductive cycle are typically resistant to radiation may be more responsive to radiation with the addition of hyperthermia.

A high rate of complete response in the patients who are treated with hyperthermia and radiation is shown by many clinical trials (Abitbol et al., 1988). The compared rates of this response are shown in Table 2.1.

Table 2.1 The rate of complete response with irradiation or hyperthermia alone.

Author	Criteria of Response	Radiation Therapy and Hyperthermia	Radiation Alone
Kim, Y. (1985)	Complete	33 %	----
Kim, J. (1982)	Complete	80 %	33 %
Scott, N.L. (1983)	Complete	87 %	39 %

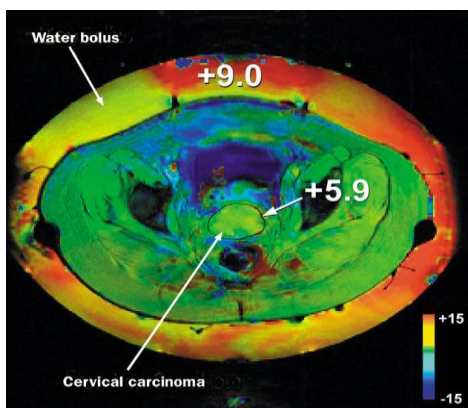


Figure 2.1 Non-invasive measurement of temperature distribution in the hybrid hyperthermia applicator (Wust et al., 2002).

The results showed above indicate the potential usefulness of radiation therapy and hyperthermia to apply superficial tumors.

The properties of hyperthermia are not only limited to its interaction with conventional treatment types (Babinová et al., 1999). There are a number of exciting areas. It may have a new area to apply, such as gene therapy. One of the major challenges in the current development of gene therapy strategies is the ability to regulate

the expression of therapeutic genes to suitable levels (Wust et al., 2002). The use of heat inducible promoters can obtain controllable gene expression. This has been shown by several preclinical studies.

More recent studies have now shown that the antitumour activity of such vascular targeting therapies can be significantly enhanced by combination with hyperthermia. Other hyperthermia combination approaches, such as with chemotherapy, are not necessarily new, but there are clearly new drugs/combinations that may have potential in this regard.

Most normal tissues are not damaged during hyperthermia if the temperature remains under 42°C. However, higher temperatures may occur in various spots (NCI Fact Sheet 7.3, 2004). This changes due to regional differences in tissue characteristics. This can cause in burns, blisters, discomfort, or pain. Perfusion techniques can cause tissue swelling, blood clots, bleeding, and other damage to the normal tissues in the perfused area; however, most of these side effects are temporary.

2.2.2 Methods to Increase Temperature

The heating patterns of a particular modality is needed before the treatment. Numerical modeling is used to predict the heating patterns. The next step is to use the heat transfer equation to calculate the temperature distribution after the pattern is obtained (Chou, 1988). Numerous papers have been published on mathematical modeling of this process. Numerical techniques, such as finite differences, finite element, moment, and finite-difference time-domain methods, have been used for numerical modeling.

Radiobiologists carefully studied the effects of hyperthermia on normal and tumor cells during the last two decades (Strohbehn and Douple, 1984). The results of these cell survival studies in the 1970s showed that cessation of cell division, defined as mitotic death or cell killing, was attained if cells were exposed to temperatures in excess of approximately 40 °C for time periods of 30 min or more. In Figure 2.2, the surviving fraction of the heated cells is plotted on the ordinate as a function of the time the cells were held at a specific temperature.

Heat is applied by increasing temperature in tissue. There are different heating techniques to achieve this. These are such as ultra sound, hot water tubes, ferromagnetic seeds and electromagnetic radiation (Yang et al., 2005). Infrared radiation can be used to heat the whole body. More deeply located tumours can be treated by applying radiation in the radiofrequency range. Small and easily accessible tumours can be heated by inserting electrodes into the tumor. These electrodes behave as small antennas.

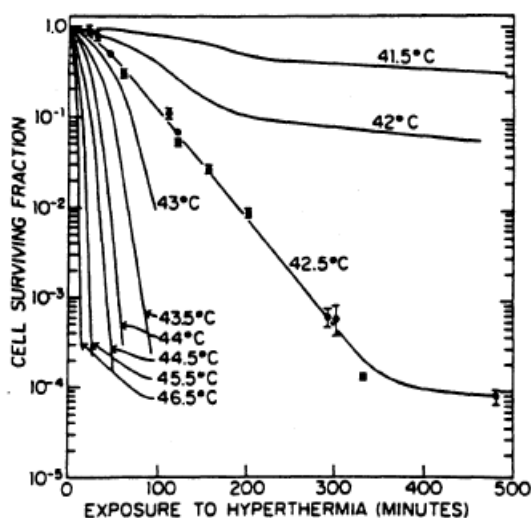


Figure 2.2 Cell survival curves (Dewey et al., 1977).

Electromagnetic or ultrasound energy is directed at the treatment volume. The energy distribution in the tissues strongly depends on tissue characteristics and is thereby inhomogeneous. The heated part depends on the physical characteristics of the energy source and on the type of applicator. The temperature distribution is not simply a result of the energy distribution. But it also depends on thermal tissue characteristics and blood flow.

The systemic temperature of human body is 37.5 °C. To reach temperatures clearly above this temperature in a defined target volume is a technical challenge and still under development. The temperature increase is induced by applying a power-density specific absorption rate (SAR; measured in W/kg) (Wust et al., 2002). Human basal metabolic rate (basal metabolism) is above 1 W/kg. Perfusion is against the

temperature rise. It counteracts it. Perfusion rates in human tumours are around 515 mL per 100 g per min, but they vary widely. To reach therapeutic temperatures of about 42 °C at least in some parts of such tumours necessitates power density of about 20-40 W/kg at the target region.

The convenient temperature distribution for clinical purposes is still unknown. The achieved temperature distributions have limited absolute values (minimum temperatures typically lie between 39.5 °C and 40.5 °C). Its reason is physical and physiological characteristics such as electrical tissue boundaries, local perfusion variations, and perfusion regulations. Only about 50 % of deeply located tumours reach at least 42°C at one particular measurement point.

The temperature distributions should be achieved as high and homogeneous as possible, although the tumour temperatures for clinical efficacy are still unclear. Monitoring and control of temperature distribution has not yet been intensively scrutinized.

2.3 TREATMENT PLANNING OF HYPERTHERMIA

If it is accepted that hyperthermia may be a useful therapeutic modality for cancer, then there is still the question of how hyperthermia should be applied clinically. Hyperthermia treatment planning is needed to design, control, document and evaluate a treatment and thus to provide the data for treatment optimization and to provide the insight to design better heating equipment. The subject of this section, treatment planning for hyperthermia, may be resolved into three components which are introduced below.

2.3.1 Specific Absorption Rate (SAR) and Its Distribution

In this part, the rate of energy absorption per unit mass is determined. Two or three dimension modelling is under specified conditions in standard phantoms or in a patient from a given treatment machine.

The heating technique is characterized under the specific conditions by the collected data during this procedure. And general identification of those sites and target volumes is allowed by this (Dunscombe et al., 1989). In addition, one group of input parameters, which is essential for the calculation of the temperature distribution, is formed by the distribution of the Specific Absorption Rate (SAR).

The objective of fulfilling Specific Absorption Rate (SAR) measurements is to describe the energy delivery equipment by determining the pattern of energy deposition.

2.3.2 Temperature and its Distribution

In a patient throughout the course of a clinical treatment, the distribution of temperature is determined in two or three dimensions. The temperature data accumulated during the clinical treatment constitute the most precious record of that treatment and are the ultimate source of data characterizing the heating session. In practice, and with currently available invasive thermometry, complete temperature distributions in vivo cannot be determined (Dunscombe et al., 1989). The state of the art is presently limited to recommending minimum procedures which could probably indicate when an appropriate hyperthermic treatment had been delivered. It remains a topic of considerable research interest to devise methods of deducing complete temperature distributions from the limited measurements possible in the clinic.

2.3.3 Treatment Planning

The selection of the optimal treatment technique is called as treatment planning. Treatment planning is fraught with difficulty. The content of available treatment machines and on the computation of the expected three dimensional temperature distribution in a patient (Dunscombe et al., 1989).

2.4 HYPER THERMIA APPLICATION METHODS

Several methods of hyperthermia are currently under study. But three methods can be distinguished in the clinical application of hyperthermia. These are known as local,

regional and whole body hyperthermia (Wust et al., 2002). In the sections that follow each of these methods is discussed in some detail.

2.4.1 Local Hyperthermia

Local hyperthermia is applied to heat a small area, such as a tumor. Different types of energy may be used to apply heat. These are including microwave, radiofrequency, and ultrasound (NCI Fact Sheet 7.3, 2004). Heating of small volumes of tumors usually up to 50 cm² in area and up to 4 cm in depth located near the surface of the body can be achieved quite easily today. The clinical experience is by Perez and Meyer with localized hyperthermia and irradiation. The majority of studies include the use of microwaves, usually at 915 MHz.

Antennas or applicators heat superficial tumours. Microwaves or radiowaves are placed on that surfaces with a contacting medium. Several types of applicators have been used clinically. These are waveguide applicators, horn, spiral, current sheet, and compact applicators, etc. (Wust et al., 2002). The main components of such a hyperthermia system are shown in Figure 2.3. The electromagnetic coupling of the applicator to the tissue is made certain by using a water bolus. The output of the power generator controls intratumoral temperature.

The resulting SAR distribution is subject to strong physical curtailment resulting in a therapeutic depth of only a few centimetres and is even further limited in regions with an irregular surface, such as the head and neck area, the supraclavicular region, or the axilla. Quality-assurance guidelines have been developed for local hyperthermia. Commercially available electromagnetic applicators (Figuree 2.4) have a typical emitting diameter of 15 cm at a frequency of 150 - 430 MHz with therapeutic depths not more than 3 cm (Wust et al., 2002).

There are several approaches to local hyperthermia. They depend on the tumor location, Local hyperthermia can be applied by external, intraluminal or interstitial methods (Yang et al., 2005), (NCI Fact Sheet 7.3, 2004).

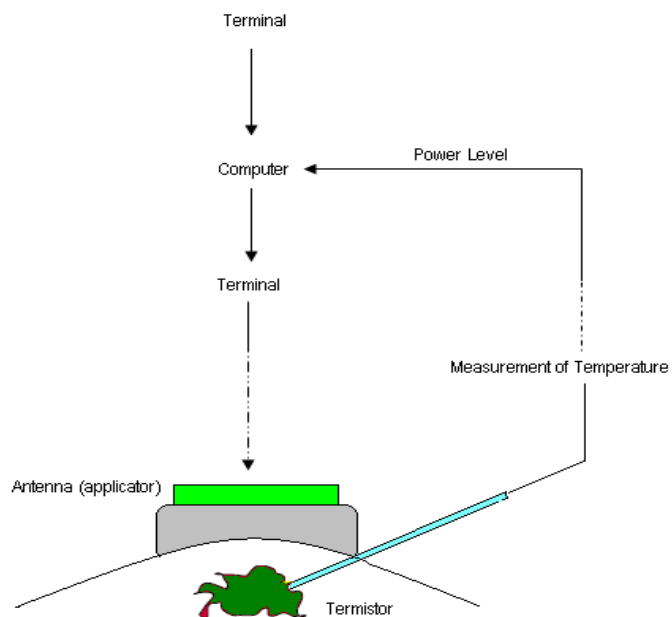


Figure 2.3 Scheme of a system for local hyperthermia (Wust et al., 2002).

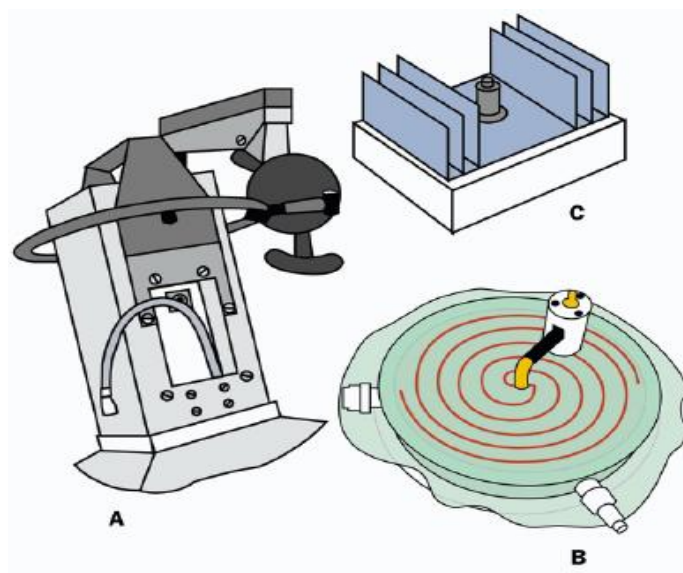


Figure 2.4 Applicator types for local hyperthermia such as (a) waveguide applicator; (b) spiral applicator; and (c) current sheet applicator (Wust et al., 2002).

Some tumors are in or just below the skin. External approaches are used to treat them. External applicators are positioned around or near the suitable region. And the tumor is exposed to energy to raise its temperature. Deep tumors within the body can be treated by using interstitial techniques, such as brain tumors. This technique is more useful than external techniques to heat tumor at high temperatures. To do this, probes or needles are used in the tumor. The probe should be properly positioned within the tumor. Imaging techniques, such as ultrasound, may be used to control it.

Local hyperthermia causes to increase the systemic temperature and absolute temperature (Yang et al., 2005). The absolute temperature increase depends on both the treatment volume to which energy is applied and the measures taken to help the patient lose energy. During hyperthermia, the tumor temperatures are increased as high as possible. And these high rates are applied as long as the tolerance limits of the surrounding normal tissues are not exceeded.

2.4.2 Regional Hyperthermia

Regional hyperthermia is a rather recent promising modality of cancer therapy based on the local heating of tumor tissue to about 44 °C usually applied in combination with radiotherapy or chemotherapy. The aim is to optimize the generated temperature distribution within the patient's body such that essentially the tumor is heated, but preferably not any sane tissue (Deufhard et al., 1997) (Strohbehn and Douple, 1984). For this reason, patient-specific treatment planning is necessary, which involves the segmentation of medical image data, the generation of geometrical patient models, and the solution of partial differential equations.

Regional hyperthermia can be applied by Deep tissue. Deep-seated tumours - eg, of the pelvis or abdomen - can be heated by arrays of antennas (Yang et al., 2005). To heat deep-seated tumors noninvasively is difficult. RF energy can be deposited into the center of the body but a large region is affected (Chou, 1988). Differential increases of blood flow in the normal and tumor tissues may result in higher temperature in tumors than normal organs. However, this temperature differential cannot be assured.

The concept behind regional hyperthermia is based on the fact that it is difficult to precisely define a tumor margin, and that the tumor may be disseminated throughout

normal tissue in given region (Strohbehn and Douple, 1984). Therefore, it is reasonable to try to heat a substantial region surrounding the known tumor volume.

The Sigma-60 applicator is a widely spread applicator (shown in Figure 2.5), which consists of four dipole antenna pairs arranged in a ring around the patient (Wust et al., 2002). Dipole antennas are schematically shown in Figure 2.5a. These external applicators are positioned around the body cavity or organ to be treated, and microwave or radiofrequency energy is focused on the area to raise its temperature. Each antenna pair can be controlled in phase and amplitude; there are restrictions in terms of the generated SAR distribution.

The major problem when using external methods such as electromagnetic applicators is that the designer only has control over the energy radiated into the tissue (Strohbehn and Douple, 1984). However, the actual temperature distribution is a function of the absorption properties of anatomical structures, thermal conductivity, and blood flow.

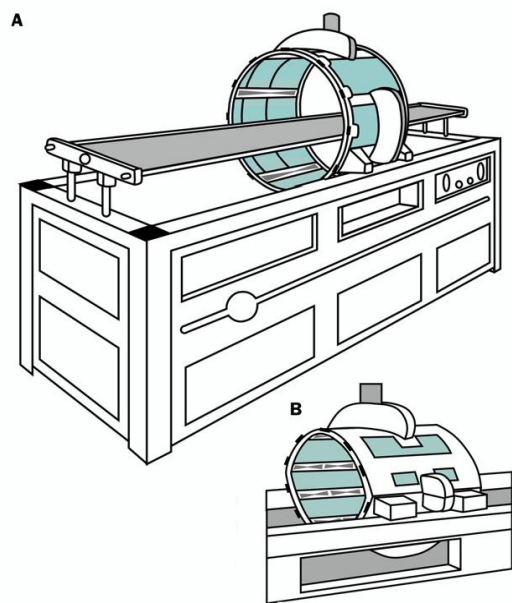


Figure 2.5 (a) Sigma-60 applicators (four dipole pairs) with treatment couch of the BSD-2000 system for regional hyperthermia. (b) A novel multiantenna applicator Sigma-Eye (12 dipole pairs) mounted on the same treatment unit as shown in (a) (Wust et al., 2002).

Regional hyperthermia is applied by perfusion of a limb, organ or body cavity with heated fluids. Deep tissue approaches may be used to treat cancers within the body, such as cervical or bladder cancer. Regional perfusion techniques can be used to treat cancers in the arms and legs, such as melanoma, or cancer in some organs, such as the liver or lung. In this procedure, some of the patient's blood is removed, heated, and then pumped (perfused) back into the limb or organ. Anticancer drugs are commonly given during this treatment.

2.4.3 Whole-Body Hyperthermia

The main expression for whole body hyperthermia is that cancer is a systemic disease and that cancer cells have in many cases metastasized throughout the body (NCI Fact Sheet 7.3, 2004) (Strohbehn and Douple, 1984). Whole body hyperthermia is one of the most efficient possibilities to treat systemic malignant diseases (Babinová et al., 1999).

For whole-body hyperthermia, several methods have been used. In whole-body hyperthermia, energy is supplied into the body, while at the same time energy losses are minimized (Yang et al, 2005).

In recent years, only radiant systems are in clinical use, with typical preheating times of 60-90 min (from 37.5 °C upwards). The Aquatherm system (Figure 2.6) is an isolated moisture-saturated chamber equipped with waterstreamed tubes (50 - 60 °C) on the inner sides, in which the patient is positioned. Long-wavelength infrared waves are emitted. A substantial increase in the skin blood circulation is induced (subcutaneous venous plexus), and energy absorbed superficially is transported into the systemic circulation. Since energy release through perspiration is blocked, the heating time is quite short (60-90 min).

The patient is positioned in a moisture-saturated cabin with hot water tubes (60°C) inside. After a systemic temperature of 41.8 °C has been achieved, the patient is thermally isolated with blankets.

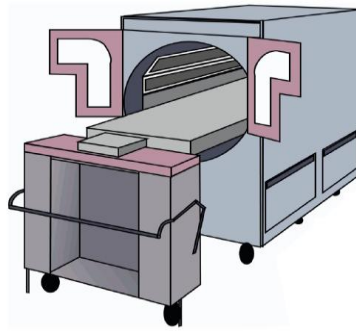


Figure 2.6 Schematic drawing of the Aquatherm system for whole-body hyperthermia (Wust et al., 2002).

The Iratherm-2000 system (Figure 2.7) uses special water-filtered infrared radiators, resulting in an infrared spectrum with a maximum near to visible light. The penetration depth in this frequency range is slightly higher (about 2 mm), but every system for whole-body hyperthermia can cause superficial overheating, resulting in thermal lesions. Water-filtered infrared radiators emit their energy from top and bottom. Thermal isolation is ensured by various transport foils. After a systemic temperature of 41.8 - 42.0 °C has been achieved, power is reduced and a steady state is adjusted.



Figure 2.7 Schematic drawing of the Iratherm system for whole-body hyperthermia (Wust et al., 2002).

CHAPTER 3

SINGULAR ANTENNA FOR HYPERTHERMIA APPLICATOR

3.1 DESIGN OF SINGULAR ANTENNA

For hyperthermia applications there are two essential problems to cope, firstly generation of heat in targeted region while keeping surrounding tissues temperature in safe limits and secondly monitoring and controlling the temperature at the targeted regions. Tumors in some areas of the body, in particular at surface locations, are relatively easy to heat with microwave or ultrasound applicators. Tumors in other locations are more difficult to bring to therapeutic temperatures, either due to their depth, inhomogeneous tissue properties, perfusion variations, irregular overlying tissue topology, or a combination of these factors. That is why the design of an effective single antenna element is needed to constructively interfere with the fields at the desired regions especially for deep regional hyperthermia applications. This represents one of the most significant challenges in hyperthermia treatment. The remedy for the first problem is to focus the fields in targeted tissues such that the fields there constructively add while in surrounding tissues not. To that end the antennas used in the system should have narrow radiation beam, small in size and frequency characteristics for enough penetration into the tissues. Typically 434 MHz at ISM band is a tradeoff frequency in terms of penetration depth and resolution considerations. The first step towards an applicator design is the development of an adequate single antenna element. The design of a hyperthermia antenna differs much from the free space applications since the antenna is radiating directly into lossy mediums, for instance the water bolus and different tissue layers, which have to be considered as antenna loads. However these conditions are constrained by inverse relationship about the electrical size of the antenna and its operating frequency. Antennas that are used in hyperthermia applications often stand inside deionized water (inside distilled water, in water capsule)

to get the better coupling of electromagnetic waves on human tissue (Gupta and Singh, 2006; Paulides et al., 2007; Ebrahimi and Attari, 2008; Juanget al., 2004; Neuman et al., 2002; Gupta and Singh, 2005; Jacobsen and Stauffer, 2002). In hyperthermia applications a distilled water bolus is used to cool the superficial heating and obtain a better matching between the antenna and the irradiated tissues.

In many applications, the microstrip antenna is chosen as a template since it has a high performance in many applications due to its lightweight, low profile with conformability and ease of integration in order systems (R. Garg et al., 2001). In the design of a microstrip antenna if a solid substrate (typically $\epsilon_r < 15$) is used then the size of the antenna is considerable huge. If a water bollus is used between the antenna and the body then most of the energy will be reflected at the interface and most of the radiation will be in lateral direction, which is strictly an unwanted situation. However if the antenna is embedded inside the water bolus and if the distilled water is considered as the merged substrate of the antenna then that will cause a considerably reduction in the antenna size with respect to its resonant frequency (M. M. Paulides, et al., 2007, R. Garg et al., 2001). In addition of the cooling of superficial tissues the antenna will also be cooled with this water bolus to sustain stable antenna characteristics during the treatment (M. M. Paulides, et al., 2007).

We examined the many antenna designs reported in the literature for our target antenna design (M. M. Paulides et al., 2007; Curto et al., 2009; Bahl et al., 1981; Andreuccetti et al., 1993; Jacobsen et al., 2005; Chen ve Chuang, 1008; Curto ve Ammann, 2006). In this context, we started with the patch antenna developed by Paulides (2007). Although we did some optimizations in this antenna, it has a very broadband radiation beam performance. Focused applicator design, that utilizes the use of a phased array system, is desirable for localized hyperthermia treatment. Many studies have been reported for different hyperthermia applicators; among them, clinically applied methods are generally based on MR techniques (M. M. Paulides et al., 2007, K. S. Cheng et al., 2010). In order to avoid superficial heating and unwanted hot spots the use of directive antennas is preferable. Our goal is to use directive antennas that will allow us to mount more antenna elements in a constrained region that will improve the efficiency of focusing. If antennas have wide radiation pattern, that will cause to increase distance between antennas. This will increase coupling between

antennas. And, that is unwanted situation. In addition, the wide radiation pattern will cause heat to build up in unwanted areas. Considering all these, we have designed a spiral antenna which embedded linear substrate strip into the water.

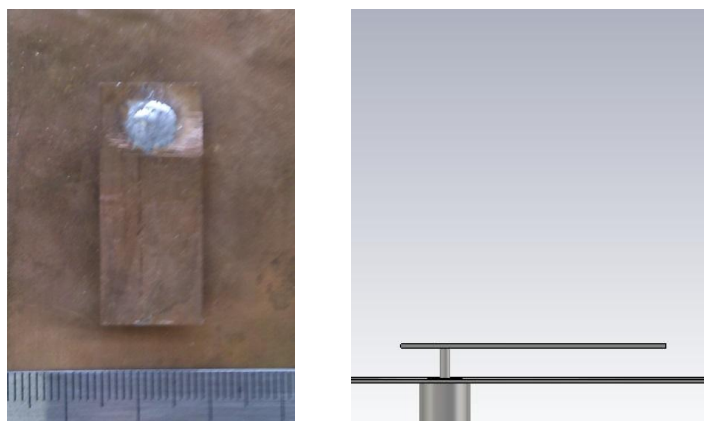


Figure 3.1 Top and Side views of the rectangular patch antenna.

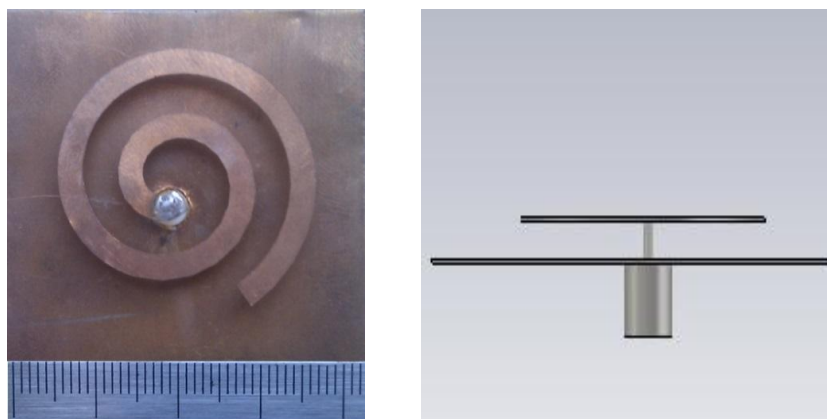


Figure 3.2 Top and Side views of the spiral antenna.

The antenna dimensions are optimized to obtain the best performance relevant to the prescribed aims. The top and side view of the realized rectangular patch and spiral antennas shown in Figure 3.1 and Figure 3.2. The antennas consist of a PEC ground plane, the spiral has two turns, the width of the microstrip is 3.25mm, the gap between the turns is 3.55 mm and the height from the antenna to the ground is 3.6mm. The

antenna is fed by a SMA connector and the inner pin of the connector has a diameter of 1.27 mm is soldered to the center of the spiral antenna. The microstrip thickness is chosen as 0.3mm to have a rigid construction since the only solid support is the inner pin. The ground has a dimension of 4.5 cm by 4.5 cm. The material properties of the deionized water at 434 MHz and room temperature are $\epsilon_r=78.4$ and the electrical conductivity $\sigma=5.55 \mu\text{S/m}$. The antenna operates only inside a deionized water bolus, in other words, both substrate of the antenna and the background environment is the deionized water. In an applicator design the water will circulate the skin to cool the possible superficial heating as well as to cool the antenna self at high powers.

The antenna sizes are optimized to reduce the size in order to have the opportunity to use more antennas for an applicator while holding the performance. The rectangular patch consist of a PEC ground plane with a patch length of 23.75mm, a width of 7.8mm, the height from the ground plane is 6mm, and it has feeding point 4.75mm from the patch's longitudinal direction shown in left side of Figure 3.1. On the other hand the spiral antenna fed at the middle has 2 turns, the width of the microstrip is 3.2mm, the gap between the turns is 3.65mm and the height from the ground is 3.4mm shown in right side of Fiure 3.2. Both antennas are fed by means of a coax having Teflon as a dielectric and the thickness of the microstrip antenna is chosen 0.65mm to have a rigid construction since the patch is not supported on a substrate but embedded in water.

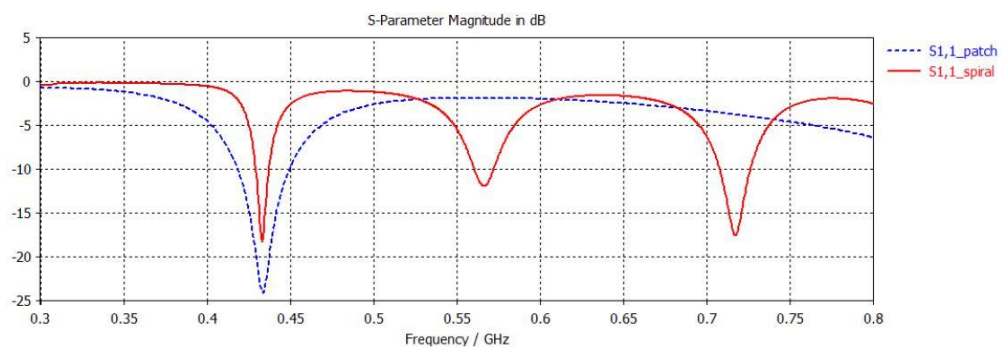


Figure 3.3 S_{11} values for patch (dashed line) and spiral (solid line) antennas.

The height of the water is chosen as 5cm assuming that will be the maximum thickness of a bolus. Although we performed simulations with different bolus thicknesses but there was not a noticeable difference in results as far as the antenna is embedded in water. The return loss values for both antennas are depicted in Figure 3.3. Both antennas resonate at 434 MHz (ISM band) with a -10 dB band width of 8 MHz for spiral and 31 MHz for patch antenna. However the spiral antenna resonates also at 567 and 718 MHz. The HPBW at $\phi = 0$ for the patch antenna is 81° and for the spiral antenna is 49° and at $\phi = 90^\circ$ for the patch antenna is 120° and for the spiral antenna is 63° . The main lobe magnitude for the patch antenna is 5.32 dB and 8.98 for the spiral antenna. At 434 MHz the spiral antenna is clearly superior to the conventional patch antenna in terms of directivity and beam width.

Antenna works completely in water, in other words, both the antenna substrate is coated with both sides of the water. It is defined multiple simulation projects and enable and disable them to fine-tune what projects need to run during the parameter sweep. S_{11} curves obtained from the parameter sweep via post-processing templates. Parameter sweep and optimisation results of the spiral antenna are shown in Figure 3.4, Figure 3.5 and Figure 3.6.

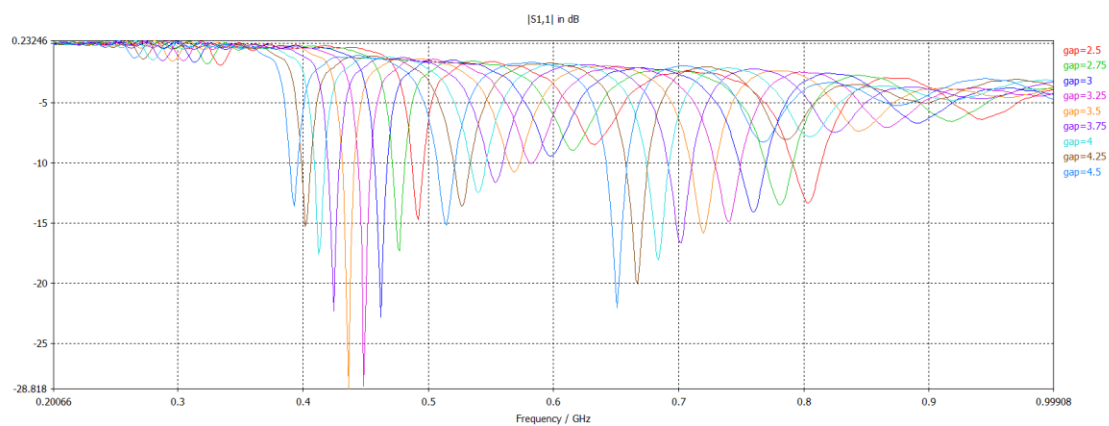


Figure 3.4 S_{11} characteristics obtained from parameter sweep for strip width of spiral antenna.

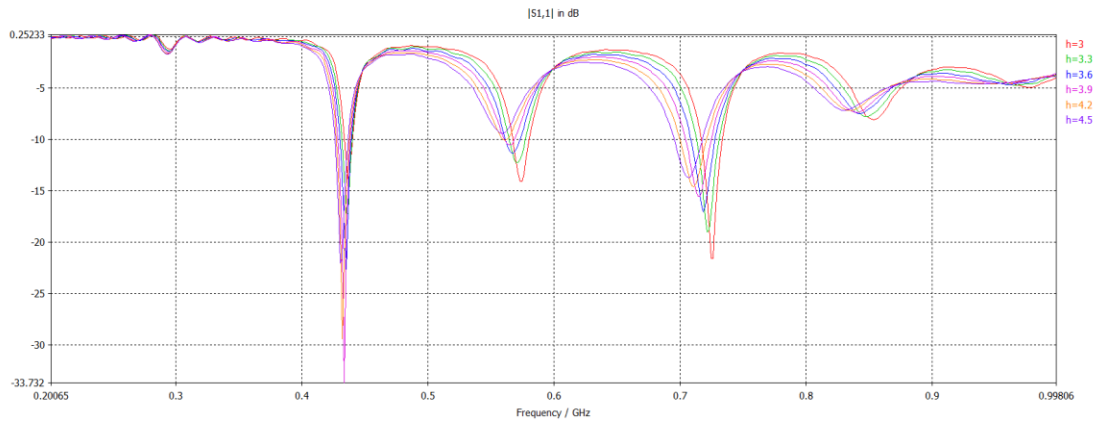


Figure 3.5 S_{11} characteristics obtained from parameter sweep for height of spiral antenna.

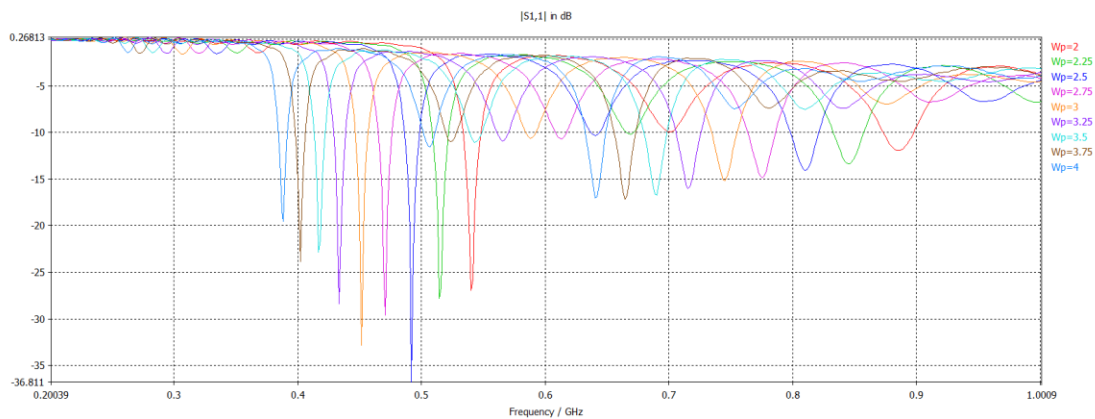


Figure 3.6 S_{11} characteristics obtained from parameter sweep for width of spiral antenna.

Both the design and simulation of the antennas are performed with CST Microwave Studio software by means of commercial electromagnetic simulation software, which uses finite integration technique in time domain as a solver. The main parameters that are influencing the resonating frequency are the width of the microstrip and the gap between the strips. Keeping the overall size constant we obtained for different ratios of these two parameters the similar resonating frequencies whereas at the proposed ratios the beam width is narrowest. For the measurements a vector network analyzer of Anritsu Vectorstar MS4642A is used. The simulated and measured return loss values inside a water bolus for the spiral are depicted in Figure 3.8 and for

the patch in Figure 3.7. A very good agreement has been obtained between the measured and simulated results both for the spiral and patch antenna, nevertheless, the software underestimates the performance of spiral antenna slightly for 566 and 716 MHz frequencies.

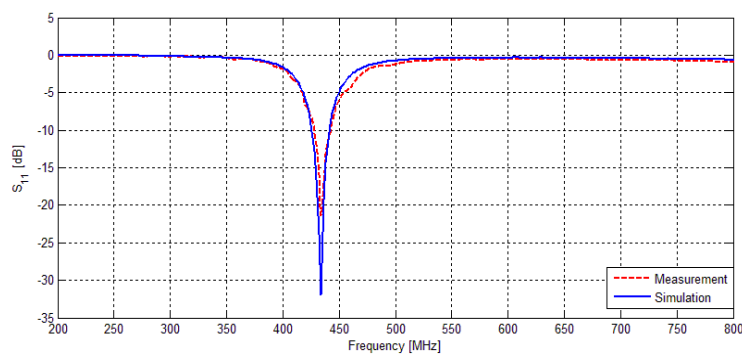


Figure 3.7 Simulation (solid line) and measurement (dashed line) S_{11} values for patch antenna.

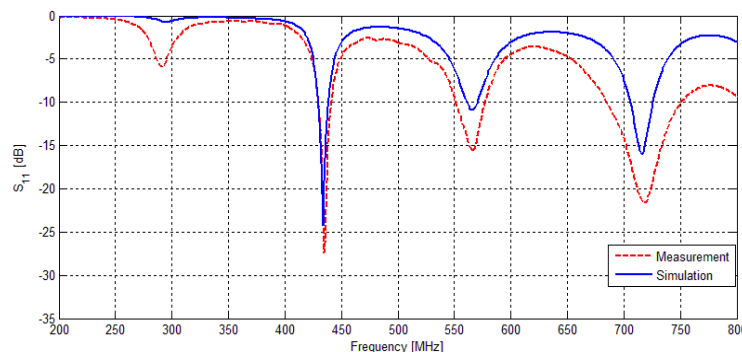


Figure 3.8 Simulation (solid line) and measurement (dashed line) S_{11} values for spiral antenna.

In antenna design, one of our most important goals is a narrow beamwidths of radiation pattern. Although we take the data with simulation results of the radiation pattern, we want to confirm them with measurement results. For this purpose, we form the proposed measurement setup is shown in Figure 3.10 for the first time in the literature. To conduct the radiation pattern measurements we filled a circular basin with

deionized water and constructed a measurement setup as depicted in Figure 3.10. The wavelength at 434 MHz inside the deionized water is $\lambda = \lambda_0 / \sqrt{\epsilon_r} = 78\text{mm}$, where λ_0 is the free space wavelength. Taking into account the far field formula the required minimum distance is $d = 2D^2 / \lambda \approx 25\text{mm}$. Hence a distance about 15cm in the measurement setup is set between the antennas. The spiral antenna is mounted to a rod and positioned at the middle of the basin and rotated manually by 5° steps. We used two additional low loss coax cables as an extension to the expensive calibration cables for the connection of the antennas in water and did perform the calibration taking into account the extended parts. We also used the time domain option of VNA to reduce the environmental noise. The comparison between the simulation and measurement results are depicted in Figure 3.11. Despite not having an ideal radiation pattern measurement setup like an anechoic chamber in free space measurements a good agreement is obtained. The small discrepancies in the measured results is probable mainly due to the manually rotation of the antenna. The half power beam width (HPBW) of the spiral antenna is smaller than 65° for each plane. Another reason to choose a spiral antenna is that it resonates at multiple frequencies. The radiation pattern of spiral antenna at 566 MHz is even narrower than at 434 MHz while at 716 MHz some distortion occurs (Figure 3.13). The simulated radiation pattern of the patch antenna is depicted in Figure 3.14. The HPBW for the patch antenna is 75° at $\phi = 0$ plane and 107° at $\phi = 90^\circ$ plane. These values are significantly greater than the spiral antenna results. The polarization of the spiral antenna shown in Figure 3.9 has right hand circular polarization (actually slightly elliptical) observed through simulations.

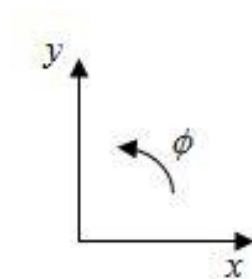


Figure 3.9 The polarization of the spiral antenna.

In case of designing an applicator the robustness of the single antenna element is important. However in our design the antenna does not have a solid substrate and the only support is the inner pin of the connector makes the antenna vulnerable. As a remedy, e.g., at three points small thin plastic pins are fixed as a support between the spiral and the ground. A slight shift in the operating frequency is observed both in the measurements and simulations. Fortunately, that shift can easily be taken into account by including the support pins in the design to set the operation at the desired frequency.

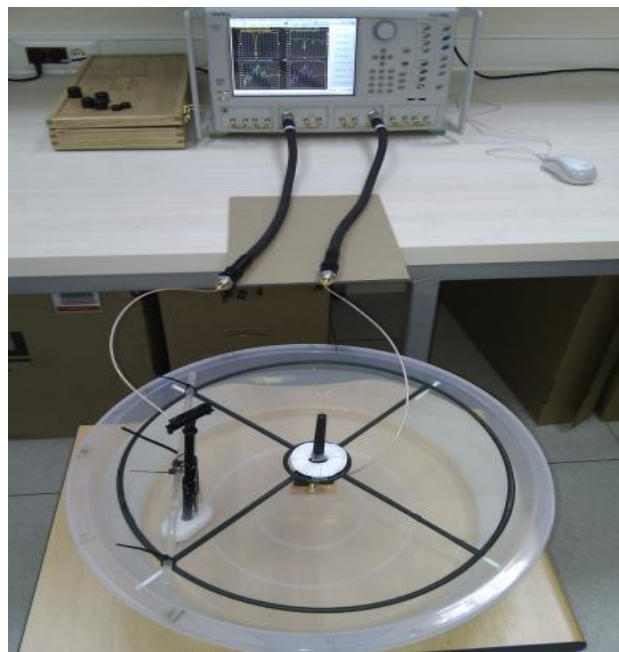


Figure 3.10 Measurement setup for manual radiation pattern measurements.

In order to investigate the performance of the antenna in presence of tissues we performed simulations with a simplistic homogeneous model of 15 cm x 15 cm area with a thickness of a 1 mm skin, 5 mm fat and 100 mm muscle taking into account the material properties at 434 MHz. The antenna should be located as close as possible to the skin in order to transfer maximum power while the antenna characteristics should remain unaltered. The S_{11} parameters of the spiral antenna with altering the water bolus thickness between 10-50 mm are depicted in Figure 3.16. Results show that the antenna reflection coefficient values are slightly shifted for 10-20 mm and at 30 mm the optimum distance is obtained. This is perceptible since the minimum far field distance

is about 25 mm. In addition we put electric field monitors at the axial cross section of the antenna to monitor the radiation behavior into the tissues. We observed similar radiation behavior (at other water bolus thicknesses as well as other cross section) as in water bolus without the tissues both for the spiral and patch antenna. The narrow radiation beam of the spiral antenna into the tissues apparently shows the adequateness of the single antenna element for a possible applicator design.

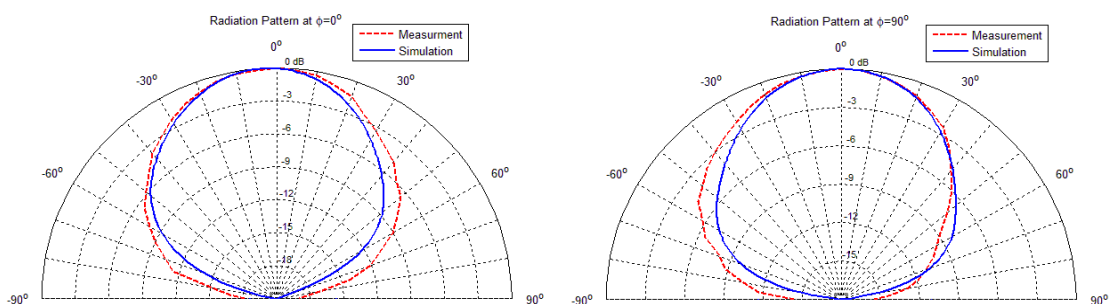


Figure 3.11 Simulated (solid line) and measured (dashed line) radiation patterns of spiral antenna at 434 MHz: for $\phi = 0$ plane (left) and $\phi = 90^\circ$ plane (right).

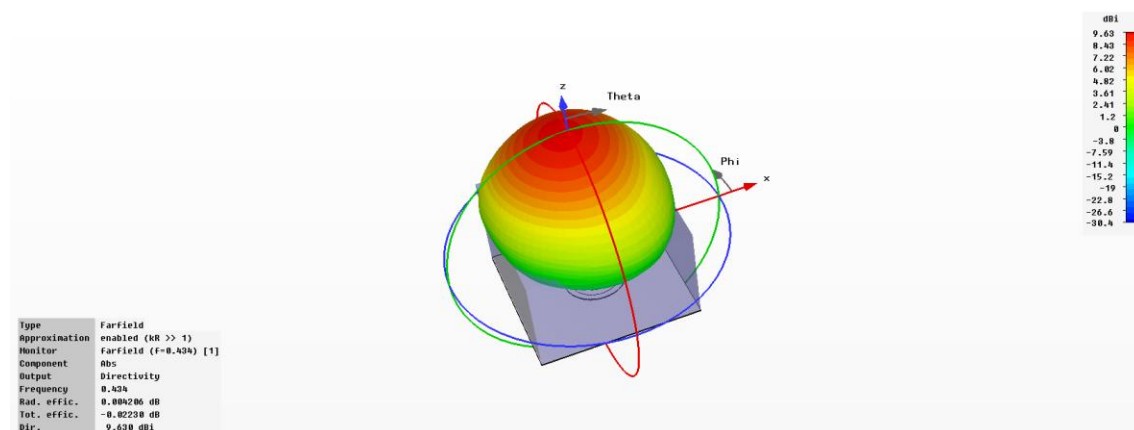


Figure 3.12 Three dimensional radiation pattern of spiral antenna at 434 MHz.

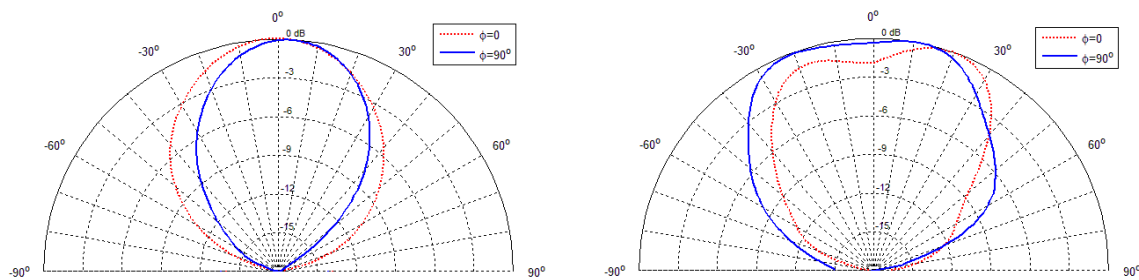


Figure 3.13 Simulated radiation patterns of spiral antenna at 566 MHz (left) and at 716 MHz (right).

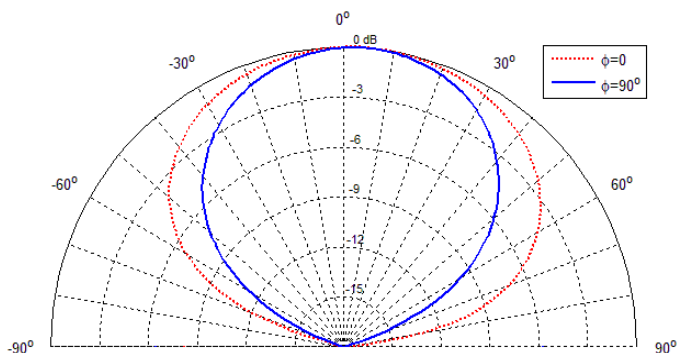


Figure 3.14 Simulated radiation patterns of patch antenna at 434 MHz.

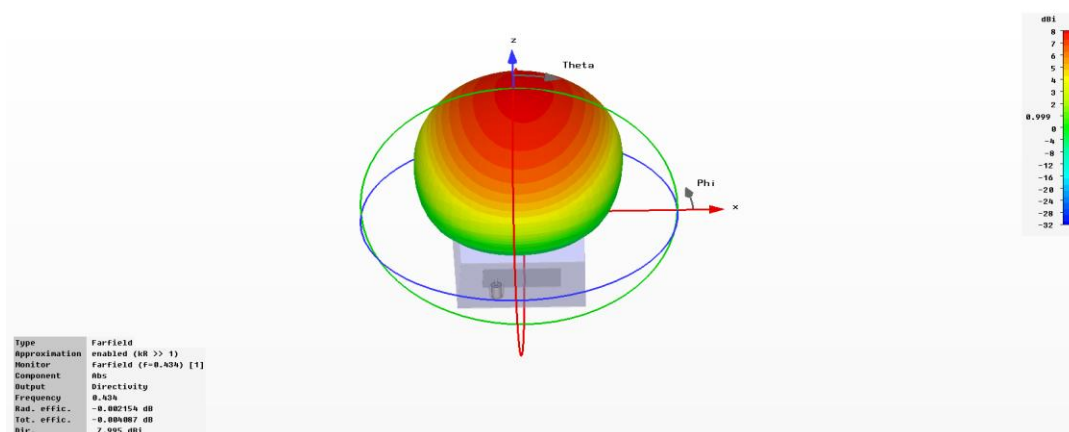


Figure 3.15 Three-dimensional radiation pattern of patch antenna obtained by simulation.

Despite the frequency and occurrence of very small slip in such a case parameters can be optimized easily and precisely considering the design of support legs. Another issue that should be mentioned is 9.7 dB the spiral antenna of the simulation results occurred profits and emission efficiency (radiation efficiency) is -0.0074 dB in other words, it is 98.3%.

Considering the antenna designs in literature (Alomainy A. et al., Xu S. et al. 2006) the focus of the studies are to heat the whole region instead of a focused smaller region. The reason for that is to use the applicator in conjunction with conventional methods like chemo and radio therapy and to reduce the uncertainty in the imaging of the infected region. That is why in their designs the narrow radiation beam was not preferred. Fortunately the advancement in the imaging technology, the hardware and software capabilities of the electromagnetic simulation tools promise now to focus the heat on a smaller region.

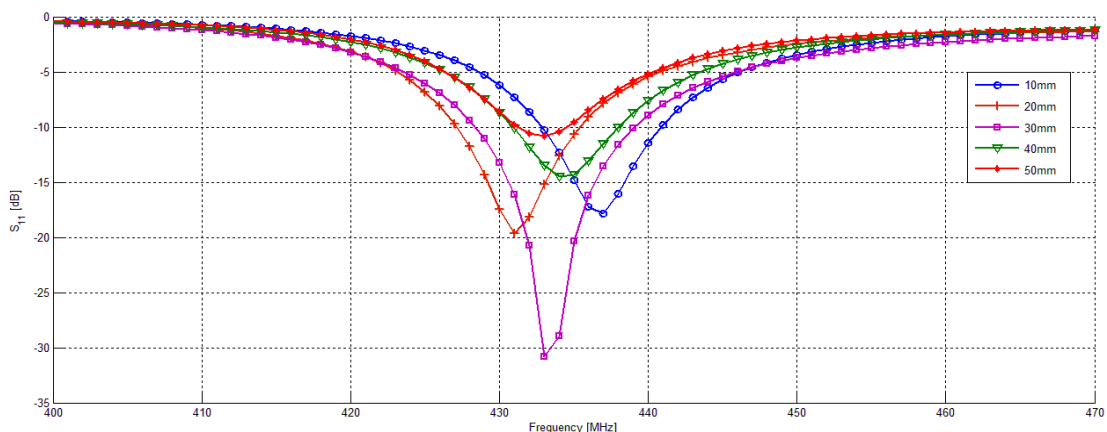


Figure 3.16 S₁₁ values for spiral antenna at different water bolus height.

CHAPTER 4

TISSUE MIMICKING GEL CHARACTERIZATION

4.1 INTRODUCTION

The application of electromagnetics in medicine have an increasing importance due to the need to develop, optimize and test with new equipments and techniques. To test and verify the proper functioning of such developed equipments human or animal subjects such as dogs, rats and rabbits can be used. However, using human subjects would require adhering to very strict regulations enforced by Food and Drug Administration (FDA) (C. Furse, 2000, K. Fukunaga, 2004). Using animal subjects, on the other hand, is very costly and required facilities (E. Zastrow, 2008). The logical route to follow would be to use tissue that mimicks and simulates materials in the design process, followed by using animal subjects, and finally after meeting the safety assessment requirements testing devices on humans (C. Gabriel et al., 1996). While Characterizing the tissue mimicking material is important to investigate the interaction between biological tissues and electromagnetic waves. Interactions of electromagnetic fields with the human body are, amongst other factors determined by the dielectric properties of tissues and cells (T. Yilmaz et al., 2008). Tissue-mimicking phantoms should be in solid form, approximate the electrical properties of the intended tissues and should not be interact with one another.

In this study, materials that mimic the relative dielectric constant and conductivity of human tissue are proposed. To this end, soft tissue simulating materials (skin, muscle fat and cancerous tissue) is presented. Here we propose, skin, muscle, fat and cancerous tissue mimicking gels for ISM band. Both relative dielectric constant (ϵ_r) and conductivity (σ) of the skin, muscle and fat mimicking material were successfully

matched with real human skin, muscle and fat for ISM band. DGBE (Diethylene glycol butyl ether), Triton X-100 (polyethylene glycol mono phenyl ether), NaCl, De-ionized water and oil are used to formulate the desired gels. The electrical properties of the resulting materials were measured with SPEAG Dielectric Assessment Kit DAK-3.5 dielectric probe kit and Anritsu Vectorstar MS4642A network analyzer.

4.2 CHARACTERIZATION OF MUSCLE MIMICKING MATERIAL

The muscle mimicking gel is characterized by mixing DGBE, Triton X-100, de-ionized water, and NaCl. To characterize the appropriate tissue mimicking gels, electrical properties of each ingredient were measured and the effect of electrical properties to one-another was investigated. Figure 4.1 and Figure 4.2 show orderly relative dielectric permittivity and conductivity of pure Triton X-100, DGBE and deionized water. The DGBE and Triton X-100 have low dielectric constant and conductivity compared to water. Although the same electrical properties can be obtained just by mixing Triton X-100, de-ionized water, and NaCl, a non-homogeneous mixture was formed that contained air bubbles because of the viscose nature of Triton X-100. To formulate a more homogeneous mixture, DGBE is used to solve Triton X-100. Then the de-ionized water and NaCl are added to the obtained solution. Human muscle has higher conductivity when compared to human skin and fat; therefore, NaCl is added to increase the conductivity of the obtained solution (C. Furse, 2000, Tuba Yilmaz et al., 2008).

The percentages of each ingredient in the mixture for ISM band are given in Table 4.1. The electrical properties of human muscle for ISM band is $\epsilon_r=52.791$, $\sigma= 1.705$ (E. Zastrow, et al., 2008, K. Fukunaga, et al., 2004). The measured electrical properties of formulated muscle mimicking gel for ISM band is $\epsilon_r=52.85$, $\sigma=1.68$.

Good agreements obtained between measured data and the reference (E. Zastrow et al., 2008). Figure 4.3 shows the order of mixing the components for the muscle tissue equivalent model. Note that electrical properties of muscle mimicking material, which is characterized, measured from 0.1 to 3 GHz and the results are shown in Figure 4.5 and Figure 4.6.

Table 4.1 Recipes for Muscle Mimicking Gels for ISM Band.

Ingredients	ISM Band
De-ionized Water	72.6
Triton X-100	18.8
DGBE	8.6
NaCl Salt	690 gr

4.3 CHARACTERIZATION OF SKIN MIMICKING MATERIAL

The skin mimicking material is characterized by mixing DGBE, Triton X-100, de-ionized water, and NaCl. As shown in Figure 4.1, DGBE and Triton X-100 have a low relative dielectric permittivity and electrical conductivity in particular high frequency. Triton X-100 in deionized water is used to reduce the relative dielectric constant and the conductivity. Triton X-100 is insoluble in pure deionized water. Adding DGBE to Triton X-100 reduces the viscosity of the mixture and allows Triton X-100 to be combined better with deionized water. Table 4.2 shows concentrations of the various ingredients, which create the skin tissue equivalent model specified.

Table 4.2 Recipes for Skin Mimicking Gels for ISM Band.

Ingredients	ISM Band
De-ionized Water	67.6
Triton X-100	28.4
DGBE	4
NaCl Salt	620 gr

When combining the materials that will form the mixture it is important they are mixed in the correct order. First of all, Triton X-100 and DGBE are mixed to reduce of the viscosity of the mixture. To avoid formation of air bubble, de-ionized water is added by using a stirrer. On behalf of correct measurement of the electrical properties, it is

important not to form air bubbles in the mixture. NaCl is added up to get desired relative dielectric permittivity and electrical conductivity. Due to the nature of its components DGBE the foam layer is formed on the surface at the end of mixture process. This layer was cleaned surface not to influence the measurement results.

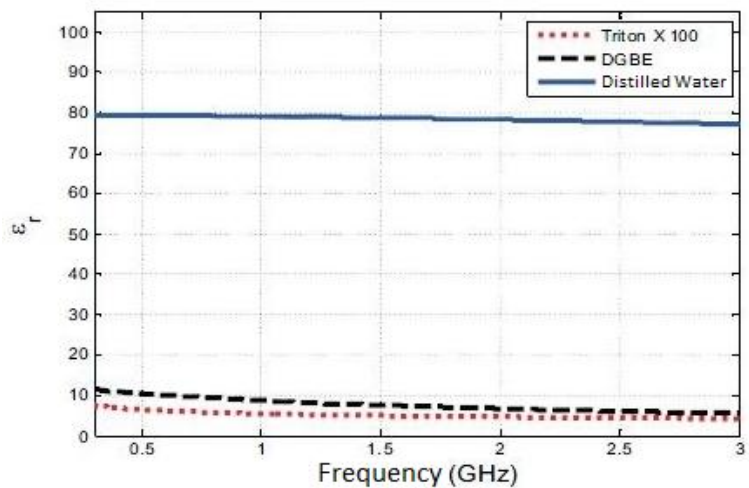


Figure 4.1 Relative dielectric permittivity comparison of Triton X-100, DGBE and deionized water.

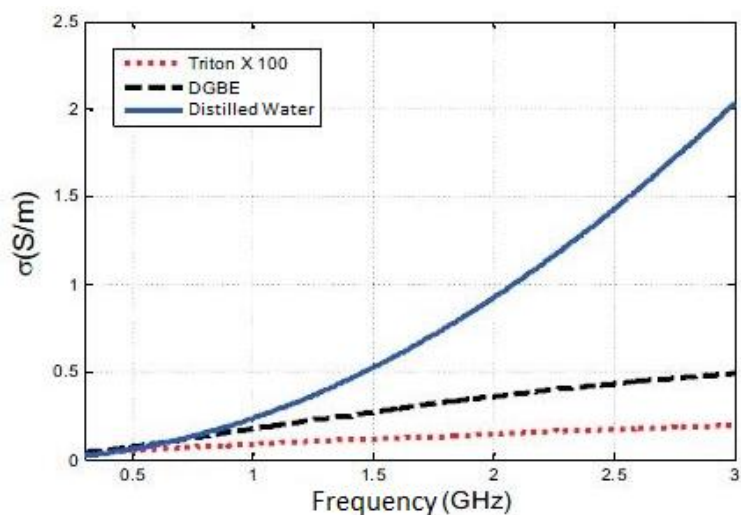


Figure 4.2 Conductivity comparison of Triton X-100, DGBE and deionized water.

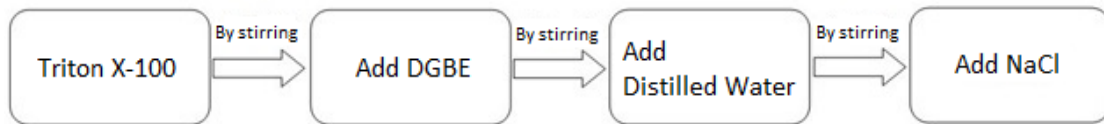


Figure 4.3 Process of preparing muscle and skin mimicking materials.

Measurement set-up for electrical property measurement is shown in Figure 4.4. Electrical properties of the skin equivalent model characterized in that measured 0.1 to 3 GHz and the results shown in Figure 4.5 and Figure 4.6. Obtained results compared with reference data mentioned and small differences correspondingly similar results were obtained. Figure 4.3 shows the order of mixing the components for the skin tissue equivalent model.

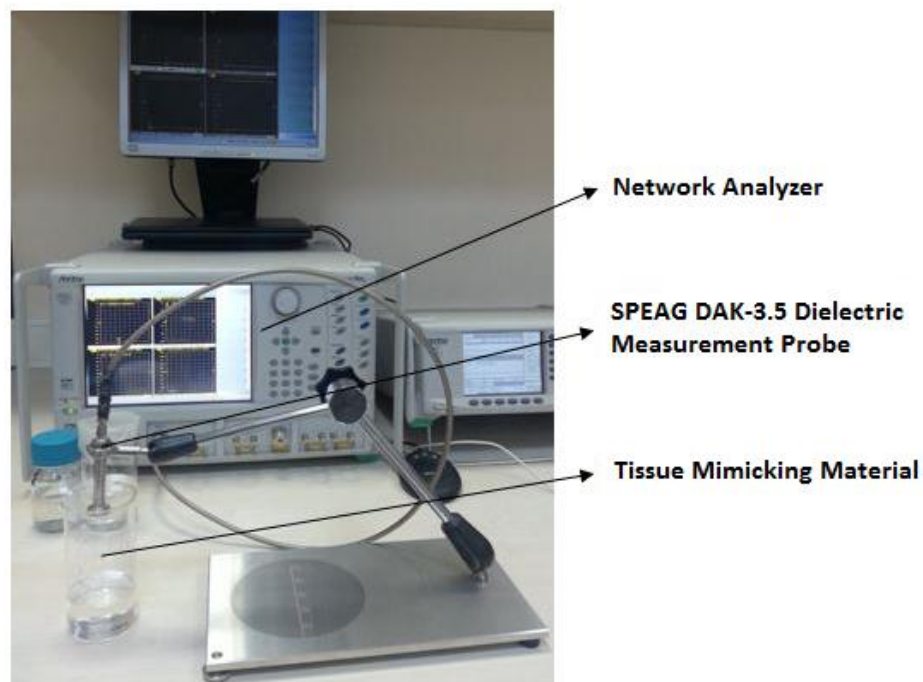


Figure 4.4 Measurement set-up for electrical property measurement.

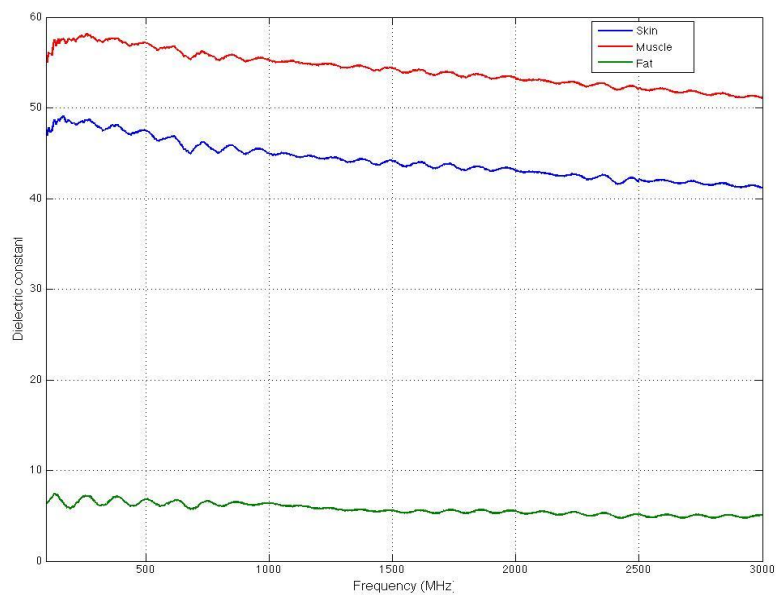


Figure 4.5 Comparison of relative dielectric permittivity of characterized skin, muscle and fat mimicking gel at room temperature.

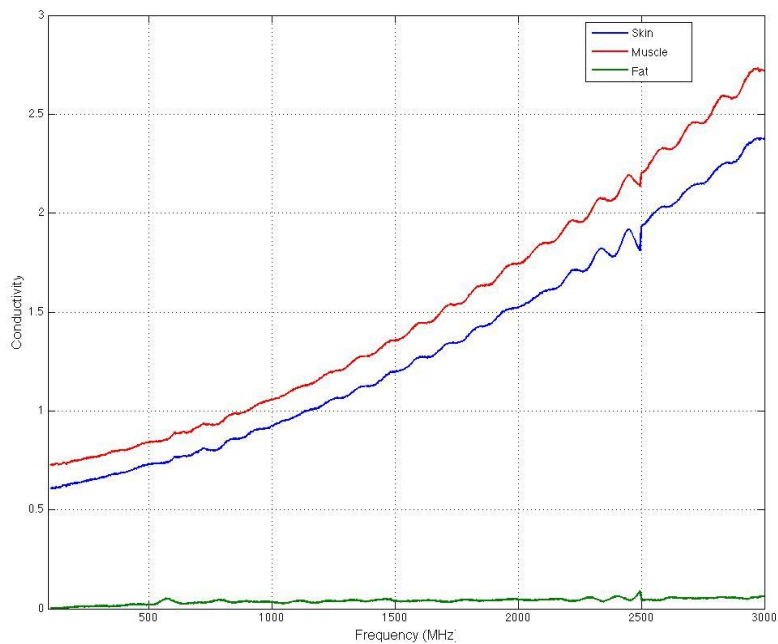


Figure 4.6 Comparison of Conductivity of characterized skin, muscle and fat mimicking gel at room temperature.

4.4 CHARACTERIZATION OF FAT MIMICKING MATERIAL

Human fat, as a low water content tissue, has very low electrical properties. The process of preparing fat mimicking material is shown in Figure 4.7. Sunflower oil and Triton X-100 were combined in order to obtain approximate electrical properties of human fat in ISM band. The percentages of each ingredient in the mixture ISM bands are given in Table 4.3.

We encountered difficulties with this mixture because the mixture of oils and other liquid chemicals are difficult to combine. The percentages of each ingredient in mixture for ISM band are given in Table 3.3.



Figure 4.7 Process of preparing fat mimicking material.

Characterized fat mimicking material's electrical properties are compared with reference data obtained from (Gabriel et al, 1996) at 434 MHz. We obtained good agreement between the data available in literature and measurements. However, it was observed that the reference data didn't comply with the desired frequency of the dielectric constant (supposed to be around 5,5-4,85). By changing the mixing ratio when we obtain the target relative dielectric permittivity, conductivity, the rates would remain low. Adding salt, it was not possible due to lack of electrical property increase mixture. The electrical properties of fat mimicking material, which is characterized, as being measured from 0.1 to 3 GHz and the results are shown in Figure 4.5 and Figure 4.6. Electrical conductivity and relative dielectric permittivity of fatty equivalent tissue model the change at the room temperature depending on time and with the results of reference, values change depending on the implementation of +4 degrees has not yet completed an overlap.

Table 4.3 Recipes for Fat Mimicking Gels for ISM Band.

Ingredients	ISM Band
Oil (%)	38,5
Triton(X-100) (%)	61,5

4.5 CHARACTERIZATION OF CANCER TISSUE MIMICKING MATERIAL

The most important feature of cancer tissue compared with healthy tissue is that of the higher electrical conductivity rate within the cancer tissue. In regards to breast cancer tissue, it is impossible to make a literal equivalent tissue because the dielectric constant needed from breast cancer tissue vary according to the content of the tissue (Lazebnik et al., 2007). Therefore, we compiled a mixture of deionized water and salt sufficient to use in measurements. The electrical property of equivalent models of the breast cancer tissues are characterized measured from 0.1 to 3 GHz; results are shown in Figure 4.8 and Figure 4.9. The percentages of each ingredient in mixture for ISM band are given in Table 4.4.

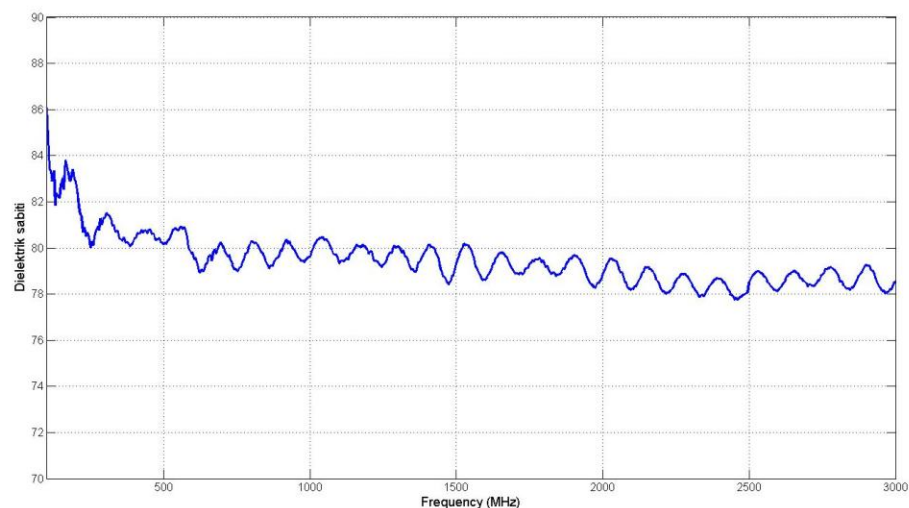


Figure 4.8 Relative dielectric permittivity of characterized breast cancer mimicking gel at room temperature.

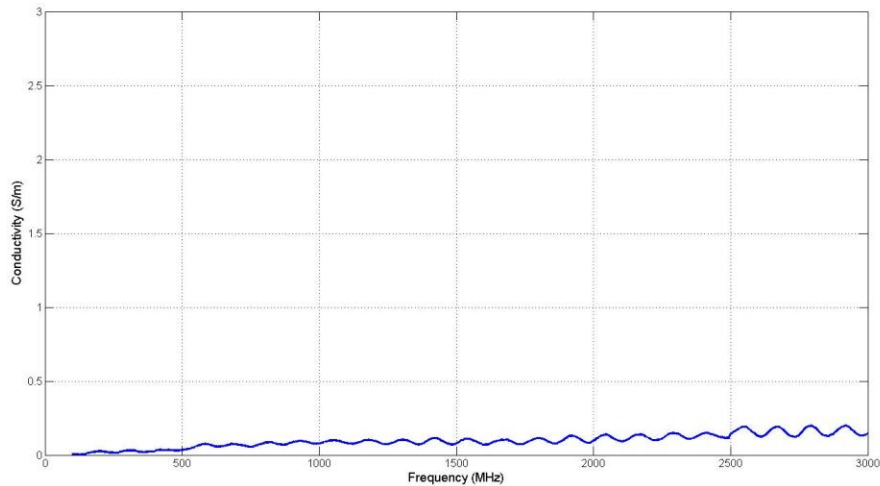


Figure 4.9 Conductivity of characterized breast cancer mimicking gel at room temperature.

Table 4.4 Recipes for Cancerous Tissue Mimicking Gels for ISM Band.

Ingredients	ISM Band
De-ionized Water	41.6
Triton X-100	47.2
DGBE	11.2
NaCl Salt	1540 gr

Also, in order to find out how long the equivalent tissue can be used and daily measurements were observed. In lieu of our observations we began taking measurements at different times, relative dielectric permittivity and conductivity in the ISM band on different days and their values were recorded and graphs were drawn over time. The electrical conductivity and relative dielectric permittivity order are shown in Figure 4.10 and Figure 4.11 according to the changes at room temperature over time. The model of +4 degrees, depending on the time changes is in Figure 4.12 and Figure 4.13. Characterized mimicking material's electrical properties are compared with reference data obtained (Gabriel et al, 1996) at 434 MHz. We obtained good agreement between the data available in literature and measurements. As a result, we observed that the electrical properties of real human tissue and characterized mimicking materials

matched in the ISM band. So, our models can be used in ISM band to investigate electromagnetic waves with interaction with human tissues. The advantages of the proposed model are listed such as:

- It contains only a few components.
- Mixing of the materials is not cost-effective.
- It must have a very simple procedure.
- To do characterization, very detailed steps and expensive facilities are not required

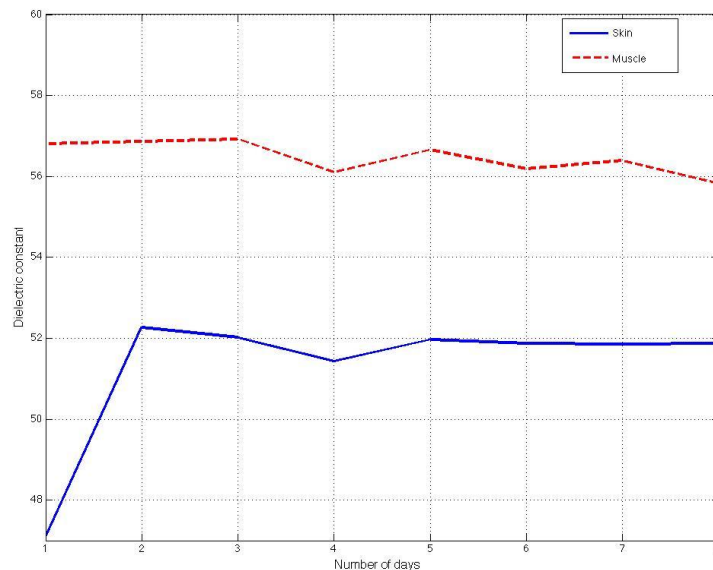


Figure 4.10 Relative dielectric permittivity changes of skin and muscle mimicking materials at room temperature.

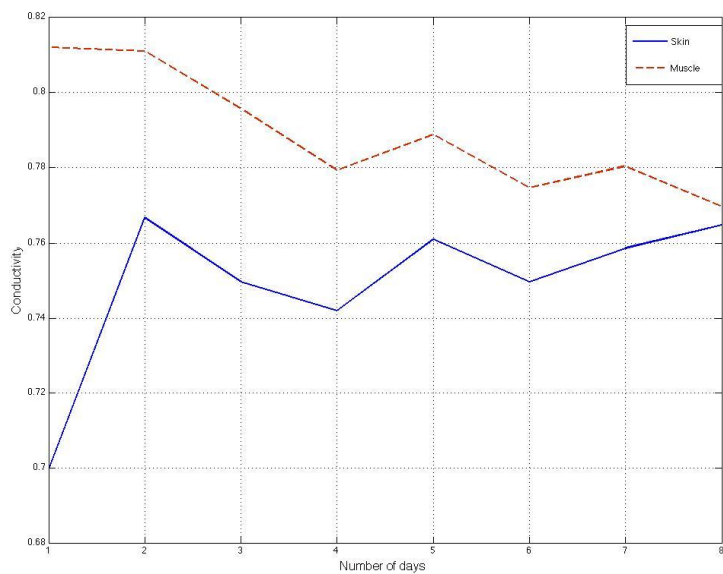


Figure 4.11 Conductivity changes of skin and muscle mimicking materials at room temperature.

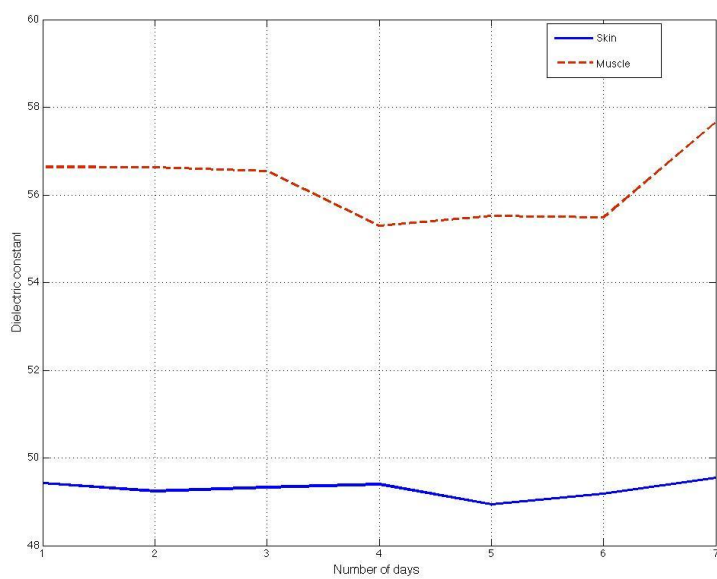


Figure 4.12 Relative dielectric permittivity changes of skin and muscle mimicking materials at +4 °C.

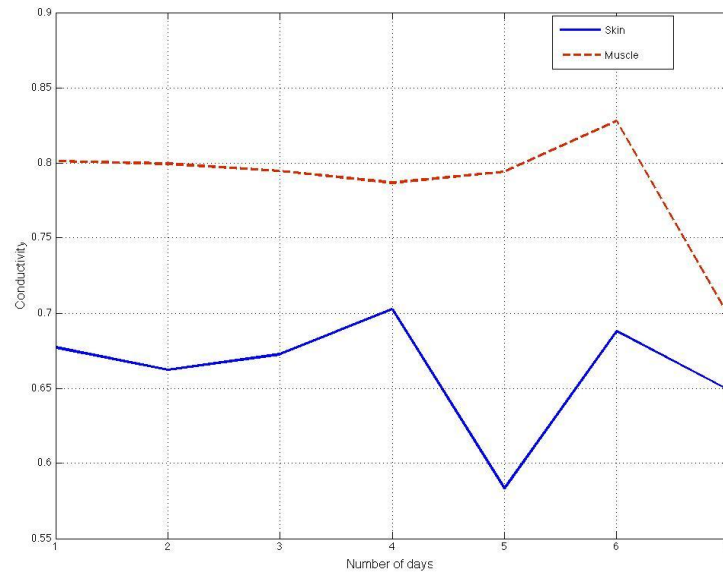


Figure 4.13 Conductivity changes of skin and muscle mimicking material at +4 °C.

In this study, two different tissue mimicking gels are characterized for in vitro testing of dual band implantable antennas. To formulate the muscle mimicking gel, DGBE, Triton X-100, de-ionized water, and NaCl were used. The fat mimicking gel is composed of DGBE, Triton and oil mixtures at several percentages. There is discrepancy between the conductivity of fat mimicking gel and the reference data for ISM band. Note that all measurements performed with Anritsu MS4342 network analyzer and SPEAG Dielectric Assessment Kit DAK-3.5 probe. We are currently searching for an alternative material that has lower conductivity to mimic human fat for ISM band. Also, we observe that these materials will not decay over time and they do not require refrigeration.

CHAPTER 5

HYPERTHERMIA APPLICATOR DESIGN

5.1 FORMING A MODEL OF HUMAN TISSUE

The electromagnetic interaction calculations in human tissues is mostly realized by finite difference time domain method (FDTD) due to be suited for simulating non-homogeneous models, scales well with the resolution increase, implicitly incorporates coupling between models and the antenna can be implemented in hardware accelerator (Taflove A. et al., 2005, ESHO Taskgroup committee, 1992). From the calculated electromagnetic field values specific absorption rate (SAR) can be calculated within the tissues. Finally by using of these values in Penne's bio-heat equation the temperature distribution can be calculated. Depending to the results the therapy and the time can be determined. In order to calculate electromagnetic interactions in tissues with simulation programs initially, it must be form a human-tissue model. The first premise of our work, we have formed a model of the leg. During forming model, real cross-sections of the human body are used to form leg model by using commercial program AutoCAD by doing interpolation. These slices have been taken from the "visible human project" data set representing an internationally known anatomic base (Visible Human Server). The leg model is attained by extrapolating of two dimensional leg slices.

Experience that we gained from the first of these geometric models created with limited resources person on the possible hosting of hyperthermia therapy in a specific application making the tissue model with commercial software such as AutoCAD is very difficult. Therefore, the availability of commercial software projects were planned in advance from computer tomography (CT) images of tissues capable of segmentation as ISEG. It has become a major problem in the tissue modeling. However, we were able to continue without interrupting our work with standard tissue models because it cannot

host the shape of individualized treatment currently this project with our content. In this context, we have obtained that ISEG software company owner of SPEAG of academics that they have prepared for eight people of different ages and different human tissue models in size. In addition to these models SEMCAD simulation programs can be integrated seamlessly. The models cannot be changed, such as the electrical properties of tissue at the desired frequency did not allow any changes because these models are not in STL format and they are given as voxel. In addition, the models couldn't be integrated in the CST.

When we have considered the ability to do the applicator for a type of cancer, we have decided to design an applicator for breast cancer to evaluate our experiences in light of their literature studies. In the treatment scenario with an applicator, the patient will lie face down on a table, the breast will hang down a space on the table and it will in the applicator placed in deionized water. In this context, the model of the breast hanging down segmentation was needed. The parts of the breast was and extremely flattened for the virtual family models were formed facedown or back onto and they were unable to use our modeling. Even if we want to form the computer tomography (CT) images that we have obtained from hospital we had trouble to create the model it is also taken to the flattened breast images. However, relatively more homogeneous and easier anatomical structure of the breast tissue in other regions of the tissues (see Figure 5.1) was an obstacle for us to design our models with the software CST. So, we have designed a breast model which is used in our study. It is shown in Figure 5.2.

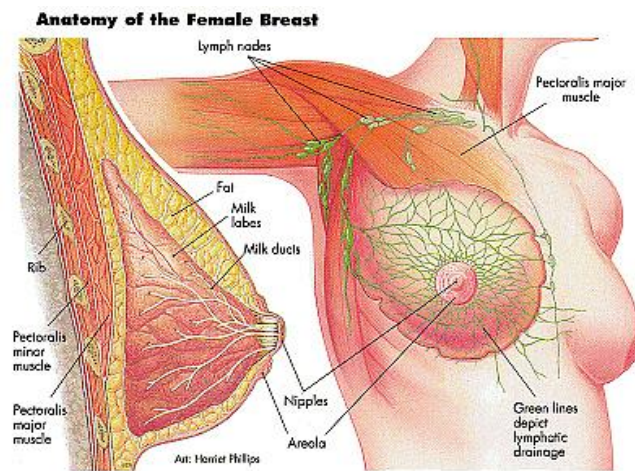


Figure 5.1 Female breast anatomy.

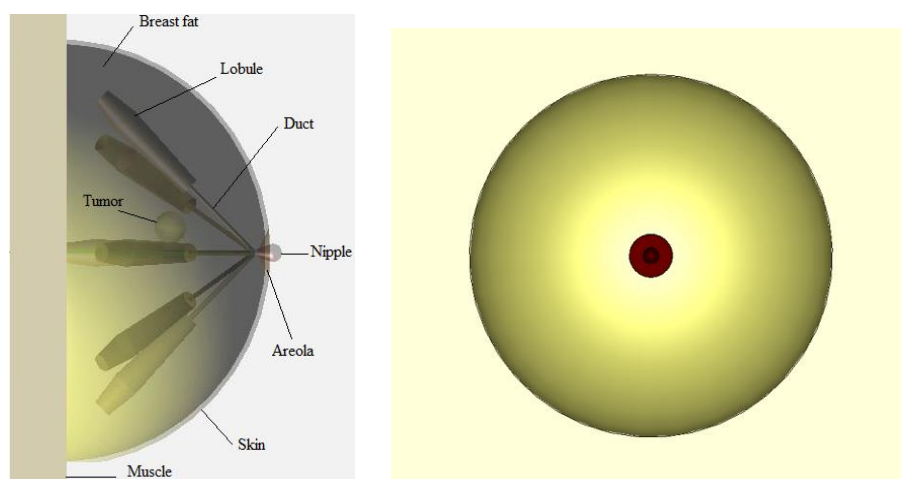


Figure 5.2 Side and top view of the breast model intended to be used in the simulation program.

5.2 APPLICATOR DESIGN

The suitability of singular antenna to be used in the design of the applicator for a specific type of cancer needs to be analyzed in more detail. The single antenna elements used for the applicator are the conventional patch antenna and the circularly shaped microstrip spiral antenna both use distilled water as substrate. The Half power beam width (HPBW) at $\phi=0^\circ$ for the patch antenna is 81° and for the spiral antenna is 49° and at $\phi=90^\circ$ for the patch antenna is 120° and for the spiral antenna is 63° . For the design details the reader is referred to look at (E. Korkmaz et al., 2014). Figure 5.5 shows the electric field lines for the patch antenna embedded in 5 cm water bolus radiating towards the tissues consist of 1 mm skin, 5 mm fat and a muscle layer at the two cross-sectional radiation planes as shown in Figure 5.3. In Figure 5.4 the electric lines depicted for spiral antenna under the same conditions. Both antennas are operating at 434 MHz. There was only about 2 MHz shift in return loss of the antennas with tissues loading.

In order to observe the radiation characteristics with using of two antenna types a simplified head phantom from CST library is used. In this model a 2cm diameter sphere in the middle of the head is added at the antenna height positions. The aim is to observe

the differences in the electromagnetic field distribution in head in a multi-antenna system. For this reason only four antenna elements is positioned and a phase correction to obtain focusing is not performed. The phantom covered with antenna elements embedded inside a water bolus is depicted in Figure 5.6. We positioned the antennas in two positions with respect to their radiation patterns at $\phi=0^\circ$ and $\phi=90^\circ$ along the azimuth of head phantom. The mutual coupling between the antennas was about -35 dB or lower for the broad radiation angle positioning and -45 dB or lower for the narrow radiation positioning of the patch while for the spiral antenna it was for all cases lower than -50 dB. Figure 5.8 shows the cross section of laterally normalized electric field distribution (left) and longitudinal cross sectional view of SAR distribution (right) when the patch antenna is positioned at the broad radiation angle.

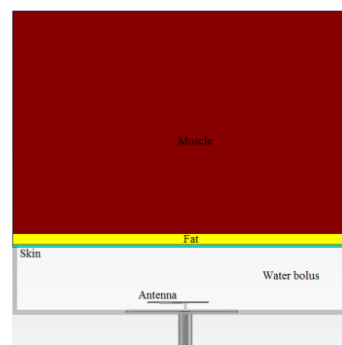


Figure 5.3 Spiral antenna model inside a water bolus (3cm) with tissues of skin, fat and muscle (left)

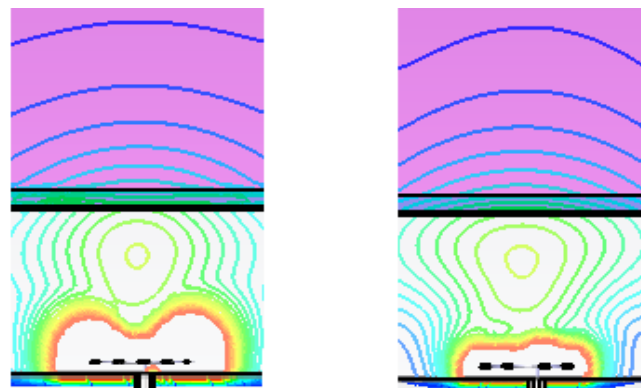


Figure 5.4 Electric field lines of spiral antenna into tissues at $\phi=0^\circ$ and $\phi=90^\circ$ planes at 434 MHz.

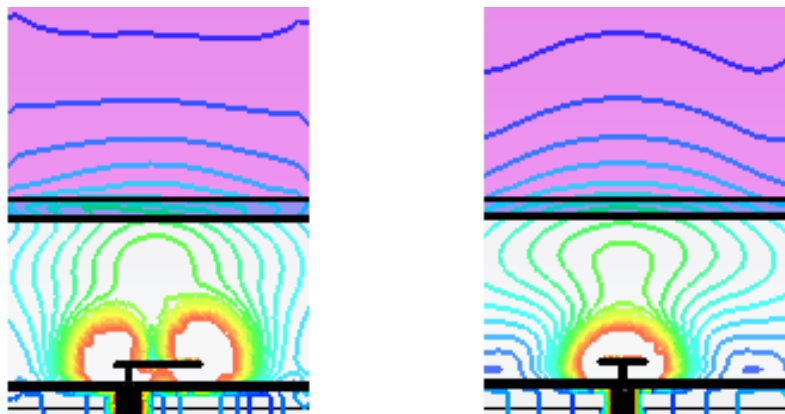


Figure 5.5 Electric field lines of spiral antenna into tissues at $\phi = 0^\circ$ and $\phi = 90^\circ$ planes at 434 MHz.

Figure 5.7 shows the same for the spiral antenna. The difference is significant such that the spiral antenna has more focusing, has less mutual coupling than the patch antenna. Although the both antenna types can be used in a hyperthermia applicator the spiral antenna is more adequate for multi-antenna configuration.

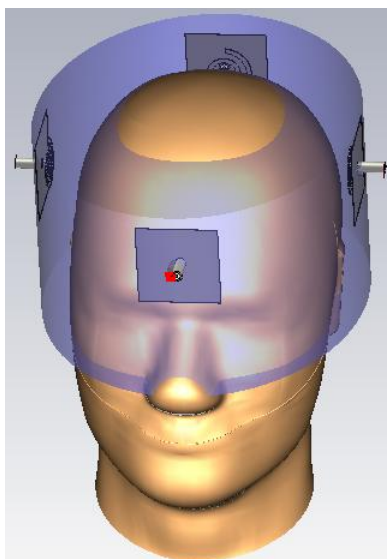


Figure 5.6 A four antenna element head model where the antennas are embedded in water bolus covering the head.

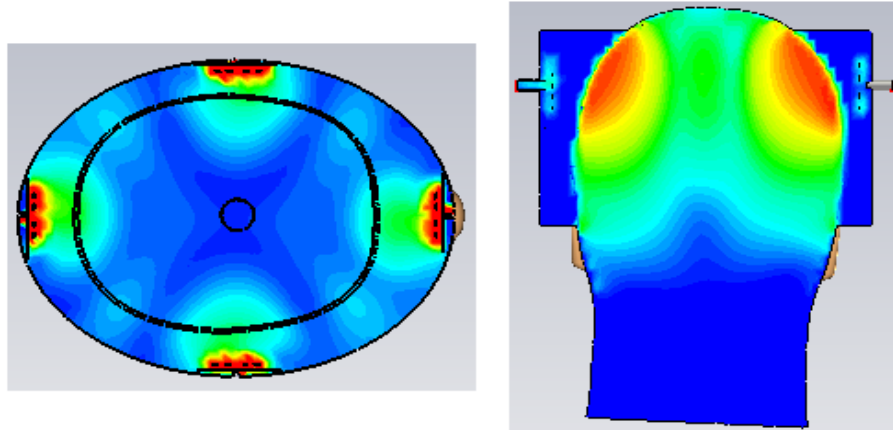


Figure 5.7 Laterally normalized electric field distribution (left) and longitudinal SAR distribution (right) for the spiral antenna.

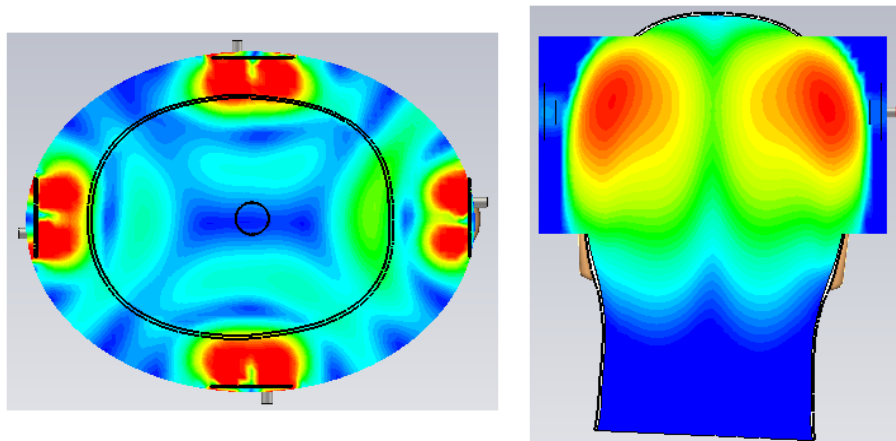


Figure 5.8 Laterally normalized electric field distribution (left) and longitudinal SAR distribution (right) when the patch antenna is positioned at the broad radiation angle.

When designing the applicator, our aim is to increase the number of antennas as much as possible we have examined coupling with each other. As it is shown in Figure 5.9 and Figure 5.10, in four-antenna array to spiral antenna coupling even in the worst case although below -50 dB, and it is calculated as -35dB for patch antennas. As it is shown in Figures 5.11 and Figure 5.12, even in the worst case, the coupling between the spiral antennas in an array of octets antennas although less than -47 dB, It stands out on the -20 dB for patch antennas. It is understood that the patch antennas couldn't be closer due to coupling but it does not constitute a problem for spiral antennas.

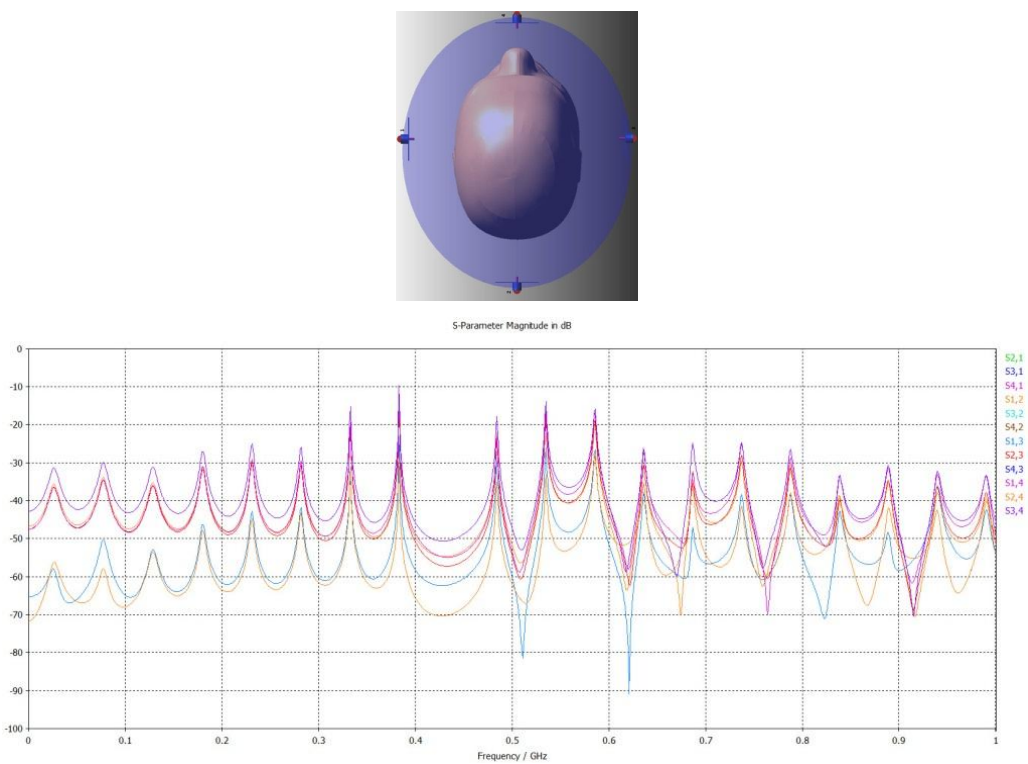


Figure 5.9 Coupling between each of four spiral antennas.

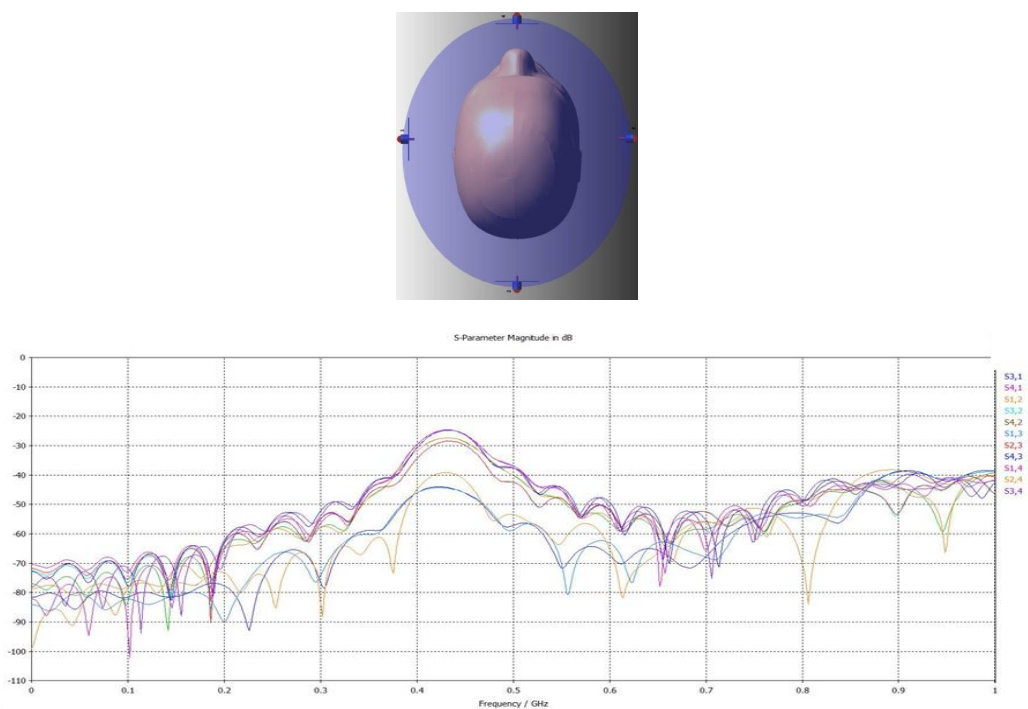


Figure 5.10 Coupling between each of four patch antennas.

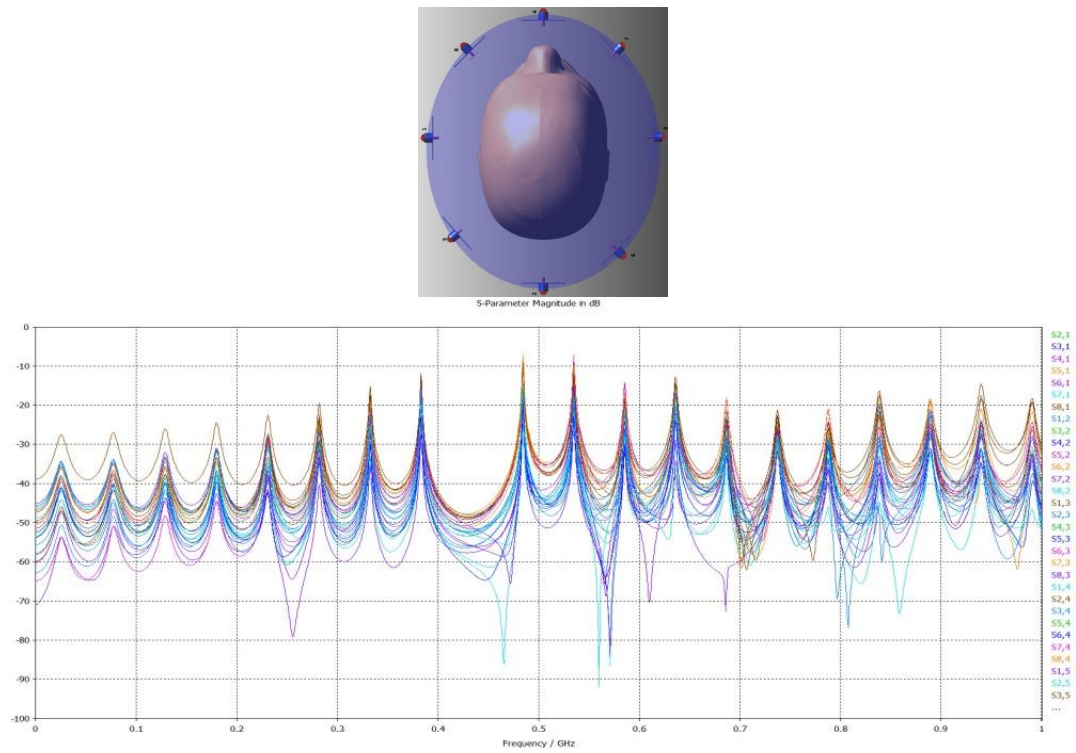


Figure 5.11 Eight spiral antennas coupling between each other.

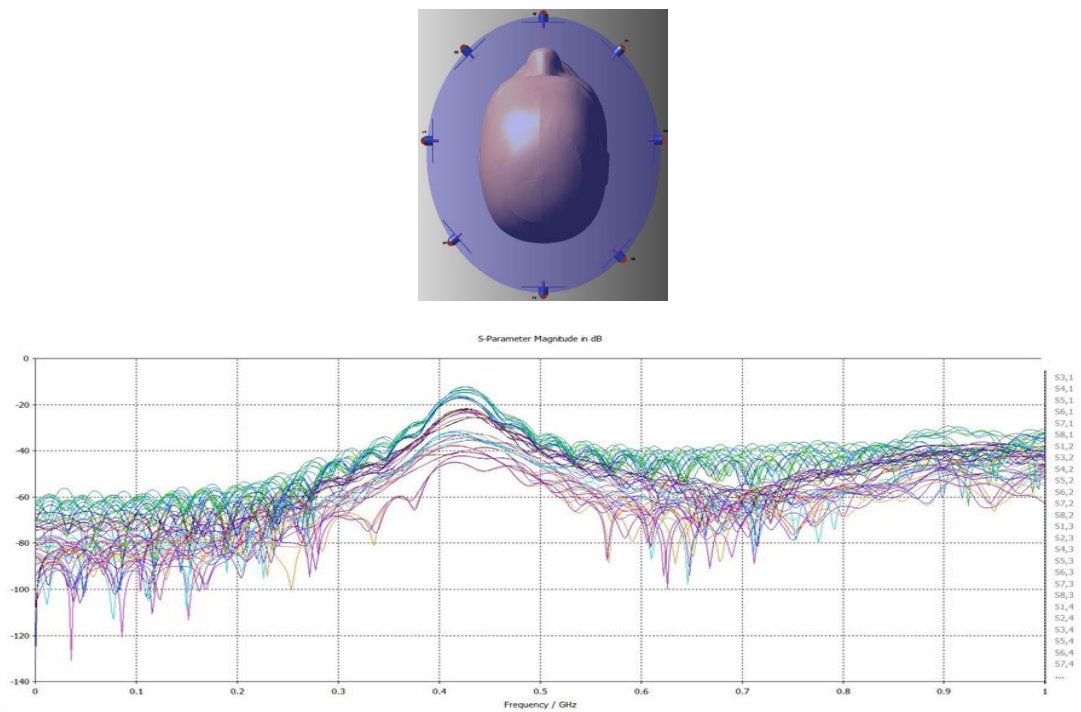


Figure 5.12 Eight patch antennas coupling between each other.

5.3 DESIGN OF A BREAST APPLICATOR

The single antenna element for the applicator design is a microstrip spiral antenna which is developed from our previous study (E. Korkmaz et al., 2013). The produced antennas operate at 434 MHz, have a half power beam width less than 65° at each plane, and its lateral size is around 3 cm. The modeled female breast and its applicator are depicted in Figure 5.13. The tissue parameters of the breast are given in Table 5.1. The breast has a spherical shape with 18 cm radius and has 9 lobules. The antennas are located approximately 3 cm distances from the skin, oriented towards the tumor and the applicator is filled by distilled water.

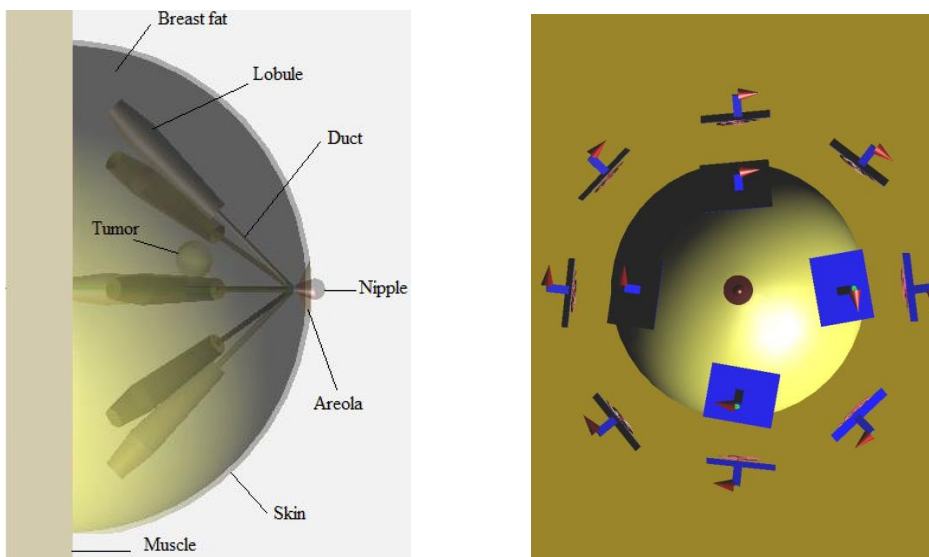


Figure 5.13 Side view of modeled female breast (left) and top view of twelve spiral antennas (right).

Tablo 5.1. Dielectric properties of tissues at 434 MHz.

Tissue Type	Dielectric Properties		
	ϵ_r	$\sigma_{eff} (S/m)$	$\rho(kg/m^3)$
Muscle	56.8660	0.8051	1041
Lobule, Areola, Duct, Nipple	15	0.4	1115
Skin	46.079	0.7019	1100
Breast Fat	5.5072	0.0352	928
Tumor	43.7	6.93	1100

The electromagnetic and thermal simulations are performed by means of commercial electromagnetic software SEMCAD X by SPEAG. The spiral antennas are fed by edge sources at the coax input of the antenna with CW sinusoidal signals at 434 MHz. The coupling between the neighbor antennas was in all cases less than -40 dB. The farthest antenna from the tumor is selected as a phase reference and all other antennas phases are delayed with the estimated phase shifts regarding the tumor position. The SAR distributions are depicted after 30 period's excitation in Figure 5.14 in three orthogonal directions at the center of the tumor. The tumor center is roughly located at 1 cm from the origin in x-y directions and 4 cm in z direction. We put some thermal sensors at different positions inside the tissues and the thermal variations at these sensors are depicted in Figure 5.15 for 60 minutes. The sensors located at superficial region reaches 42 °C earlier then the deeper regions and tumor location. The temperature distributions at the tumor location in three orthogonal directions are depicted in Figure 5.16. Sensors placed on the surface reach to 42 °C earlier than deep place.

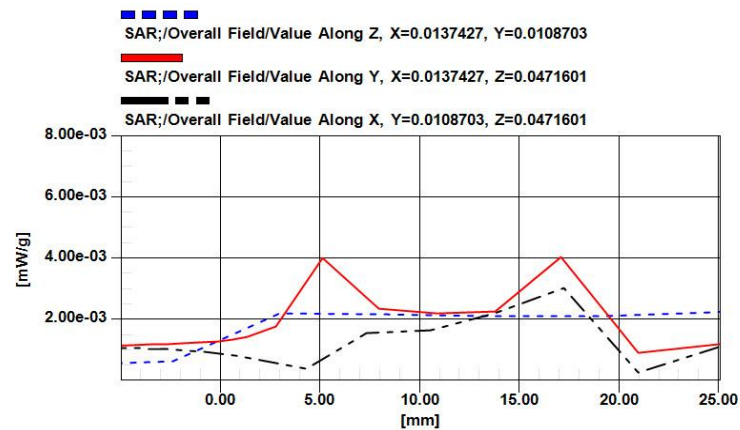


Figure 5.14 The SAR values at the center of cancer region in three orthogonal directions.

Since breast has a quasi-spherical shape we decided to design a hemispherical applicator. In our first design we did perform simulations with 12 antennas but due to the lossy character of the tissues the constructive interference on the focusing region was not satisfactory to obtain a remarkable temperature increase (E. Korkmaz, et al.,

2013). Hence, taking advantage of the directivity of our antennas we designed a hemispherical array with 12 antennas on the lower orbit of sphere, 8 antennas at the intermediate orbit, and 4 antennas around the top of the sphere (around nipple location) all 24 antennas focusing to the center as shown in Figure 5.17. The coupling between the antennas at 434 MHz was ever worst case less than -30 dB that enabled us to use so many patients breast will suspended through a hole into the applicator which is completely embedded in distilled water.

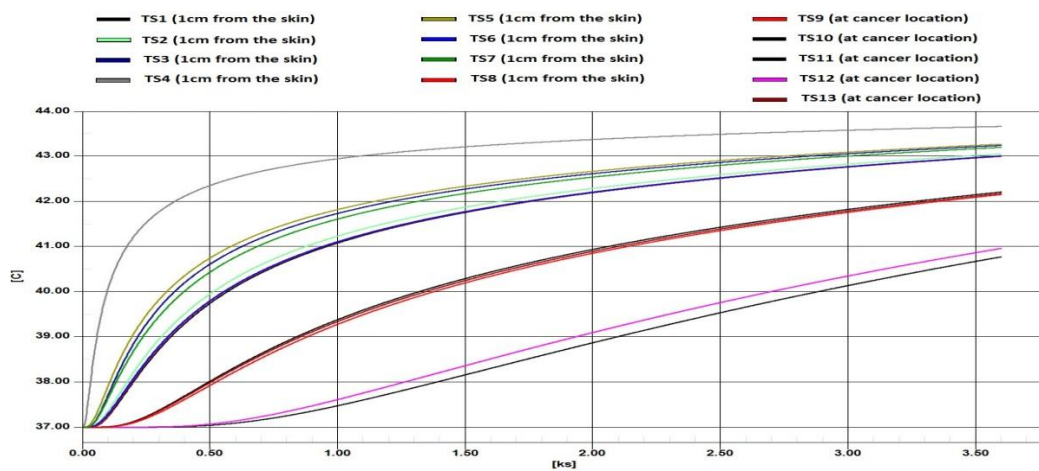


Figure 5.15 The temperature increase during the 60 minutes at various locations of the model.

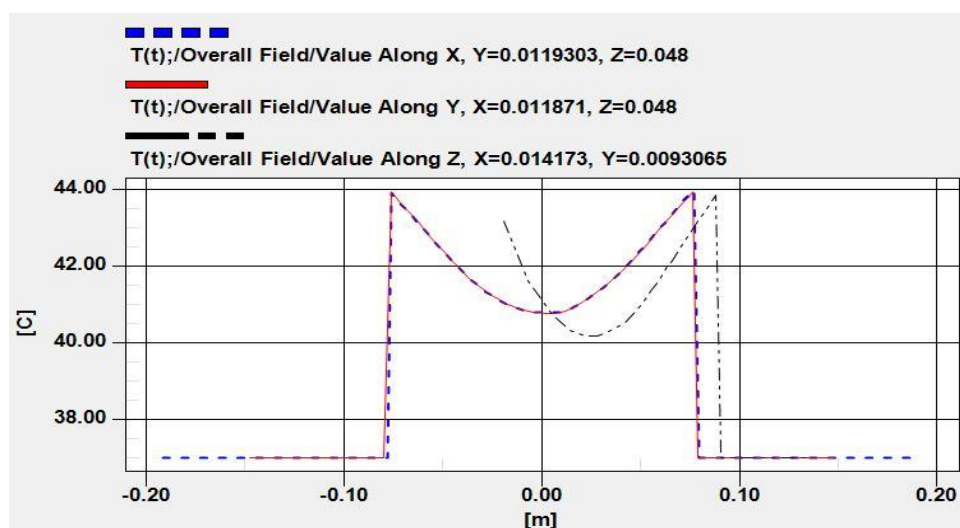


Figure 5.16 Temperature distribution at the tumor center in three orthogonal directions.

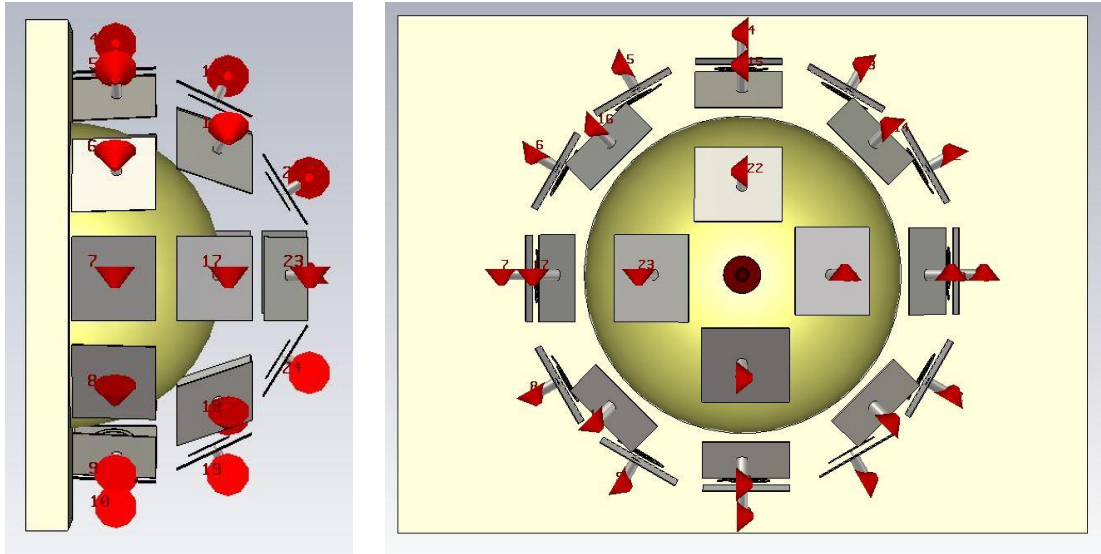


Figure 5.17 Side view of the modeled and top view of realized hemispherical breast applicator.

We need designed hemispherical breast applicator with 24 antennas and furthermore carried simulations toward utilizing SEMCAD X software program utilizing breast model which is shown in Figure 5.17. The phase of each individual antenna is adapted to focus the tumor region. Antennas are fed by 1.6 W power and simulated for 30 minutes at 434 MHz. As a initial temperature, we chose the normal human body temperature as 37,5 °C. Temperature distribution for three orthogonal axes which taken from the center of cancerous part is shown in Figure 5.18. Figure 5.19 illustrates the temperature distribution of each axis. Here, the origin of z-axis is breast-muscle interface. Cancerous areas are about above 3,5-4 cm. In addition, Figure 5.20 shows temperature increase on different points of the breast model during 30 minutes. Surface warming has been completely removed and when the heat is over 44 °C focusing on an area of 2 cm in diameter, temperature quickly decreases away from the center. As it is seen similar result in all three planes, Three-dimensional focusing is observed in all three planes. A focusing and heat distribution in this ratio is based on the successful results so far made and published studies.

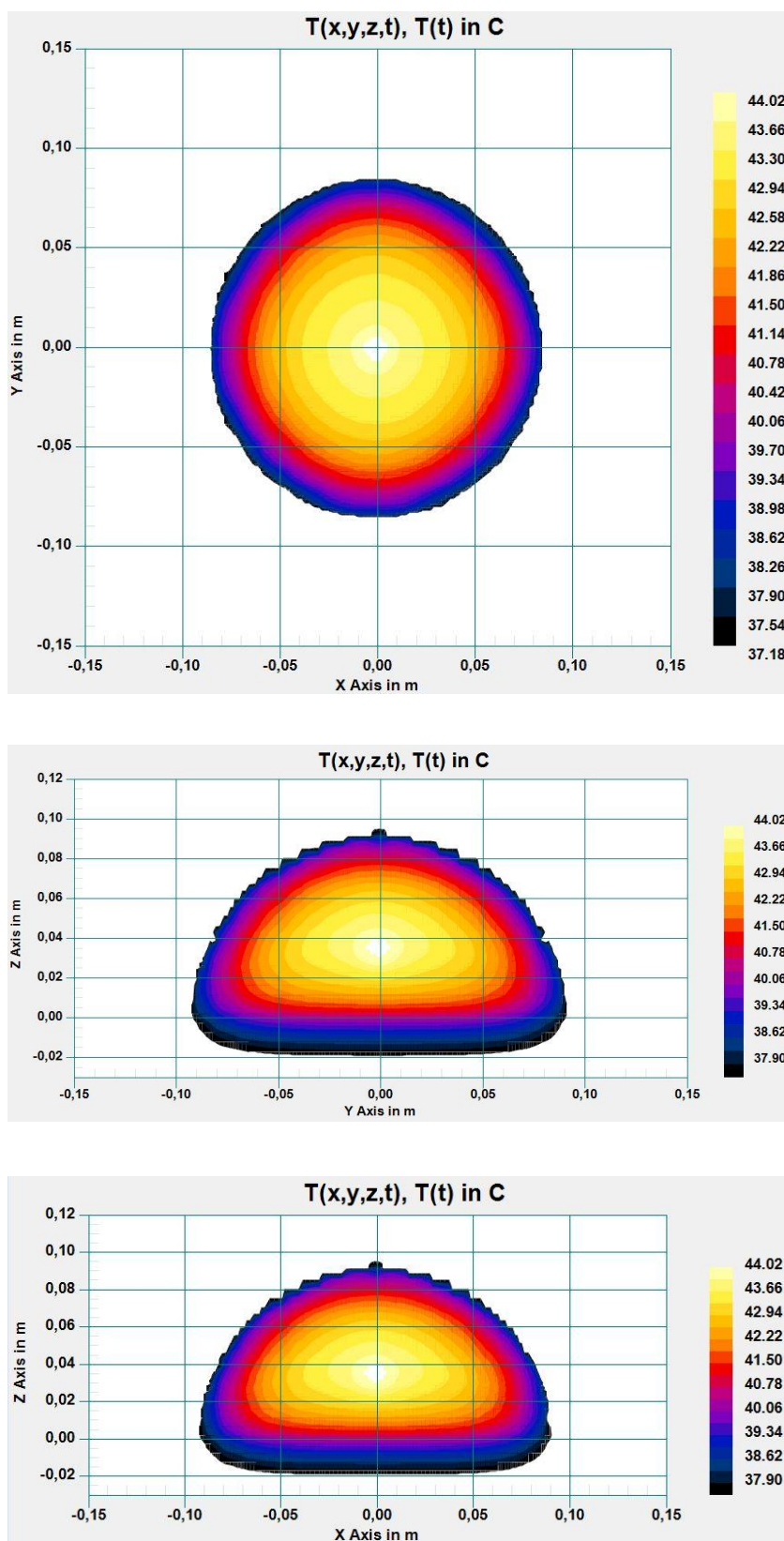


Figure 5.18 Two dimensional temperature distribution at the cancerous point with three cross sections.

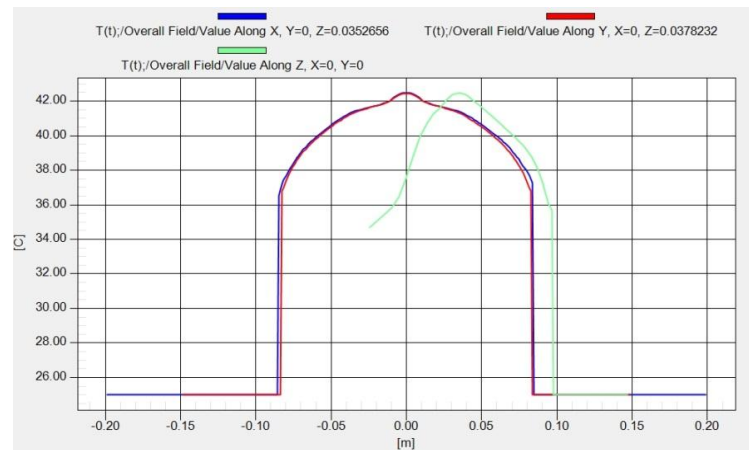


Figure 5.19 One-dimensional temperature distribution in each of three orthogonal sections through the breast model at 434 MHz exposure for 30 minutes.

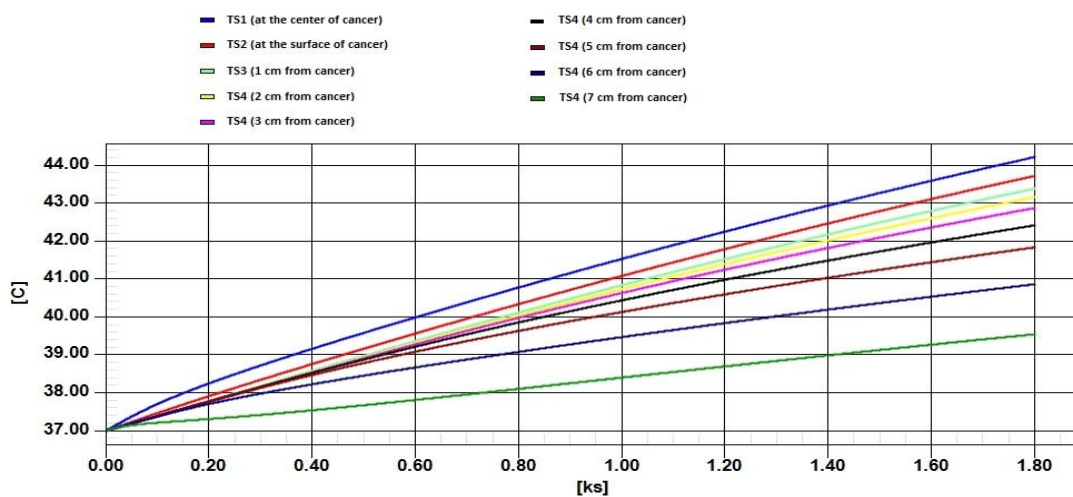


Figure 5.20 Temperature increase during exposure in 30 minutes at various locations of the model at 434 MHz.

5.4 SIMULATIONS WITH REAL BREAST PHANTOM

In treating tissue with hyperthermia treatment, an array of antennas can be used to focus electromagnetic energy into the required tissue by varying the phase and amplitude of each antenna in the array. Focused applicator design, that utilizes the use of a phased array system, is desirable for localized hyperthermia treatment. Realistic breast phantoms also used to observe the temperature distribution (Li X. et al., 2005). These

phantoms, which include more parts, are anatomically realistic. Real breast phantom is depicted in Figure 5.21. The fundamental principle is that the tumor is a lossy dielectric object surrounded by a different kind of lossy dielectric medium (normal breast tissues), which causes reflection and scattering due to the boundary condition. One of the most important role of applicator is to be focused. The electrical location basically represents the equivalent time-delay or phase shift at the tumor with respect to the antenna element locations. Cancerous tissue is shown in Figure 5.21. Shifting phase at each feed is required in order to adjust the focus. As we mentioned before, we could focus the temperature distribution on tumor. Two dimensional temperature distribution at the cancerous point with three cross section is shown in Figure 5.24. Then we shifted cancerous tissue to left and right to observe focusing at the different locations. Temperature distribution is shown in Figure 5.22 and Figure 5. 23 respectively

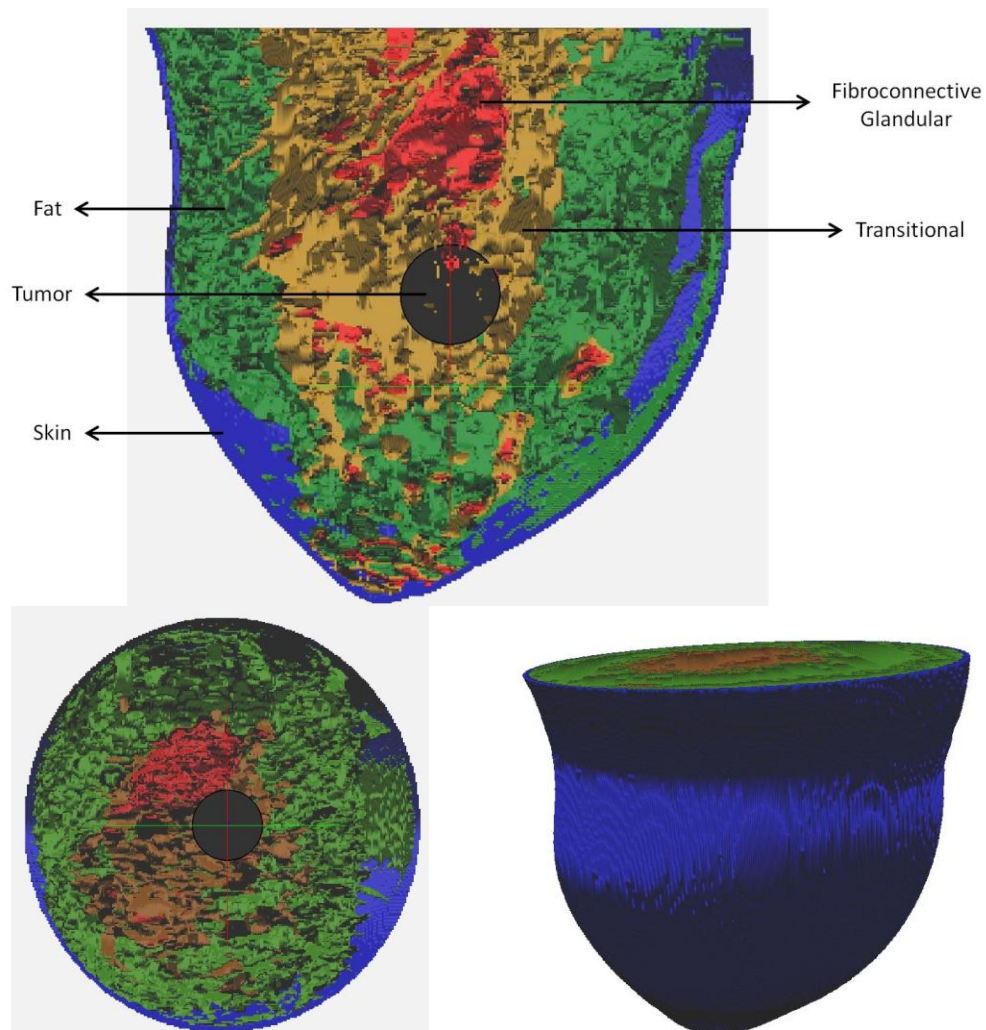


Figure 5.21 Side and top view of modeled detailed female breast model (Li X., et al, 2005).

Tablo 5.2. Dielectric properties of breast tissues at 434 MHz.

Tissue Type	Dielectric Properties		
	ϵ_r	$\sigma_{eff} (S/m)$	$\rho(kg/m^3)$
Transitional	56.8660	0.8051	1041
Fiberconnective Glandular	15	0.4	1115
Skin	46.079	0.7019	1100
Breast Fat	4.33	0.02	928
Tumor	43.7	1.23	1100

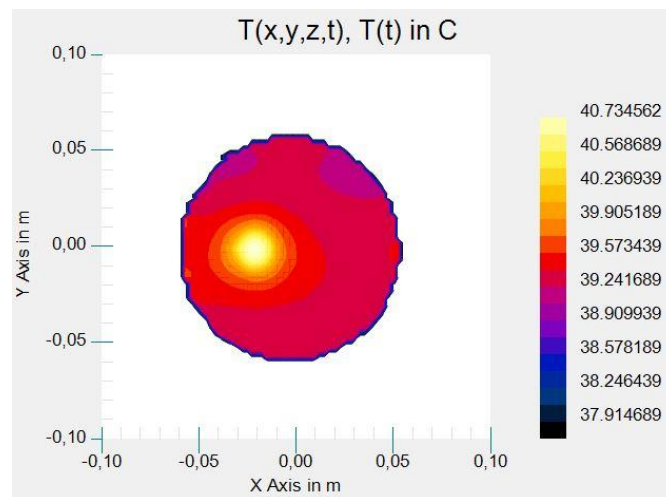


Figure 5.22 Two dimensional temperature distribution at the cancerous point with three cross.

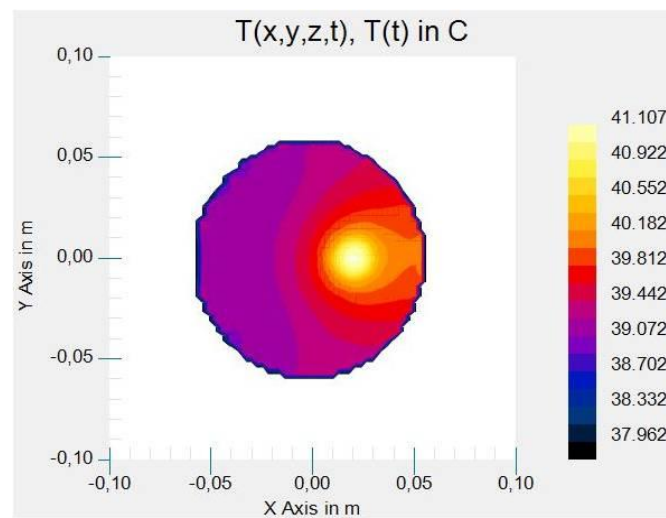


Figure 5.23 Two dimensional temperature distribution at the cancerous point with three cross.

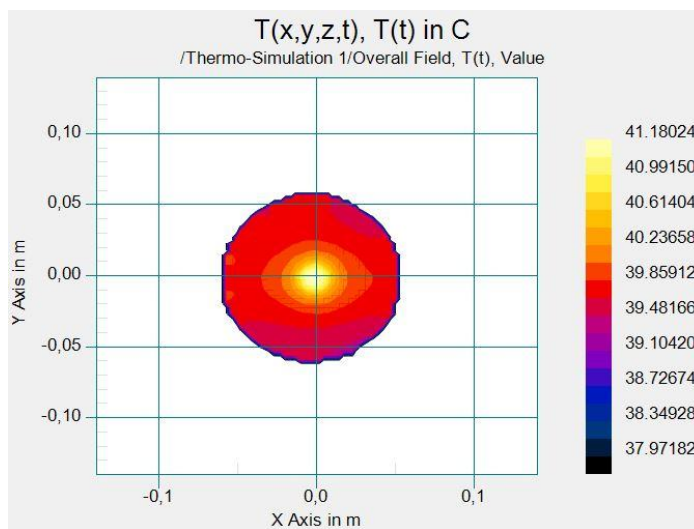
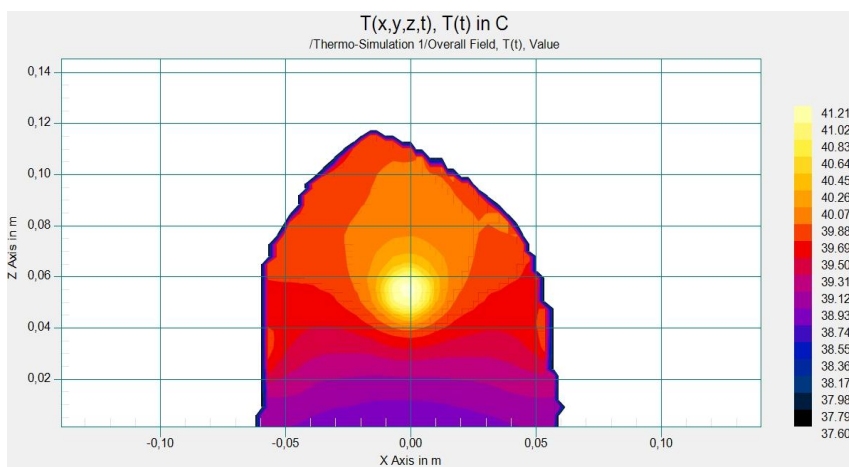
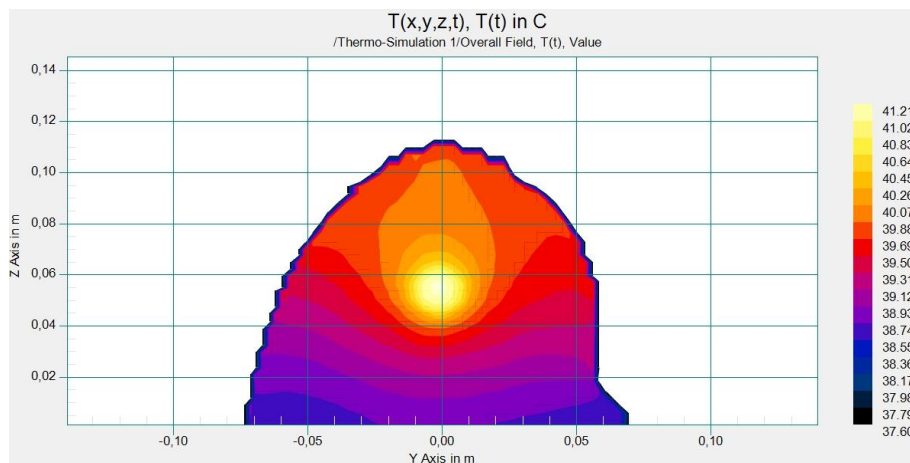


Figure 5.24 Two dimensional temperature distribution at the cancerous point with three cross section.

CHAPTER 6

IMPLEMENTATION AND MEASUREMENT WITH HEMISPHERICAL BREAST APPLICATOR

6.1 DESIGN OF MICROWAVE COMPONENTS

It is needed some electronic components such as RF amplifiers and RF splitters to complete the applicator. We have designed some of them by ourselves. The operating principle of such layout is the following. The RF signal at 434 MHz from signal source splits into 2 channels by using T-splitter. Then by means of 2 solid state amplifiers we can adjust amplitude of every signal. Due to these adjustments electric field focusing in the desire region is available. Directional couplers prevent reaching reflected wave to generator.

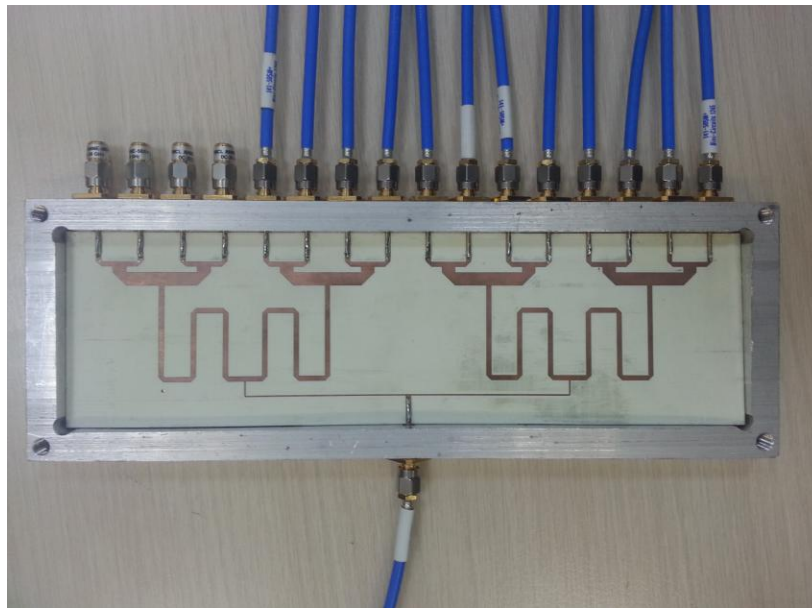


Figure 6.1 1x16 RF splitter used in applicator.

Reflected wave will be absorbed by 50 Ohm load. Modern solid state amplifiers are simple and stable in operation and can derive the necessary amplification. Therefore, we have firstly designed the RF splitter. We need two 1x16-out RF power splitters to feed 24 antennas. Feeding point is at rear and there are 8 outputs on the both sides. The RF power supply has to be independent for each antenna. Then, we have observed that this design is not practical. So, we re-designed and produced new one within the Fatih University which is shown in Figure 6.1. The measurement results are shown in Figure 6.2. In the ideal case, output signal is -12 dB but additionally 0.5 dB loss will be occurred. 50 Ω loads are connected to the off-position connector not to be reflected.

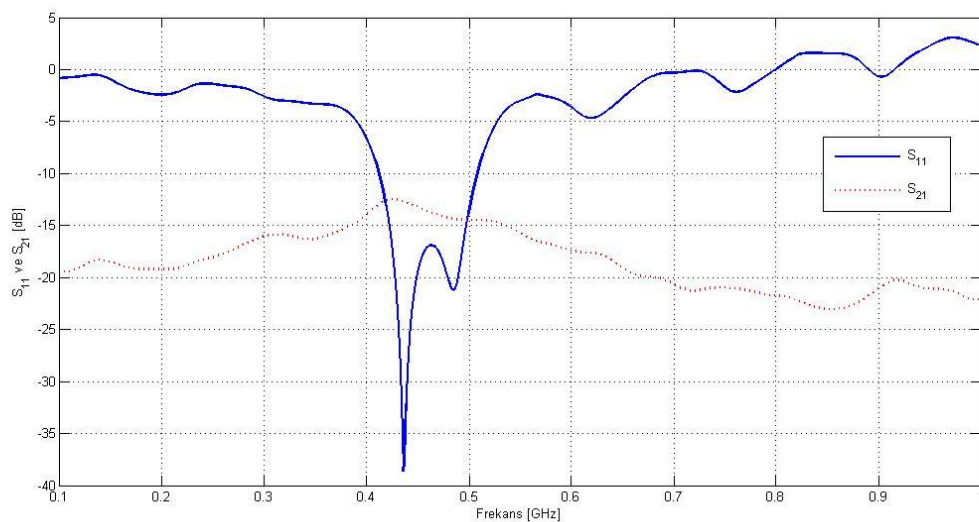


Figure 6.2 Measurement results of 1x16 RF splitter.

Furthermore, we are supposed to make phase control of the antennas for non-symmetrical structures. In this context, the Voltage-controlled 1x16 RF phase shifter as shown in Figure 6.3 is designed and manufactured. This is with phase range 180°, control voltage 0-12 V. We observe that the measurement results consistent with simulation results.

Signal generator which is used in measurements is able to generate up to 20 dBm (100 mW) power. So, power of each antenna is very low. Therefore, we need RF power amplifier. Initially, we have designed a RF power amplifier with 30 dB gain and up to 6 W output power. RF Amplifiers was working probably at the beginning, and then it is burned perhaps due to not properly solder by manually. Thus, it was obtained through the purchase of high power amplifiers producing 25 W power. Owing to all possibilities, we produced and designed amplifiers which can be connected to the output of the RF splitters and produces maximum power of 100 mW and 25 dB gain. But when the intake of other amplifiers happened, it did not need to use.

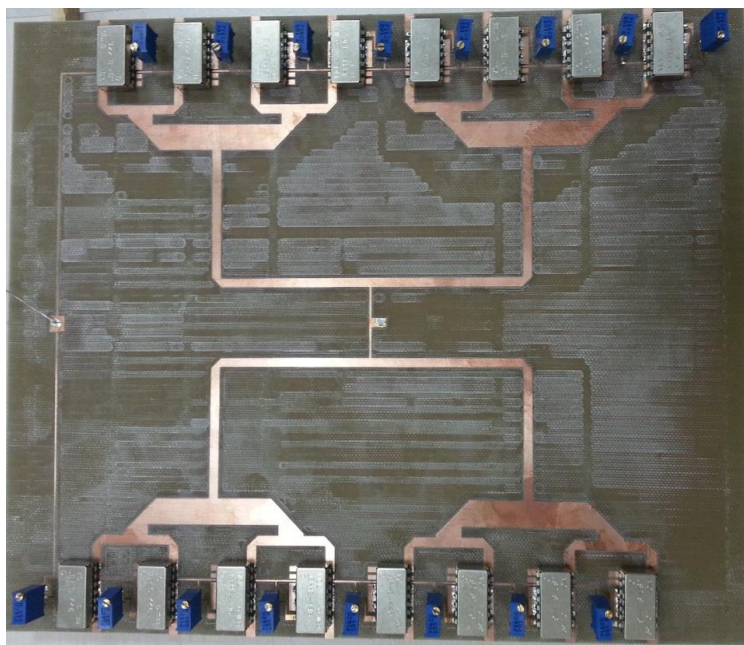


Figure 6.3 Voltage-controlled 1x16 RF phase shifter.

Since breast has a quasi-spherical shape we decided to design a hemispherical applicator. And then we produced breast applicator with 12 antennas on the lower orbit of sphere, 8 antennas at the intermediate orbit, and 4 antennas around the top of the sphere (around nipple location) all 24 antennas focusing to the center as shown in Figure 6.4. A structure was needed for a global structure to attach antennas in the correct position. Therefore, carving inside a cube-shaped plastic hemisphere shape was obtained. This hemisphere holder mounted 24 antennas as previously designed.

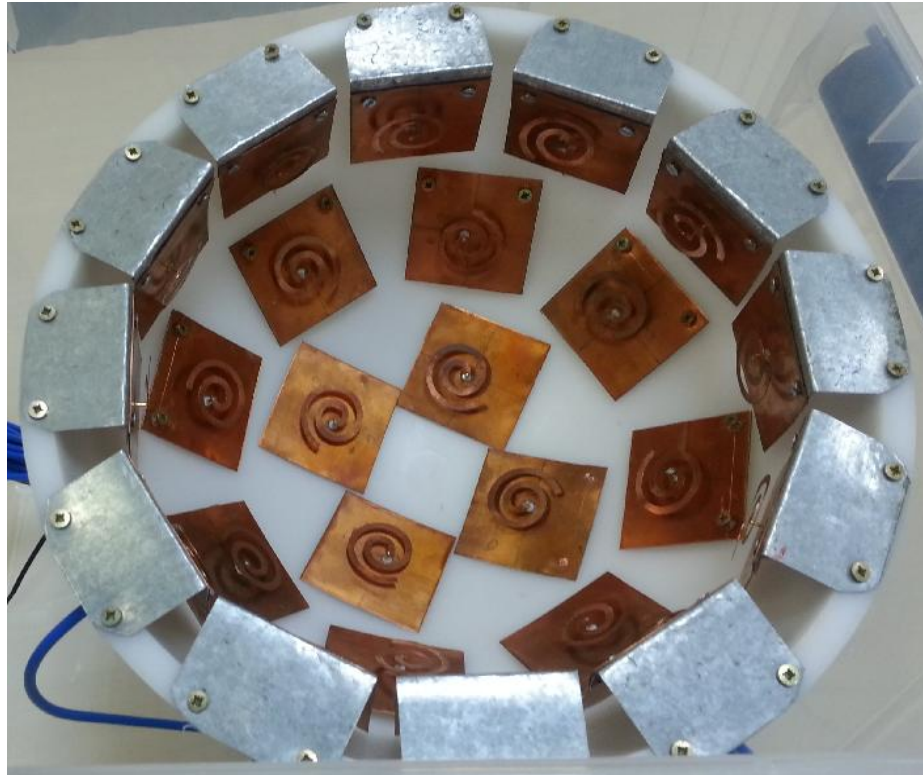


Figure 6.4 Realized hemispherical breast applicator.

6.2 MEASUREMENT WITH HEMISPHERICAL BREAST APPLICATOR

The measurement setup is shown in Figure 6.5. Signal generator is connected to a two way T-splitter and the two outputs are connected to two identical RF amplifiers which can give a maximum power of up to 50 W. The outputs of amplifiers are connected to 1x16 way RF-splitters. Two groups of twelve antennas are connected to splitter outputs and remaining outputs are connected to 50 Ω loads to avoid mismatch reflections. The applicator is placed in a handmade anechoic room with RF absorbers to reduce possible radiation effects.

In order to observe the temperature distribution we first filled all glass beakers shown in Figure 6.6 with salty de-ionized water. The conductivity of salty water is about 0.53 S/m at 434 MHz. Then we nested all three beakers concentrically by hanging them from the mouth to a holder such that smallest beaker is located at the center of applicator. The beakers are numbered such that the inner one is beaker 1 and the outer one is beaker 3. In the second measurement we only changed the content of beaker 1

with cancer mimicking tissue gel. The beakers did also serve as temperature isolation to observe the temperature distribution fairly.

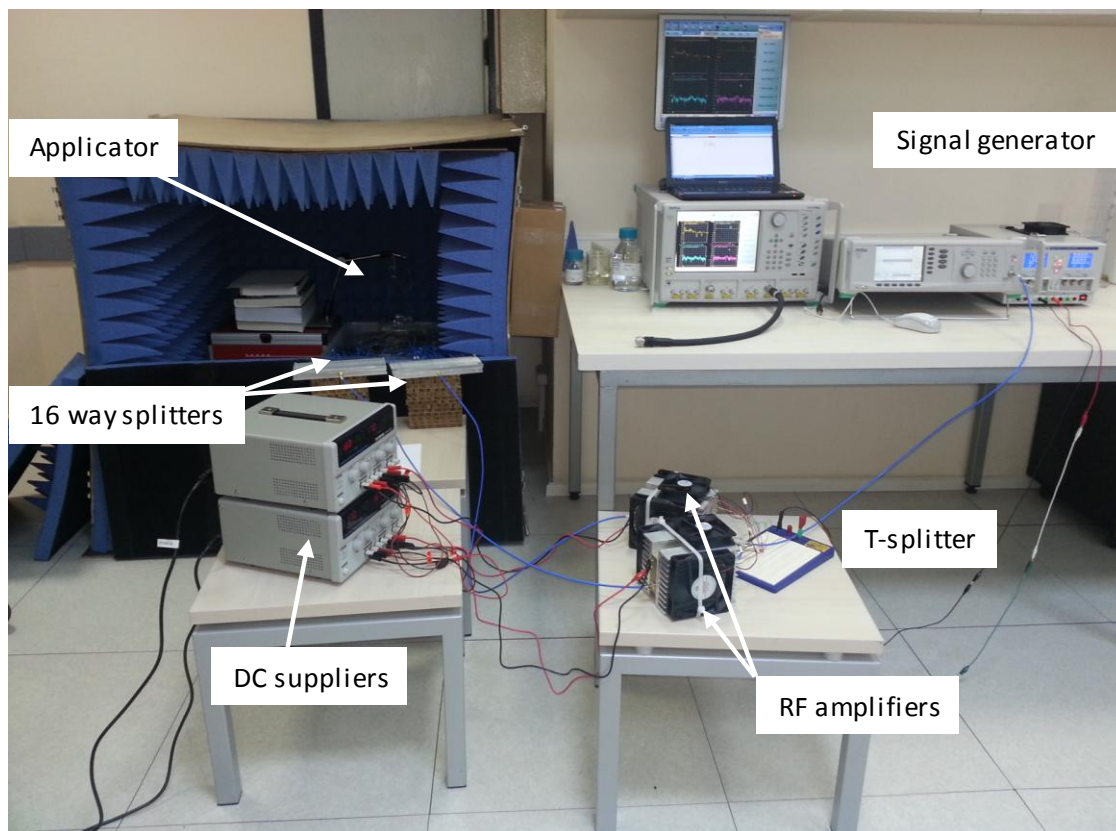


Figure 6.5 General view of experimental setup.



Figure 6.6 Different beakers used during the measurements and placement into the applicator.

We adjusted the power level of signal generator such that all individual antennas are fed by 0.8 W power. The idea is to increase the temperature about 5 °C to elevate from 37.5 °C body temperatures up to 42.5 °C treatment temperatures. Then we exposed the beakers to RF radiation for 70 minutes. The temperature difference in time when all beakers are salty water is shown in Figure 6.7. The temperature change after 70 minutes when the inner beaker is cancer mimicking gel about 6 °C while in other case the change is about 5 °C. Temperature difference in time when beaker 1 is cancer mimicking gel is shown in Figure 6.8. In both cases the surrounding beakers temperature change are insignificant. We also performed measurements with tissue mimicking gels and similar results are obtained.

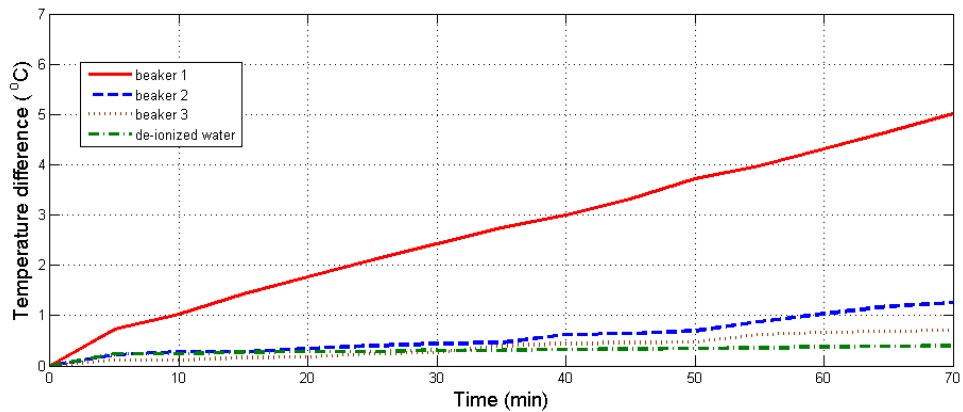


Figure 6.7 Temperature difference in time when all beakers are salty water.

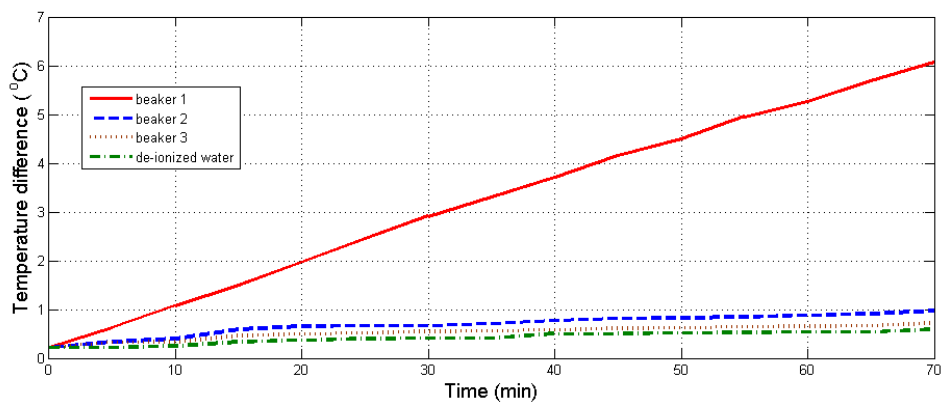


Figure 6.8 Temperature difference in time when beaker 1 is cancer mimicking gel.

In the second experiment equivalent tissue gels we obtained earlier was used. According to this, skin tissue in the outer beaker, fatty tissue in the second beaker and cancer tissue in the inner beaker were used. Because of the high conductivity of the cancerous tissue A little more than 1 °C degree heat has been reached at the same time. Focusing has similar features with the experiment. These results are considered excellent when compared with similar in the literature.

CHAPTER 7

CONCLUSION

As time goes by the diagnosis's of cancer are on the rise, currently there is not a wide variety of treatment options available to patients in need of cancer treatment with the exception of different combinations of traditional methods depending on the type of cancer. Many patients are as concerned about their method of treatment as they are about the disease itself. This would be a step forward in the direction of giving patients as well as doctors not only more options but a better prognosis with the implementation of thermotherapy and hyperthermia.

This doctoral thesis had as a main aim to bring some new scientific contributions to the topics of medical applications of EM field, especially then to microwave thermotherapy or hyperthermia. In the scope of this dissertation, a novel preclinical female breast applicator with 24 directive spiral antennas forming a hemispherical array is presented.

For the applicator a compact novel microstrip spiral antenna with a narrower radiation pattern is introduced which can be considered as an adequate choice to use it in a multi-antenna system for semi-deep or deep hyperthermia applications. The narrow radiation pattern and small size are desirable characteristics to place more antennas in an array configuration and to reduce the constructive interference at superficial regions such that a better focus on the targeted region is obtained. The half power beam width (HPBW) of the spiral antenna is smaller than 65° for each plane. The operation at multi-frequencies can be used in case of penetration depth and focusing considerations.

The electromagnetic interactions inside the tissues are studied and thermal results are presented. The desired temperature in the focused tumor region can be reached and controlled with the developed applicator while the hot spots are avoided. Both measurement and simulation results verify the capability of the applicator to focus at a very small region in three dimensions.

For the confirmation of the simulation results with measurement results the tissue mimicking materials are characterized and recipes are reported. The characterized tissue mimicking materials are inexpensive and have simple recipes that are easy to formulate. Recipes are developed for skin, muscle, fatty and breast cancer tissue which is needed for a breast model. There is a discrepancy between the conductivity of fat mimicking material and the reference data for ISM band.

In order to design an applicator it is a necessity to create models of human tissues for use in the simulations. For the first simulations we designed a relatively simple breast model to study the efficiency of the applicator. For a real breast model a segmentation tool is needed to extract the 3D model from the CT or MR image slices. After validation with the simplified breast model the efficiency of the applicator is analysed on a real non homogeneous breast model belonging to a specific person. The simulation results belonging to this real breast model verified again the 3D focusing capability of the designed applicator.

In order to perform the measurements and verify the simulation results there was a need for a measurement setup. Considering the budget of the project where this thesis is a part of it and, the available devices and infrastructure a reasonable measurement setup is constructed. Three beakers concentrically nested by hanging them from the mouth (opening) to a holder such that the smallest beaker which has a 2cm radius and is located at the center of the applicator. The phase of each individual antenna is adapted to focus the tumor region. By changing material at the center of the applicator, we observed a temperature difference over time in the inner beaker while the surrounding beakers temperature changes were insignificant. The beakers also served as temperature isolation to observe the temperature distribution fairly. The measurement results verified the 3D thermal focusing of the applicator.

This study, which is successfully completed, is promising for breast cancer both in conjunction with conventional techniques and as stand alone treatment. However, additional studies are needed to apply our findings and designs on patients in clinics. It is possible to apply the clinical phase of the applicator made of thermal dosimeters and to include the real-time thermal imaging systems. Methods for non-invasive treatments using thermal probes cannot be used. Also; infrared thermal imaging systems to penetrate tissue cannot be used because three-dimensional temperature distribution in the tissue is required. MR-based methods thermal monitoring integrated with applicator is an option. However it is extremely costly and raises flexibility due to difficulties in integration. Therefore, there is a need to improve the microwave imaging system using the same applicator with microwave thermal imaging techniques.

Results obtained by research in the frame of my doctoral thesis were presented in several peer reviewed prestigious international scientific conferences and journal. In addition some of the obtained results are in preparation to submit it for

REFERENCES

- Abitbol, A. A., James G. Schwade, Alan A. Lewin, Charles F. Gottlieb, Mark J. Hagmann, and Taudeusz M. Babij, *Hyperthermia: A potential useful adjunct to radiation therapy*, IEEE Engineering in Medicine & Biology Society 10th Annual International Conference, 1988.
- Alomainy A., Y. Hao, X. Hu, C. G. Parini, and P. S. Hall “*UWB on-body radio propagation and system modeling for wireless body-centric networks*,” IEE Proc., Commun., vol.153, no.1, pp. 107-114, Feb. 2006.
- American Cancer Society, *Hyperthermia to Treat Cancer*,
<http://www.cancer.org/treatment/treatmentsandsideeffects/treatmenttypes/hyperthermia> Son erişim tarihi: 29/10/2014.
- Andreuccetti D., M. Bini, A. Ignesti, R. Olmi, S. Priori, and R. Vanni, *High permittivity patch radiator for single and multi-element hyperthermia applicators*, IEEE Transactions on Biomedical Engineering, vol. 40, no. 7, pp. 711–715, 1993.
- American Cancer Society, *Hyperthermia to Treat Cancer*,
<http://www.cancer.org/treatment/treatmentsandsideeffects/treatmenttypes/hyperthermia> Son erişim tarihi: 29/10/2014.
- Anguera J., et.al., *Small and High Directivity Bow-Tie Patch Antenna Based on the Sierpinski Fractal*, Microwave and Optical Technology Letter, Vol.31, No.3, p. 239-241, November 2001.
- Babincová, M., P. Sourivong, D. Leszczynska and P. Babinec, *Blood-specific whole-body electromagnetic hyperthermia*, Medical Hypotheses, Vol. 55, No. 6, pp. 459–460, November 1999.
- Bahl I. J., S. S. Stuchly, J. W. Lagendijk, and M. A. Stuchly, *Microstrip loop radiators for local hyperthermia*, in IEEE MTT-S International Microwave Symposium Digest, pp. 465– 467, June 1981.
- BSD Medical, USA
http://www.bsdmedical.com/international/products_hyperthermia.php
Son erişim tarihi: 29/10/2014.

- Cancer Research UK, *Diagram showing a tumour forcing its way through normal tissue*,
<http://www.cancerhelp.org.uk/help/default.asp?page=100>
 Son erişim tarihi: 29/10/2014.
- Censor, Y., “*Mathematical aspects of radiation therapy treatment planning: Continuous inversion versus full discretization and optimization versus feasibility*”, in C. Borgers and F. Natterer (Editors), *Computational Radiology and Imaging: Therapy and Diagnosis*, , The IMA Volumes in Mathematics and its Applications, Vol. 110, pp. 101-112, Springer-Verlag, New York, USA, 1999.
- Cheng K. S., M.W. Dewhurst, P.R. Stauffer, and S. Das, *Effective learning strategies for real-time image-guided adaptive control of multiple source hyperthermia applicators*, *Med. Phys.*, vol. 37, no. 3, pp. 1285–1297, 2010.
- Chen W. T. and H. R. Chuang, *Numerical computation of the EM coupling between a circular loop antenna and a full-scale human-body model*, *IEEE Transactions on Microwave Theory and Techniques*, vol. 46, no. 10, part 1, pp. 1516–1520, 1998.
- Chou Chung-Kwang, *Application of Electromagnetic Energy in Cancer Treatment*, *IEEE Transactions on Instrumentation and Measurement*, Vol. 31, No. 4. December 1988.
- Cukier, Daniel. *Coping with Chemotherapy and Radiation Therapy*. McGraw-Hill Companies, Blacklick, OH, USA, 2005.
- Curto S., P. McEvoy, X. Bao, and M. J. Ammann, *Compact patch antenna for electromagnetic interaction with human tissue at 434MHz*, *IEEE Transactions on Antennas and Propagation*, vol. 57, no. 9, pp. 2564–2571, 2009.
- Curto S. and M. J. Ammann, *Electromagnetic interaction between resonant loop antenna and simulated biological tissue*, *Microwave and Optical Technology Letters*, vol. 48, no. 12, pp. 2418–2421, 2006.
- Dewey WC, Hopwood LE, Sapareto SA. et al., *Cellular response to combination of hyperthermia and radiation*, *Radiology*. 123: 463–474, 1977.
- Deuflhard, P., M. Seebass et al., *Hyperthermia Treatment Planning in Clinical Cancer Therapy: Modelling, Simulation, and Visualization*, 15th IMACS World Congress, Berlin-Dahlem, June 1997.
- Duncombe, P. B., C. Cetas Tomas, et al., *Hyperthermia Treatment Planning*, AAPM Report No. 27, August 1989.
- Ebrahimi-Ganjeh M. A. and A. R. Attari, *Study of water bolus effect on SAR penetration depth and effective field size for local hyperthermia*, *Progress In Electromagnetics Research B*, vol. 4, pp. 273–283, 2008.

- ESHO Taskgroup Committee, *Treatment planning and modelling in hyperthermia*, a task group report of the European Society for Hyperthermic Oncology. Tor Vergata, Rome, Italy, 1992.
- Falk M. H., R.D. Issels, “*Hyperthermia in oncology*”, *International Journal of Hyperthermia*, 17(1), pp. 1-18, 2002.
- Fukunaga K., S. Watanabe, and Y. Yamanaka *Dielectric Properties of Tissue-Equivalent Liquids and Their Effects on Specific Absorption Rate*, *IEEE Transactions on Electromagnetic Compatibility*, vol. 46, no. 1, pp 126-129, February 2004.
- Furse C. M., *Design of an antenna for pacemaker communication*, *Microwave RF*, vol. 39, no. 3, pp. 73–76, Mar. 2000.
- Gabriel C., S. Gabriel, and E. Corthout, *The dielectric properties of biological tissues: I. Literature survey*, *Phys. Med. Biol.*, 41, pp. 2231-2249, 1996.
- Gabriel S., R. W. Lau, and C. Gabriel, *The dielectric properties of biological tissues: II. Measurements in the frequency range 10 Hz to 20 GHz*, *Phys. Med. Biol.*, 41, pp. 2251-2269, 1996.
- Garg R., P. Bhartia, I. Bahl, A. Ittipiboon, “*Microstrip Antenna Design Handbook*,” Norwood, MA: Artech, 2001
- Gellermann J, et al. *Comparison of MR-thermography and planning calculations in phantoms*, *Med. Phys* 2006;33:3912–3920.
- Gupta R. C. and S. P. Singh, *Development and analysis of a microwave direct contact water-loaded box-horn applicator for therapeutic heating of bio-medium*, *Progress in Electromagnetics Research*, vol. 62, pp. 217–235, 2006.
- Gupta R. C. and S. P. Singh, *Analysis of the SAR distributions in three-layered bio-media in direct contact with a waterloaded modified box-horn applicator*, *IEEE Transactions on Microwave Theory and Techniques*, vol. 53, no. 9, pp. 2665–2671, 2005.
- Hamza-Lup, F. G., L. Davis, and Omar A. Zeidan, “Web-based 3D Planning Tool for Radiation Therapy Treatment”, *Association for Computing Machinery (ACM)*, Columbia, Maryland, 18–21 April 2006, pp. 159-162, ACM 2006.
- Hafstrom L, Rudenstam CM, Blomquist E. et al. *Regional hyperthermic perfusion with melphalan after surgery for recurrent malignant melanoma of the extremities*, *J Clin Oncol*. 9: 2091–2094, 1991.
- Hildebrandt B., Wust P., Ahlers O., Diein A., Sreenivasa G., Kerner T., Felix R., Riess H., *The cellular and molecular basis of hyperthermia*, *Critical Reviews in Oncology/Hematology*, Vol. 43, pp. 33-56, 2002.
- Hynynen K, McDannold N. *MRI guided and monitored focused ultrasound thermal ablation methods: a review of progress*, *Int. J. Hyperthermia* 2004;20:725–738.

- Isik O., Korkmaz E., *Electromagnetic Modeling of Thermal Fields Induced in Human Femur Tissue*, IEEE AP-S International Symposium on Antennas and Propagation & USNC/URSI Na, Toronto / Kanada, Jul. 2010.
- Işık O., Korkmaz E., *İnsan Dokularında Elektromanyetik Etkileşim ve Lokal Isı Artışı Modellemesi*, 14.Biyomedikal Mühendisliği Ulusal Toplantısı, İzmir/Türkiye, May. 2009, Proceedings of BIYOMUT 2009, paper no 144.
- Işık O., *Modeling of Electromagnetic behavior and Local Temperature Increase in Human Tissues*, August 2009, MS Thesis, Fatih University.
- Isik O., E. Korkmaz, S. Kara, M. A. Nassor, B. Turetken, *Development of a Hyperthermia Applicator with Compact Microstrip Antennas*, Proceedings of the IEEE International Symposium on Antennas and Propagation, Chicago, USA, 2012.
- iSEG, Switzerland, <http://www.speag.com/news-events/news/simulation/iseg-v3-1-release/> Son erişim tarihi: 29/10/2014.
- J. van der Zee, "Heating the patient: a promising approach?" *Annals of Oncology*, 13(8), pp. 1173-1184, 2002
- Jacobsen S. and P. R. Stauffer, *Multifrequency radiometric determination of temperature profiles in a lossy homogeneous phantom using a dual-mode antenna with integral water bolus*, IEEE Transactions on Microwave Theory and Techniques, vol. 50, no. 7, pp. 1737–1746, 2002.
- Jacobsen S., H. O. Rolfsnes, and P. R. Stauffer, *Characteristics of microstrip muscle-loaded single-arm Archimedean spiral antennas as investigated by FDTD numerical computations*, IEEE Transactions on Biomedical Engineering, vol. 52, no. 2, pp. 321–330, 2005.
- Juang T., D. Neuman, J. Schlorff, and P. R. Stauffer, *Construction of a conformal water bolus vest applicator for hyperthermia treatment of superficial skin cancer*, IEEE Engineering in Medicine and Biology Society, vol. 2, pp. 3467–3470, 2004.
- Kim J. and Y. Rahmat-Samii, *Implanted antennas inside a human body: Simulations, designs, and characterizations*, IEEE Trans. Microw. Theory Tech., vol. 52, no. 8, pp. 1934–1943, Aug. 2004.
- Korkmaz E., O. Isik, S. Kara, M. A. Nassor, B. Turetken, *Design of Compact Microstrip Antennas Embedded in Water Bolus for Hyperthermia Applications*, Proceedings of the IEEE International Symposium on Antennas and Propagation, Chicago, USA, 2012.
- Korkmaz E., Isik O., Kara S., *Electromagnetic Modeling of a Female Breast Hyperthermia Applicator*, Proceedings of the IEEE International Symposium on Antennas and Propagation, Orlando, USA, 2013.
- Korkmaz Erdal, Omer Isik, Mohammed Ahmed Nassor, *A Compact Microstrip Spiral Antenna Embedded in Water Bolus for Hyperthermia Applications*, International

Journal of Antennas and Propagation, vol. 2013, Article ID 954986, 6 pages, 2013, doi: 10.1155/2013/954986.

- Korkmaz E., Isik O., *Electromagnetic Hyperthermia Modeling in Human Intra-Abdominal Region*, International Symposium on Antenna Technology and Applied Electromagnetics [ANTEM] and the Amer, Ottawa / Kanada, Jul. 2010.
- Kowalski, Marc E., and Jian-Ming Jin, *Model-Based Optimization of Phased Arrays for Electromagnetic Hyperthermia*, IEEE Transactions on Microwave Theory and Techniques, Vol. 52, No. 8, pp. 1964-1977, August 2004.
- Legendijk J. J. W., *Hyperthermia treatment planning*, 2000 Phys. Med. Biol. 45 R61-R76.
- Lazebnik vd., *A large-scale study of the ultrawideband microwavedielectric properties of normal, benign and malignant breast tissues obtained from cancer surgeries*, 2007, Physics in Medicine and Biology, vol. 52, pp. 6093-6115.
- Li X., E. J. Bond, B. D. Van Veen, and S.C. Hagness, "An overview of ultrawideband microwave imagining for early-stage breast cancer detection," IEEE Antennas Propag. Mag., Vol. 47, pp. 1934, Feb. 2005.
- Li Z., M. Vogel, P. F. Maccarini, V. Stakhursky, B. J. Soher, S. Das, O. A. Arabe, W. T. Joines, and P. R. Stauffer, *Improved hyperthermia treatment control using SAR/temperature simulation and PRFS magnetic resonance thermal imaging*, Int. J. Hyperthermia, vol. 27, no. 1, pp. 86–99, 2011.
- Lindholm C-E. *Hyperthermia and Radiotherapy*. Ph.D. Sweden: Thesis, Lund University, Malmo. 1992.
- Muller C. *Therapeutische Erfahrungen an 100 mit kombination von Rontgenstrahlen un Hochfrequenz, resp. Diathermie behandelten bosartigen Neubildungen*. Munchener Medizinische Wochenschrift. 1912; 28: 1546–1549.
- National Cancer Institute, *Hyperthermia in Cancer Treatment*, <http://www.cancer.gov/cancertopics/factsheet/Therapy/hyperthermia>
Son erişim tarihi: 29/10/2014.
- Neuman D. G., P. R. Stauffer, S. Jacobsen, and F. Rossetto, *SAR pattern perturbations from resonance effects in water bolus layers used with superficial microwave hyperthermia applicators*, International Journal of Hyperthermia, vol. 18, no. 3, pp. 180–193, 2002.
- Paulides M. M., J. F. Bakker, N. Chavannes, and G. C. Van Rhoon, *A patch antenna design for application in a phasedarray head and neck hyperthermia applicator*, IEEE Transactions on Biomedical Engineering, vol. 54, no. 11, pp. 2057–2063, 2007.

- Paulides M.M., Bakker J.F. and van Rhooon G.C., *A head and neck hyperthermia applicator: theoretical antenna array design*, 23rd Annual meeting of the European Society for Hyperthermic Oncology, 2006, Berlin, Germany.
- Paulides M.M., *Development of a clinical head and neck hyperthermia applicator*, PhD dissertation, October 18, 2007, Erasmus University Rotterdam.
- Paulides M. M, J.F Bakker, L. W. Hofstetter, W. C. Numan, R. Pellicer, E. W. Fiveland, M. Tarasek, G. C. Houston, G. C. van Rhooon, D. T. Yeo, G. Kotek, *Laboratory prototype for experimental validation of MR-guided radiofrequency head and neck hyperthermia*, 59(9), pp. 2139-2154, May. 2014.
- Pennes, H. H., *Analysis of Tissue and Arterial Blood Temperatures in the Resting Human Forearm*, Journal of Applied Physiology , Vol. 1, 93-122, 1948.
- Pennes, H. H., *Analysis of Tissue and Arterial Blood Temperatures in the Resting Human Forearm*, Journal of Applied Physiology , Vol. 85, pp. 5-34, 1998.
- Sağlık Bakanlığı, Kanser Daire Başkanlığı, *2008 Yılı Türkiye Kanser İnsidansları*, http://kanser.gov.tr/Dosya/kayitcilik/2008-Rapor_1.pdf
Son erişim tarihi: 29/10/2014.
- Salomir R, et al. *Local hyperthermia with MR-guided focused ultrasound: spiral trajectory of the focal point optimized for temperature uniformity in the target region*. J. Magn. Reson. Imaging 2000;12:571–583.
- Salomir R. *On-line correction and visualization of motion during MRI-controlled hyperthermia*. Magnetic Resonance Imaging 2001 ;45:128–137.
- Seebass M., R. Beck, J. Gellermann, J. Nadobny, P. Wust, *Electromagnetic phased arrays for regional hyperthermia - optimal frequency and antenna arrangement*. Int. J. Hyperthermia, 2001.
- Seegenschmiedt MH, Vernon CC. *A Historical perspective on hyperthermia in oncology* In: Seegenschmiedt MH, Fessenden P, Vernon CC, eds. Thermoradiotherapy and Thermochemotherapy. Vol 1, Berlin Heidelberg: Springer/Verlag, 1995.
- Sherar M. D., F: F. Liu, D. J. Newcombe, B. Cooper, W. Levin, W. B. Taylor, and J. W. Hunt, “*Beam shaping for microwave waveguide hyperthermia applicators*,” Int. J. Radiat. Oncol. Biol. Phys. (UK), vol. 25, 849-857, 1993.
- Smith E. Egyptian surgical papyrus dated around 3000 B.C. (cited by: van der Zee J: *Heating the patient: a promising approach?*, Ann Oncol. 2002; 13: 1173–1184.
- Stang J., M. Haynes, P. Carson, M. Moghaddam, *A Preclinical System Prototype for Focused Microwave Thermal Therapy of the Breast*, IEEE Tans. On Biomedical Engineering, Vol. 59, No. 9, pp. 2431-2438, September 2012.

- Stauffer P. R., P. Maccarini, K. Arunachalam, O. Craciunescu, C. Diederich, T. Juang, F. Rossetto, J. Schlorff, A. Milligan, J. Hsu, P. Sneed, and Z. Vujaskovic, *Conformal microwave array (CMA) applicators for hyperthermia of diffuse chestwall recurrence*, *Int. J. Hyperthermia*, vol. 26, no. 7, pp. 686–698, 2010.
- Taflove A. and Hagness SC., *Computational Electromagnetics: The Finite Difference Time-Domain Method*, Artech House, Norwood, 3rd edition, 2005. ISBN 1-580-53832-0.
- Van den Berg P. M., DeHoop, A.T., Segal, A., ve N. Praagman, *A Computational Model of the Electromagnetic Heating of Biological Tissue with Application to Hyperthermic Cancer Therapy*, *IEEE Transactions on Biomedical Engineering*, Vol. 30, No. 12, 797-805, 1983.
- Visible Human Server, Computer Science Department, Ecole Polytechnique Federale de Lausanne, <http://visiblehuman.epfl.ch/index.php>
- Wust, P., B. Hildebrandt, G. Sreenivasa et al., *Hyperthermia in combined treatment of cancer*, *The Lancet Oncology*, Vol. 3, pp. 487–497, 2002.
- Vernon C. C., Hand J. W., Field S. B., Machin D., Whaley J. B., van der Zee J., van Putten W. L. J., van Rhoon G. C., van Dijk J. D. P., Gonzalez D. G., Liu F., Goodman P., and Sherar M., “Radiotherapy with or without hyperthermia in the treatment of superficial localized breast cancer: Results from five randomized controlled trials,” *Int. J. Radiat. Oncol. Biol. Phys.*, vol. 35, pp. 731--744, 1996.
- Vujaskovic Z., Kim D. W., Jones E., Lan L., McCall L., Dewhurst M. W., Craciunescu O., Stauffer P., Liotcheva V., Betof A., and Blackwell K., “A phase I/II study of neoadjuvant liposomal doxorubicin, paclitaxel, and hyperthermia in locally advanced breast cancer,” *Int. J. Hyperthermia*, vol. 26, no. 5, pp. 514--521, 2010.
- Wust P., R. Beck, J. Berger, H. Föhling, M. Seebaß, W. Wlodarczyk, W. Hoffmann, J. Nadobny, *Electric field distributions in a phased-array applicator with 12 channels: Measurements and numerical simulations*. *Med. Phys.* 27, pp. 2565-2579, 2000.
- Wust P, et al. *Thermal monitoring: invasive, minimal-invasive and non-invasive approaches*, *Int. J. Hyperthermia* 2006;22:255–262.
- Xu S., Y. Rahmat-Samii, “*Shaped-reflector antenna designs using particle swarm optimization: An example of a direct-broadcast satellite antenna*,” *Microw. Opt. Technol. Lett.*, vol. 48, no.7, pp.1341-1347, Jul. 2006.
- Yang, X., J. Du, Y. Liu, *Advances in Hyperthermia Technology*, *IEEE Engineering in Medicine and Biology 27th Annual Conference*, Shanghai, China, September 1-4, 2005, pp. 6766-6769.
- Yilmaz Tuba, Tutku Karacolak, Erdem Topsakal, *Characterization of Skin Mimicking Gels for Implantable Antennas Operating at ISM Band (2.4 GHz - 2.48 GHz)*, *National Radio Science Meeting, URSI*, January 3-6, 2008.

Zastrow E., S. K. Davis, M. Lazebnik, F. Kelcz, B. D. Van Veen, S. C. Hagness,
*Development of Anatomically Realistic Numerical Breast Phantoms With Accurate
Dielectric Properties for Modeling Microwave Interactions With the Human Breast,*
IEEE Transactions on Biomedical Engineering, vol. 55, no. 12, pp. 2792-2800,
December 2008.

3D-Doctor, USA, <http://www.ablesw.com/3d-doctor/>
Son erişim tarihi: 29/10/2014.

APPENDIX A

DECLARATION STATEMENT FOR THE ORIGINALITY OF THE THESIS, FURTHER STUDIES AND PUBLICATIONS FROM THESIS WORK

A.1 DECLARATION STATEMENT FOR THE ORIGINALITY OF THE THESIS

I hereby declare that this thesis comprises my original work. No material in this thesis has been previously published and written by another person, except where due reference is made in the text of the thesis. I further declare that this thesis contains no material which has been submitted for a degree or diploma or other qualifications at any other university.

Signature:

Date: July 6, 2015

A.2 PUBLICATIONS FROM THESIS WORK

Academic Journals

- Erdal Korkmaz, Omer Isik, and Mohammed Ahmed Nassor, "A Compact Microstrip Spiral Antenna Embedded in Water Bolus for Hyperthermia Applications", International Journal of Antennas and Propagation, Vol. 2013, No. 954986, Oct. 2013, pp. 1-6.

Conference Proceedings

- Erdal Korkmaz, Omer Isik and Huseyin Sagkol, "Non-invasive RF Hyperthermia for Cancer Treatment ", Mediterranean Conference on Information & Communication Technologies, Saïdia, Morocco, May. 2015, 1, 1,pp. 40.

- Erdal Korkmaz, Omer Isik and Huseyin Sagkol, "A Directive Antenna Array Applicator for Focused Electromagnetic Hyperthermia Treatment of Breast Cancer", 9th European Conference on Antennas and Propagation (EuCAP), Lisbon, Portugal, Apr. 2015, 1, 1.
- Erdal Korkmaz, Omer Isik, Sadik Kara, "Electromagnetic Modeling of A Female Breast Hyperthermia Applicator", IEEE International Symposium on Antennas and Propagation and USNC-URSI National Radio Science Meetin, Orlando, Florida, USA, Jul. 2013, IEEE APS URSI 2013, 1, 1,pp. 4.
- O. Isik, E. Korkmaz, S. Kara, M. A. Nassor, B. Turetken, "Development of a Hyperthermia Applicator with Compact Microstrip Antennas", Proceedings of IEEE International Symposium on Antennas & Propagation, Chicago ABD, Jul. 2012, 1, pp. 1.
- E. Korkmaz, M. A. Nassor, S. Kara, O. Isik, B. Turetken, "Design of Compact Microstrip Antennas Embedded in Water Bolus for Hyperthermia Applications", Proceedings of IEEE International Symposium on Antennas , Chicago ABD, Jul. 2012, 1, pp. 1.
- O. Işık, E. Korkmaz, B. Turetken, " Antenna Arrangement Considerations for Microwave Hyperthermia Applications", The XXX General Assembly and Scientific Symposium of the International Union of Radio Science, İstanbul, Turkey, Aug. 2011, IEEE Proceedings of The XXX General Assembly and Scientific Symposium of the International Union of Radio, KP1, 10,pp. KP1.10.
- Erdal Korkmaz, Omer Isik, "Electromagnetic Hyperthermia Modeling in Human Intra-Abdominal Region", Proceedings of the 14th International Symposium on Antenna Technology and Applied Electromagnetics [, Ottawa / Kanada, Jul. 2010, IEEE International Symposium on Antenna Technology and Applied Electromagnetics [ANTEM] and the AMEREM, 14, 237,pp. 237.
- O. Isik, E. Korkmaz, "Electromagnetic Modeling of Thermal Fields Induced in Human Femur Tissue", Proceedings of the 2010 IEEE AP-S International Symposium on Antennas and Propagation & USNC/URSI Na, Toronto / Kanada, Jul. 2010, IEEE AP-S International Symposium on Antennas and Propagation & USNC/URSI Na, 111,pp. pp. 10.

APPENDIX B

ACKNOWLEDGEMENT

This thesis was a part of the supported project by The Scientific and Technological Research Council of Turkey (TUBITAK) under number 111E087. Preliminary study of this work was supported by the Scientific Research Found of Fatih University under the project number P500609002-2. The author is thankful to SPEAG for their support of academic license for SEMCAD X and real breast phantoms.

CURRICULUM VITAE

CONTACT INFORMATION

Ömer IŞIK
Fatih University, Electrical and Electronics Engineering,
34500 Büyükçekmece
Istanbul, Turkey
Phone: (0212) 866 33 00 (Ext. 5596)
Email: omer@fatih.edu.tr

EDUCATION

Ph.D., Electrical and Electronics Engineering, Fatih University, Istanbul, Turkey, June 2015.

Dissertation: "Modeling of Electromagnetic Interaction in Human Tissues and Local Temperature Increase for Cancer Treatment and Development of a Hyperthermia Applicator"

M.S., Electrical and Electronics Engineering, Fatih University, Istanbul, Turkey, June 2010.

Thesis: "Modeling of Electromagnetic Behavior and Local Temperature Increase"

B.S., Electrical and Electronics Engineering, Gaziantep University, Gaziantep, Turkey, June 2006.

PROFESSIONAL EXPERIENCE

- Research Assistant, Electrical and Electronics Engineering Department, Fatih University, Istanbul, Turkey, (2008 - present).

PUBLICATIONS

Academic Journals

- Erdal Korkmaz, Omer Isik, and Mohammed Ahmed Nassor, "A Compact Microstrip Spiral Antenna Embedded in Water Bolus for Hyperthermia Applications", International Journal of Antennas and Propagation, Vol. 2013, No. 954986, Oct. 2013, pp. 1-6

Conference Proceedings

- Erdal Korkmaz, Omer Isik and Huseyin Sagkol, "Non-invasive RF Hyperthermia for Cancer Treatment ", Mediterranean Conference on Information & Communication Technologies (MedICT 2015), Saïdia, Morocco, May. 2015, Lecture Notes in Electrical Engineering by Springer Verlag, 1, 1,pp. 40.
- Erdal Korkmaz, Omer Isik and Huseyin Sagkol, "A Directive Antenna Array Applicator for Focused Electromagnetic Hyperthermia Treatment of Breast Cancer", 9th European Conference on Antennas and Propagation (EuCAP), Lisbon, Portugal, Apr. 2015, 1, 1.
- Erdal Korkmaz, Omer Isik, Sadik Kara, "Electromagnetic Modeling of A Female Breast Hyperthermia Applicator", IEEE International Symposium on Antennas and Propagation and USNC-URSI National Radio Science Meetin, Orlando, Florida, USA, Jul. 2013, IEEE APS URSI 2013, 1, 1,pp. 4.
- O. Isik, E. Korkmaz, S. Kara, M. A. Nassor, B. Turetken, "Development of a Hyperthermia Applicator with Compact Microstrip Antennas", Proceedings of IEEE International Symposium on Antennas & Propagation, Chicago ABD, Jul. 2012, 1, pp. 1.
- E. Korkmaz, M. A. Nassor, S. Kara, O. Isik, B. Turetken, "Design of Compact Microstrip Antennas Embedded in Water Bolus for Hyperthermia Applications", Proceedings of IEEE International Symposium on Antennas , Chicago ABD, Jul. 2012, 1, pp. 1.
- O. Işık, E. Korkmaz, B. Turetken, " Antenna Arrangement Considerations for Microwave Hyperthermia Applications", The XXX General Assembly and Scientific Symposium of the International Union of Radio Science, İstanbul, Turkey, Aug. 2011, IEEE Proceedings of The XXX General Assembly and Scientific Symposium of the International Union of Radio, KP1, 10,pp. KP1.10.
- Erdal Korkmaz, Omer Isik, "Electromagnetic Hyperthermia Modeling in Human Intra-Abdominal Region", Proceedings of the 14th International Symposium on Antenna Technology and Applied Electromagnetics, Ottawa, Canada, Jul. 2010, IEEE International Symposium on Antenna Technology and Applied Electromagnetics [ANTEM] and AMEREM, 14, 237,pp. 237.
- O. Isik, E. Korkmaz, "Electromagnetic Modeling of Thermal Fields Induced in Human Femur Tissue", Proceedings of the 2010 IEEE AP-S International Symposium on Antennas and Propagation & USNC/URSI, Toronto, Canada, Jul. 2010, 111,pp. pp. 10.

Posters

- Ömer Işık, Erdal Korkmaz, "İnsan Dokularında Elektromanyetik Etkileşim ve Lokal Isı Artışı Modellemesi", 14.Biyomedikal Mühendisliği Ulusal Toplantısı, İzmir/Türkiye, May. 2009, IEEE Proceedings of BIYOMUT 2009, 1, 1,pp. pp. 1.

RESEARCH PROJECTS

- 2008-2010 Assistant Researcher, “Modeling of Electromagnetic Behavior and Local Temperature Increase” supported by Fatih University.
- 2011-2014 Assistant Researcher, “Kanser Tedavisinde İnsan Dokularındaki Elektromanyetik Etkileşim ve Lokal Isı Artışı Modellemesi ve Hipertermi Aplikatörünün Geliştirilmesi” supported by TÜBİTAK.
- 2013-2014 Coordinator, Researcher, “Hipertermi Aplikatörünün Prototipinin Tasarımı ve Üretimi” supported by Ministry of Science, Industry and Technology.
- 2014-2015 Assistant Researcher, “Elektromanyetik Alan Ölçen RF Alan Ölçücü” supported by Ministry of Science, Industry and Technology.

TECHNICAL SKILLS

- Programming languages: Fortran, C
- Analytical and statistics programs: Matlab, CST, Semcad X, Antenna Magus
- Word processing and publication: Microsoft Word